FLOODED ISLANDS
PRE-FEASIBILITY STUDY

RMA DELTA MODEL CALIBRATION REPORT

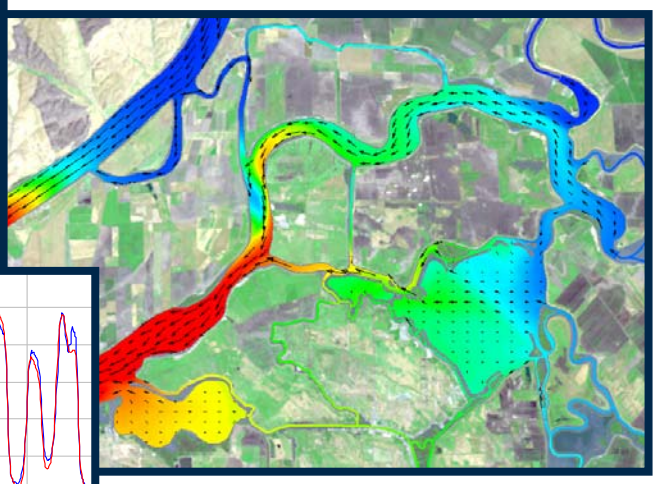

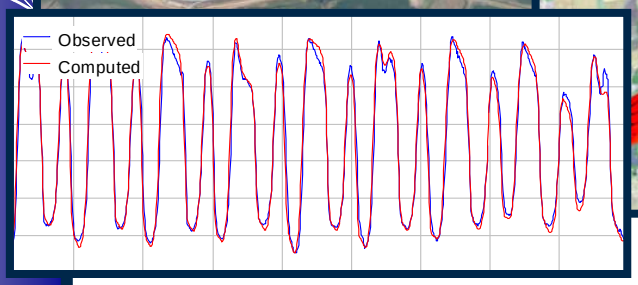

Prepared For:

California Department of Water Resources

For Submittal To:

California Bay-Delta Authority

June 30, 2005

Prepared By:

RMA Resource Management Associates

FLOODED ISLANDS
PRE-FEASIBILITY STUDY
RMA DELTA MODEL CALIBRATION REPORT

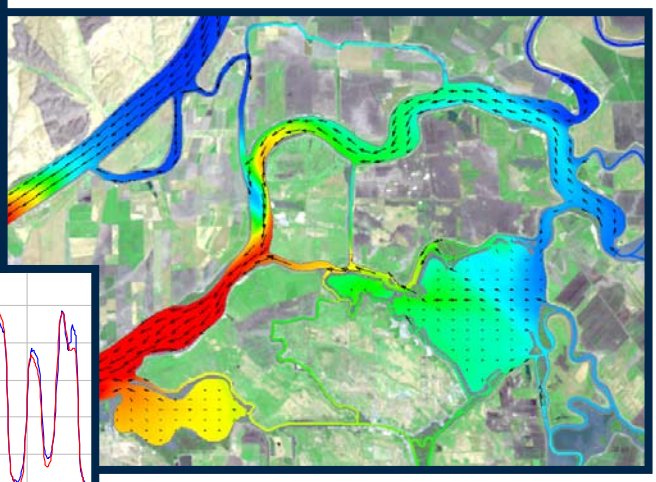

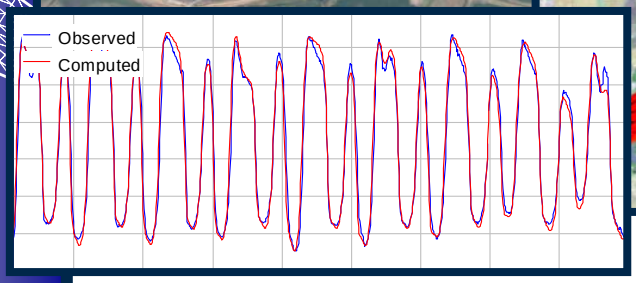

Prepared For:
California Department of Water Resources
1416 Ninth Street
Sacramento, CA 94236

Contact:
Donald Kurosaka
Project Manager
916-653-6636

For Submittal To:
California Bay-Delta Authority
650 Capitol Mall, 5th Floor
Sacramento, CA 95814

Prepared By:
Resource Management Associates
4171 Suisun Valley Road, Suite J
Fairfield, CA 94534

Contact:
John DeGeorge
707-864-2950

June 30, 2005

RMA Resource Management Associates

TABLE OF CONTENTS

LIST OF FIGURES

LIST OF TABLES

1 INTRODUCTION

The RMA finite element model of the San Francisco Bay and Sacramento – San Joaquin Delta has been calibrated and refined through many previous studies. During the spring and summer of 2002, the USGS placed a number of temporary flow and CTD meters in and around the area of Franks Tract. This new data has significantly enhanced the understanding of flow and salinity transport in the central Delta. Data from these gauges and the other permanent flow, stage and EC stations in the Delta were utilized to further refine and calibrate the RMA finite element model in the central Delta. This document serves to describe the calibration process and demonstrate the capability of the calibrated model to predict flow, stage and EC in the Delta.

1.1 BACKGROUND

Resource Management Associates, Inc. (RMA) has developed a series of finite element models for one-, two- and three-dimensional simulation of flow, salinity, water quality and sediment transport in streams and estuaries.

Through numerous modeling projects, RMA has developed several finite element representations of the San Francisco Bay and Delta system that emphasize various areas in the Bay and Delta. During the Suisun Marsh Levee Breach modeling project sponsored by CALFED, considerable detail was added to the representation of Suisun Bay and the western Delta. Work with CALFED on subsequent studies allowed for further model refinement in the Delta, leading up to the current effort, which represents the most detailed and accurate version of the RMA Delta model to date.

The RMA Bay-Delta and Delta models have been successfully calibrated and applied in numerous studies to evaluate the water quality responses of treated wastewater discharges to San Francisco Bay and Delta, and the potential impacts of various Suisun Marsh and Delta levee

breach scenarios. Depending on the requirements of the study, the RMA Bay-Delta model may be run for the entire system with the tidal boundary condition applied at the Golden Gate, or it may be run for the Delta region only with tidal boundary condition applied at Martinez. The full Bay-Delta model is run when a study involves large changes in Delta tidal prism or Net Delta Outflow that might alter stage or salinity at Martinez, such as the Delta levee breach scenarios. If the focus of a study is limited to the Delta and alternative configurations are not expected to alter stage or salinity at Martinez then the Delta only version of the model is utilized. This reduces computational effort and removes uncertainty associated with propagating the stage and salinity signal from the Golden Gate to Martinez. Simulations in support of the Flooded Islands Pre-Feasibility Study utilized the Delta only version of the model.

1.2 OBJECTIVES

This objective of this calibration effort was to prepare the model for detailed evaluation of flow and salinity impacts associated with alternative configurations proposed in the Flooded Islands Study. Measurable salinity impacts at the primary export locations and throughout the Delta result from small changes in flow and mixing processes at the tidal time scale integrated over weeks and months. Understanding and accurately representing the changes in short time scale flow and mixing processes in the model is critical to predicting the impacts of proposed alternatives. April through October 2002 was selected for the detailed calibration period due to the availability of extensive monitoring data collected by the USGS as part of a special study of the Franks Tract Region. 2002 was considered a dry year, although the period encompasses a significant range of inflows, exports, and tidal conditions. Particular emphasis was placed on improving hydrodynamic and salinity representations in and around Franks Tract, as dynamics in this area strongly affect the rest of the Delta. Because the calibration was focused on the Delta region, the Delta only version of the RMA Bay-Delta model was run with the tidal boundary applied at Martinez.

The emphasis of the Pre-Feasibility phase of the Flooded Islands Study is on relative ranking of a wide range of proposed alternatives. As the project moves toward recommendation of a single preferred alternative, absolute prediction of water quality impacts over a range of

water year types becomes more important in evaluating the benefits of the project. At that time, further model calibration and verification should be conducted that include other water year types.

1.3 REPORT ORGANIZATION

The model formulation is described briefly in Section 2, with the detailed description of the numerical model programs, including the governing equations, presented in Appendix A. In Section 3, the configuration of the RMA Delta model is described including geometric extents of the finite element mesh, data sources and model coefficients. Section 4 details the calibration period model boundary conditions, inputs and operations. Results for stage, flow and salinity are plotted and discussed in Sections 5, 6 and 7, respectively. Conclusions are summarized in Section 8.

2 MODEL FORMULATION

RMA has developed a set of finite element models for the simulation of hydrodynamic and water quality responses in shallow estuaries. The program RMA2 (King, 1986) is a generalized free surface hydrodynamic model that is used to compute two-dimensional depth-averaged velocity and water surface elevation. RMA11 (King, 1995) is a generalized two-dimensional depth-averaged water quality model which computes a temporal and spatial description of conservative and non-conservative water quality parameters. RMA11 uses the results from RMA2 for its description of the flow field.

The model uses a depth-averaged approximation in the western Delta and Suisun Bay where significant vertical gradients in salinity are often present. Vertical gradients in salinity may lead to three dimensional circulation patterns that will not be represented by a two-dimensional depth-averaged model. Instead, the three dimensional processes are approximated by two-dimensional mixing parameters. The calibration results presented in this report show that the model was able to very accurately transport salinity from the tidal boundary at Martinez, through Suisun Bay, to Jersey Point and False River for the 2002 period simulated. In other modeling work using the full RMA Bay Delta model with the salinity boundary applied at the Golden Gate, the two-dimensional representation has been shown work well during most conditions. The approximation has the most difficulty during the transient recovery of salinity following a large net delta outflow. In this case the model salinity recovers more slowly than the real system. Generally the model catches up to the observed salinity within one to two weeks following a large storm event. There is some concern that calibrated mixing coefficients would not be appropriate if the system configuration was changed significantly. Modeling of the Jones Tract levee failure has shown that the model performs adequately given a large change in tidal prism. In the modeling of the Feasibility Study alternatives, there were no changes proposed that would strongly affect the flows through Suisun Bay, and, therefore, the calibration of mixing coefficients will probably not be affected. This issue may be explored further during future calibration/verification efforts.

The RMA2 model is capable of representing the influence of the depth-averaged (horizontal) baroclinic distribution in the computation of the hydrodynamics. Because fresh water is less dense than saline water, horizontal salinity gradients lead to higher water surface elevations in the Delta and larger spring-neap tidal variation than would be calculated neglecting the density gradient, Note that the depth-averaged model does not explicitly represent vertical salinity gradients and associated gravitational circulations (a fully three-dimensional model would be required). A "salinity-coupled" version of the RMA2 program has been developed which includes the relevant water quality transport routines from the RMA11 program in order to compute the salinity distribution throughout the model domain during the hydrodynamic simulation. The salinities (or EC) values are then utilized in the computation of the baroclinic term of the flow equation. Salinity transport and flow are not computed simultaneously. Rather, the salinities from the previous computational time step are used to compute the fluid densities for the current hydrodynamic time step. Once a converged solution for the flow computation is achieved, the resulting flow field is utilized for the computation of the salinity transport.

In addition to two-dimensional depth-averaged elements, the models described also employ one-dimensional channel elements. Special "transition" elements allow the one-dimensional elements to be readily interfaced to the two-dimensional depth-averaged elements. For systems such as the San Francisco Bay-Delta, the two-dimensional depth-averaged elements are typically used to represent the open waters of the bays and large river channels while the one-dimensional elements are used for reproducing flow and transport for many of the more simple channels of the Delta.

The RMA suite of finite element hydrodynamic and water quality models employed for this study have been used extensively since 1977 in engineering applications to examine flow and transport of constituents in surface water systems. Originally developed with the support of the U.S. Army Corps of Engineers Waterways Experiments Station, the models have undergone continued development and refinement by RMA. One of the most important additions has been the capability to accurately represent wetting and drying in shallow estuaries.

The RMA2 flow model and the earlier version of the water quality model, RMA-4 form the basis for the U.S. Army Corps of Engineers (USACE) TABS-MD modeling system. The

public domain versions of the RMA2 and RMA-4 (an earlier water quality model) models are based upon the USACE version of the models, and are available as part of the commercially available "Surface Water Modeling System" (SMS) package. RMA has extended its own version of the two-dimensional flow and water quality models to allow application to more complex water quality, sediment transport and flow problems in estuaries, wetlands and floodplains.

The RMA hydrodynamic and transport programs are generalized models. However, features of the models may be discussed in the context of applying these codes to the simulation to flow and water quality transport in the Bay-Delta estuary.

2.1 RMA2

Hydrodynamics are simulated using RMA2, a two-dimensional depth-averaged finite element model that solves the shallow water equations in primitive variables to provide temporal and spatial descriptions of velocities and water depths throughout the regions of interest. The program uses a finite element approach with Galerkin's criterion applied to the method of weighted residuals. For the two-dimensional approximations, the model employs 6-node triangular and 8-node quadrilateral element. Three node line elements are used for approximating one-dimensional channel flow. Quadratic shape functions are used interpolate the velocity variables while linear shape functions are used for the depth, h. The quadratic functions allow for a curved element edge geometry. Because these equations can be highly non-linear, they are solved by a Newton-Raphson iterative technique. Time dependent solutions employ a Crank-Nicholson implicit finite difference scheme. Values of time integration constant, θ, can be varied by input. Typically a value of .526 is used for the RMA2 time dependent simulations. The time step used for modeling the depth-averaged flow and water quality transport in the Delta is 7.5 minutes.

The model uses the Smagorinsky formulation for modeling of turbulent momentum transfer. RMA2, capable of simulating the de-watering of tidal flats, is well suited for modeling of inter-tidal hydrodynamics in the marshes and mudflats that characterize the Bay-Delta system.

A full description of the governing equations for flow and additional RMA2 model details are provided in Appendix A.

2.2 RMA11

The results of the RMA2 flow simulation (x and y velocity components, and depth of water) are saved every time step for all nodal locations to a binary file. The flow result file then may be used by the finite element water quality model, RMA11, to compute salinity transport or the transport of other water quality constituents with more complex interactions. EC or salinity transport may also be computed during the flow simulation using the "salinity-coupled" version of the RMA2 model.

The RMA11 water quality model is capable of simulating water temperature, DO/BOD, algae growth and decay including interaction with the nitrogen and phosphorous cycles, cohesive and non-cohesive sediment transport, coliform with associated decays, and arbitrary conservative and non-conservative constituents with user defined interactions.

RMA11 solves a set of differential equations representing the conveyance of dissolved or suspended material by advection and turbulent mixing. These equations are derived from a statement of conservation of mass. Eddy diffusion is also used to approximate the complex process of time dependent transport by turbulent mixing. In the inter-tidal water quality simulation mode, advection is the dominant transport mechanism. Turbulent diffusion occurs in the presence of velocity and concentration gradients. Calibrated scaling constants are developed for the longitudinal and transverse diffusion terms. The scaling constant for the longitudinal diffusion is multiplied by the current velocity to develop the longitudinal diffusion coefficient. The transverse diffusion coefficient is set in the user input as some fraction of the longitudinal coefficient.

The RMA11 model may also be executed in a steady-state mode. This method is used to develop the initial spatial distribution of Delta EC from a limited number of known EC observations. During the current calibration effort, the initial condition EC is developed in the Delta with a diffusive solution to known EC values.

The full description of the governing equations for constituent transport is presented in Appendix A.

3 MODEL CONFIGURATION

3.1 GEOMETRIC EXTENTS

RMA's Sacramento – San Joaquin Delta network was developed using an in-house GIS-based graphical user interface program. The program allows for development of the finite element mesh over layers of bathymetry points, bathymetry grids and contours, USGS digital line graph (DLG) and digital orthoquad (DOQ) images, and aerial photo surveys processed by USGS.

The RMA model of the Delta, shown in Figure 3-1, extends from the Martinez to the confluence of the American and Sacramento Rivers, and to Vernalis on the San Joaquin River. A two-dimensional depth-averaged approximation is used to represent the Suisun Bay region, the Sacramento-San Joaquin confluence area, Sherman Lake, the Sacramento River up to Rio Vista, Big Break, the San Joaquin River up to its confluence with Middle River, False River, Franks Tract and surrounding channels, Old River south of Franks Tract, and the Delta Cross Channel area. The Delta channels and tributary streams are represented using a one-dimensional cross-sectionally averaged approximation.

The model network used for the alternative analysis approximated Mildred Island as off-channel storage of the one-dimensional elements surrounding the island. A test simulation was performed with Mildred Island represented with two-dimensional depth–averaged elements, but there was no significant improvement in accuracy of the model with regard to overall flows or salinity transport in the Delta. Since the added two-dimensional detail did not significantly improve the result but did increase computation time, it was not used in this calibration. When detailed flows in the neighborhood Mildred Island are needed, the two-dimensional representation will be used.

Current model calibration efforts focused on refinement of the finite element mesh in and around Franks Tract and False River, in the Delta Cross Channel, in and around Big Break, and in Lower Mokelumne River.

The size and shape of elements are dictated by changes in bottom elevation and other hydraulic and salinity considerations. Wetting and drying of the tidal mudflats has been represented in sufficient detail to provide a good definition of change in the tidal prism with change in tidal stage.

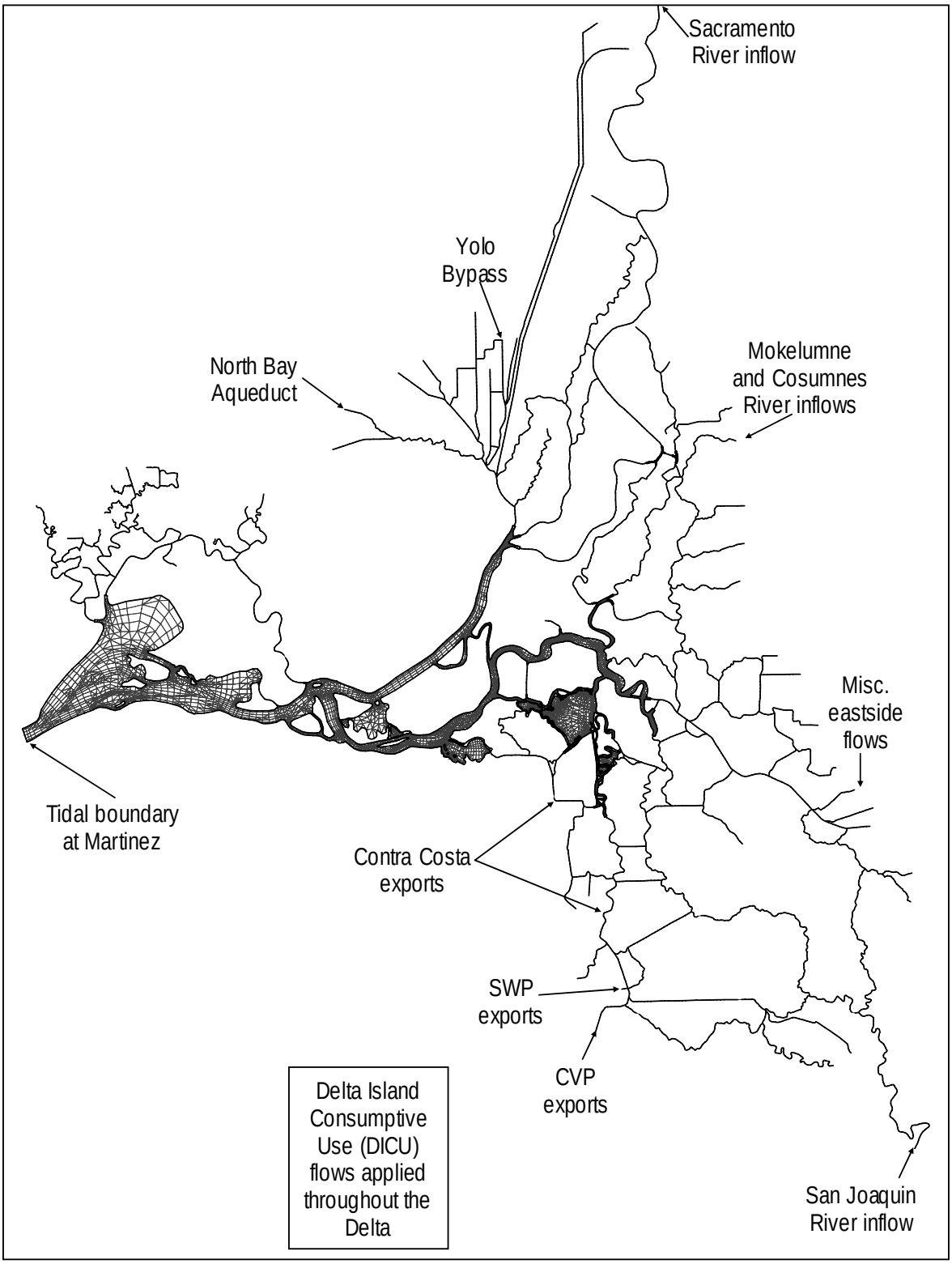

Figure 3-1 Model configuration of the Sacramento - San Joaquin Delta.

3.2 BATHYMETRY

Bottom elevations and the extent of mudflats were based on bathymetry data collected by NOAA, DWR, USACE and USGS. These data sets have been compiled by DWR and can be downloaded from DWR's Cross Section Development Program (CSDP) website at http://baydeltaoffice.water.ca.gov/modeling/deltamodeling/models/csdp/index.html. Additional data were collected around Franks Tract by DWR and USGS in 2004. USGS 10 m resolution Delta Bathymetry grids were obtained from the Access USGS website at http://sfbay.wr.usgs.gov/access/Bathy/Delta/.

RMA's grid development software, RMASIM, has the capability of displaying bathymetry data in point form or in the USGS bathymetry grid format. Figure 3-2 illustrates RMASIM with USGS bathymetry grid data displayed over a color aerial photo image in the Big Break area.

Three-dimensional views of Suisun Bay and the confluence area, and of the Franks Tract area of the model are shown in Figures 3-3 and 3-4, respectively.

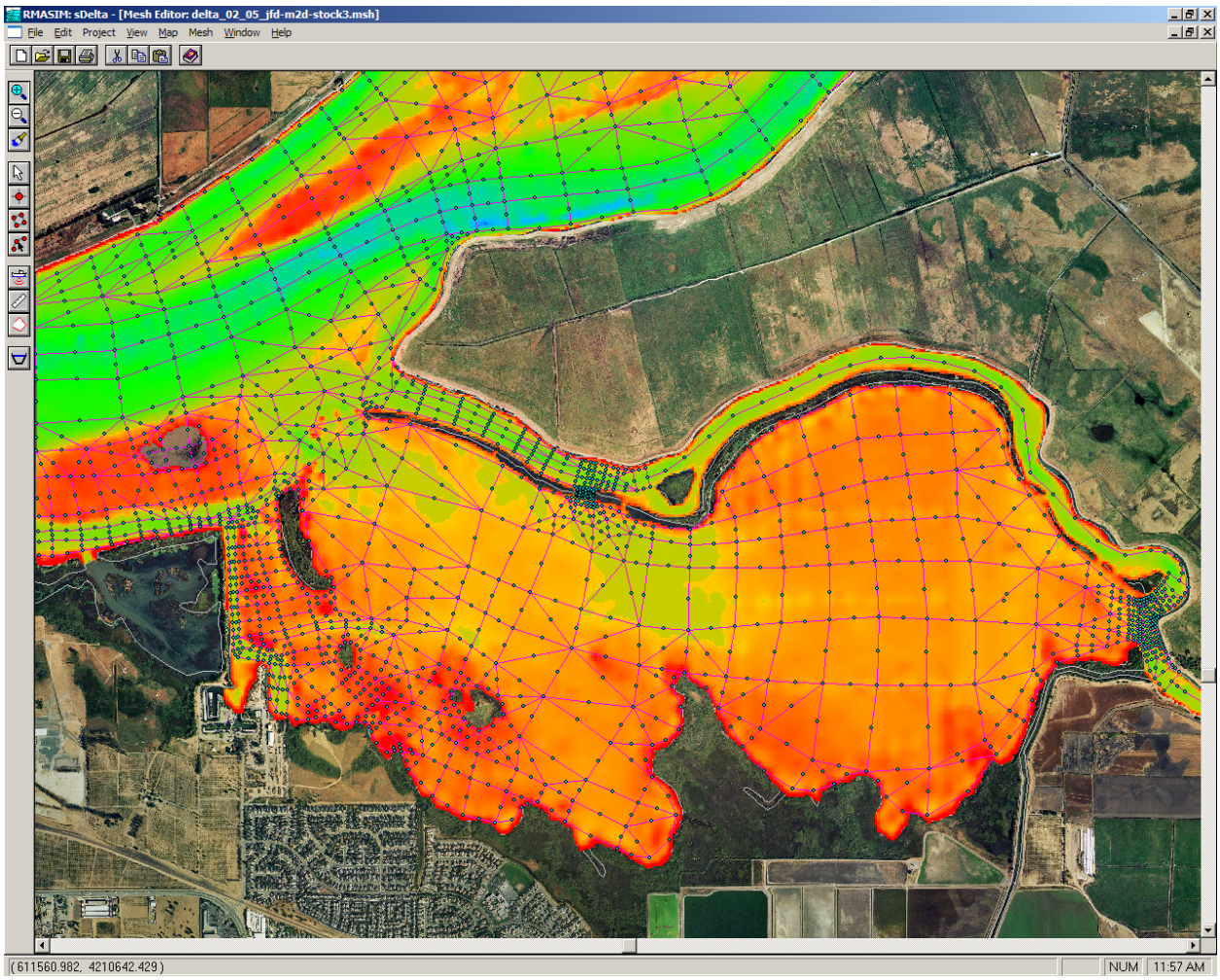

Figure 3-2 RMASIM displaying USGS bathymetry grid.

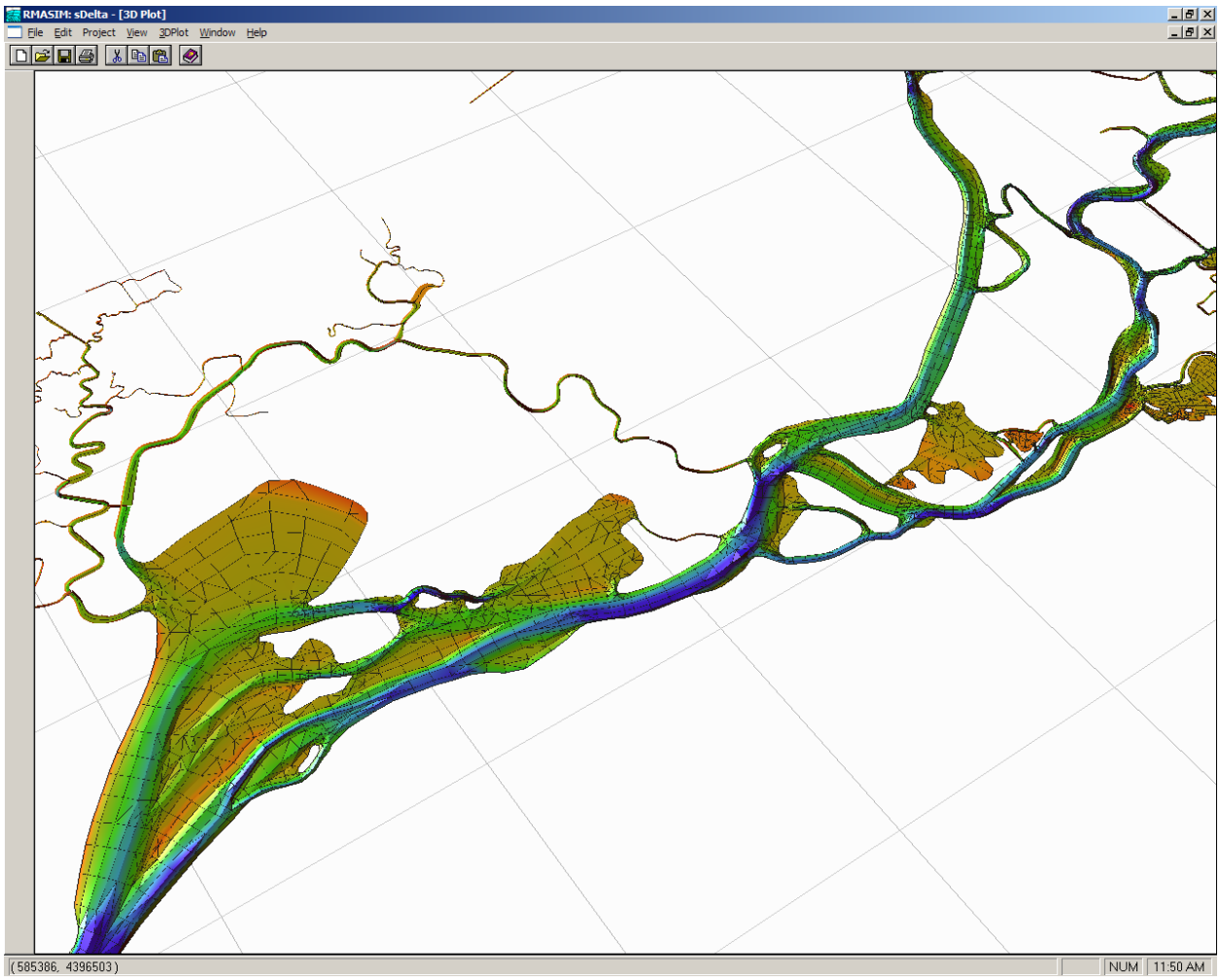

Figure 3-3 3-D view of Suisun Bay and the confluence area of the finite element mesh, shown in RMASIM.

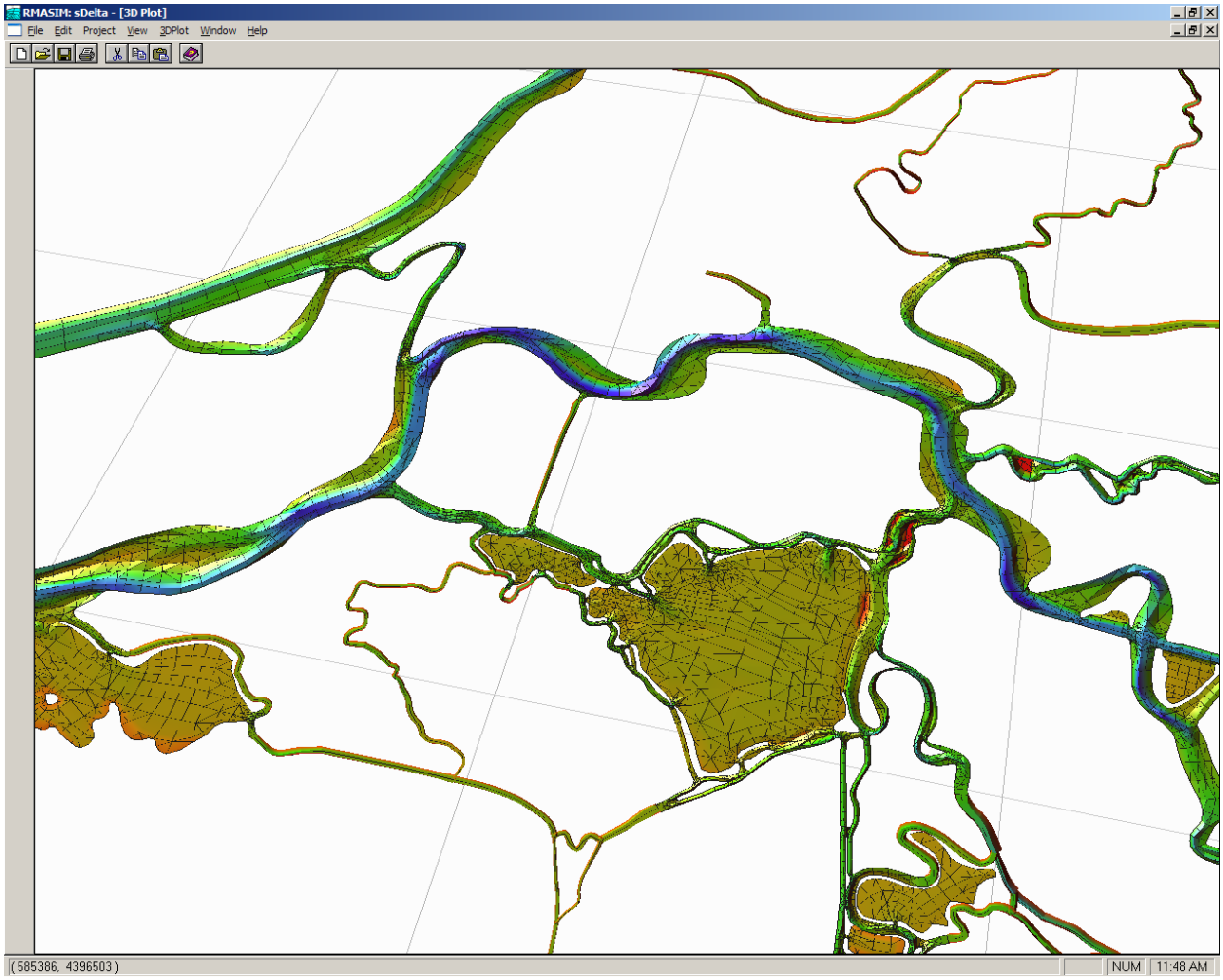

Figure 3-4 3-D view of the Franks Tract area of the finite element mesh, shown in RMASIM.

3.3 MODEL COEFFICIENTS

RMA2 represents turbulent and sub-grid scale transport of momentum using the "eddy viscosity" approximation. The Smagorinsky method with fixed minimum values is use to estimate eddy viscosity in each element. For the calibration simulation, the minimum eddy viscosity is universally set at 0.1 N-s/m^2 and the Alpha factor is 0.05 (see Appendix A for discussion of Smagorinsky method). Other model coefficients, including Manning's n and diffusion, are applied by element type. Table 3-1 lists model coefficients by location.

Table 3-1 Model coefficients.

Location	Manning's n	Longitudinal diffusion factor	Lateral diffusion factor	Min longitudinal diffusion (m^2/s)	Min lateral diffusion (m^2/s)
1-D Delta channels	0.029	200.0	0.05	2.0	1.0
Suisun Bay	0.024	60.0	0.2	2.0	2.0
SJR 2-D	0.027	75.0	0.05	1.0	0.5
Sacramento R 2-D	0.024	100.0	0.05	2.0	0.5
Mudflats	0. 035	200.0	0.1	2.0	1.0
Marsh	0.06	200.0	0.1	2.0	1.0
False River	0.03	150.0	0.05	2.0	0.5
Franks Tract no egeria	0.03	300.0	0.05	3.0	1.0
Franks Tract egeria beds	0.095	300.0	0.1	3.0	1.5
Franks Tract some egeria	0.05	300.0	0.1	3.0	2.0
FT shallow breaches	0.04	200.0	0.1	3.0	2.0
West False River	0.03	150.0	0.05	2.0	0.5
Sacramento R 1-D	0.026	200.0	0.05	2.0	1.0
Dutch Slough	0.029	300.0	0.05	2.0	1.0
Old River 2-D	0.029	120.0	0.05	2.0	0.75
Three Mile Slough	0.03	95.0	0.05	2.0	0.5
SJR near Sacramento R	0.024	70.0	0.1	2.0	1.0

4 CALIBRATION PERIOD

4.1 OVERVIEW

The current version of RMA's Bay-Delta model has been developed and continually refined during several studies over the past 30 years. The current and most intense calibration effort has been performed for the period of April 1 through October 1, 2002 to coincide with USGS flow, velocity and EC data collected in and around Franks Tract. Flow, Stage and EC data from the permanent Delta stations are also available during this period. Water year 2002 is classified as a dry year.

Because the calibration effort is focused on the Delta, the RMA Bay-Delta model was run for the Delta region only. Hydrodynamic model operation requires specification of the tidal stage at Martinez and inflow and withdrawal rates at other external boundaries. Gate and barrier operations are also included in the model.

4.2 TIDAL BOUNDARY

The tidal boundary is set at Martinez using observed 15-minute stage data from IEP. The tide used for the calibration period is plotted in Figure 4-1. EC data at the tidal boundary is plotted in Figure 4-2. The average of surface and bottom EC was used.

4.3 RIVER INFLOWS

Daily average inflow boundary conditions are applied for the Sacramento River, San Joaquin River, Cosumnes River, Mokelumne River, Calaveras River, and miscellaneous eastside flows. The model interpolates between the daily average flows at noon each day.

Dayflow data (from http://www.iep.ca.gov/dayflow/index.html) are used to set boundary conditions for Sacramento, San Joaquin, Cosumnes and Mokelumne Rivers. Calaveras flows are DWR DSM2 flows from the RCAL009 station on the IEP website (http://iep.water.ca.gov/cgi-

bin/dss/dss1.pl?station=RCAL009). The miscellaneous eastside flows boundary condition is set using Dayflow values for "MISC" less the Calaveras River flows.

Inflow locations are shown in Figure 3-1. Sacramento and San Joaquin River flows and NDO for the calibration period are plotted in Figure 4-3.

4.4 DELTA EXPORTS

Delta exports applied in the model include SWP, CVP, Contra Costa exports at Rock Slough and Old River intakes, and North Bay Aqueduct. Exports are plotted for the calibration period in Figure 4-4.

Daily average export flows from Dayflow (http://www.iep.ca.gov/dayflow/index.html) are used for the CVP and North Bay Aqueduct. Contra Costa's Old River export flows are from IEP at ROLD034 (http://iep.water.ca.gov/cgi-bin/dss/dss1.pl?station=ROLD034). Contra Costa's Rock Slough export flows are computed as the difference between the Dayflow values for "CCC" and the IEP values for the Old River intake. Hourly SWP export flows are computed from hourly IEP time series data of :

1. water surface elevations outside Clifton Court Forebay;
2. water surface elevations inside Clifton Court Forebay; and
3. Gate opening height of the five Clifton Court Forebay Gates.

These data are input into the gate flow equations shown below, which were developed by Hills (1988).

$$Q_1 = H_1\left\{0.44 + 215.224\left(Elev_{outside} - Elev_{inside}\right)^{1/2}\right\}$$

$$Q_2 = H_2\left\{4.46 + 181.804\left(Elev_{outside} - Elev_{inside}\right)^{1/2}\right\}$$

$$Q_3 = H_3\left\{4.76 + 173.378\left(Elev_{outside} - Elev_{inside}\right)^{1/2}\right\}$$

$$Q_4 = H_4\left\{3.38 + 173.378\left(Elev_{outside} - Elev_{inside}\right)^{1/2}\right\}$$

$$Q_5 = H_5 \left\{ 2.38 + 168.790 \left(Elev_{outside} - Elev_{inside} \right)^{1/2} \right\}$$

$$Q_{total} = Q_1 + Q_2 + Q_3 + Q_4 + Q_5$$

Where,

$Q_i =$ flow through gate i (cfs),

$H_i =$ gate height/gate position of gate i (ft),

$Elev_{outside} =$ stage outside Clifton Court Forebay (ft),

$Elev_{inside} =$ stage inside Clifton Court Forebay (ft), and

$Q_{total} =$ total Clifton Court gates inflow (cfs).

The Clifton Court inflow equations are discussed in detail in Chapter 12 of *Methodology for Flow and Salinity Estimates in the Sacramento-San Joaquin Delta and Suisun Marsh* (DWR, 2004).

4.5 DELTA ISLAND CONSUMPTIVE USE

DICU values were applied on a monthly average basis and were derived from monthly DSM2 input values. Net monthly average DICU flows are plotted in Figure 4-4.

To appropriately distribute DICU flows in the model, RMA developed a utility program to match nodes in DSM2 to elements in the RMA model using UTM coordinates. This program was used to specify the RMA2 element inflows and withdrawals for each month, and salinity loadings from the agricultural returns. DICU flows incorporate channel depletions, infiltration, evaporation, and precipitation, as well as Delta island agricultural use. Table 4-1 summarizes the total monthly diversions (incorporates agricultural use, evaporation and precipitation), drains (agricultural returns), seeps (channel depletions) and total flows used for DICU flows. Total flows are negative, meaning net withdrawal from the system. These flows are distributed to multiple elements throughout the Delta, as shown in Figure 4-5.

Table 4-1 Summary of monthly DICU flows in cfs.

Month	Diversions (-)	Drains (+)	Seeps (-)	Total(-)
April	2109.9	1121.8	1006.4	1994.5
May	3978.0	1710.4	973.4	3241.0
June	4850.2	1995.6	1006.4	3860.9
July	4943.0	2011.0	973.4	3905.4
August	2659.8	1265.9	973.4	2367.3
September	1231.2	848.4	1006.2	1389.1

4.6 CONTROL STRUCTURES

Permanent gates and temporary barriers represented in the model include the Delta Cross Channel, Old River near Tracy (DMC) barrier, Old River at Head barrier, Middle River barrier, Montezuma Slough salinity control gates, Grant Line Canal barrier, and Lawler buffer ditch culvert. Control structure locations are shown in Figure 4-6. The control structures are represented as follows.

- **Delta Cross** – a single operable gate 120' wide.
- **Old River near Tracy (DMC) temporary barrier** – six circular culverts with tide gates and a single weir. The culverts are 4' diameter and 56' long with a Manning's n value of 0.02 and invert elevation of -6' MSL. The weir is 75' wide with a crest elevation of 2' NGVD.
- **Old River at Head temporary barrier** –six circular culverts and a single weir. The culverts are 4' diameter and 56' long with a Manning's n value of 0.02 and invert elevation of -4' MSL. The weir is 200' wide with a crest elevation of 10' NGVD.
- **Middle River temporary barrier** – six circular culverts with tide gates and a single weir. The culverts are 4' diameter and 40' long with a Manning's n value of 0.02 and invert elevation of -4' MSL. The weir is 140' wide with a crest elevation of 1' NGVD.

- **Montezuma Slough salinity control gates** – three operable tide gates and a flashboard structure. The gates are each 36' wide and the flashboard is 66' wide. The flashboard structure is either in or out (no partial installation during this period).
- **Grant Line Canal temporary barrier** – six circular culverts with tide gates and a single weir. The culverts are 4' diameter and 40' long with a Manning's n value of 0.02 and invert elevation of -6.5' MSL. The weir is 125' wide with a crest elevation of 0.5' NGVD.
- **Lawler buffer ditch culvert** – a single circular culvert. The culvert is 2.8' diameter and 69' long with a Manning's n value of 0.024.
- **Rock Slough tide gate** – permanent tide gate.

The calibration period operation schedule for the Delta Cross Channel is detailed in Table 4-2. Temporary barrier operations are given in Table 4-3. The Montezuma Slough salinity control gate operation schedule is detailed in Table 4-4. The gate status "Closed" means no flow is passing through the Gate. "Open" means the gate is not affecting flow in the channel. "Operating" means the gate is affecting flow based on specified components (weirs, culverts or tide gates) and their associated parameters.

Gate and barrier operations data are provided by DWR and IEP.

Table 4-2 Delta Cross Channel gate operation schedule for the calibration period.

Date	Hour	Gate status
01Jan2002	0.00	Closed
24May2002	10.40	Operating
28May2002	10.40	Closed
31May2002	10.40	Operating
03Jun2002	20.28	Closed
04Jun2002	5.50	Operating
04Jun2002	20.50	Closed
05Jun2002	5.50	Operating
05Jun2002	20.50	Closed
06Jun2002	5.50	Operating
06Jun2002	20.50	Closed
07Jun2002	5.50	Operating
09Jun2002	23.50	Closed
10Jun2002	7.50	Operating
10Jun2002	23.50	Closed
11Jun2002	7.50	Operating
11Jun2002	23.50	Closed
12Jun2002	7.50	Operating
12Jun2002	23.50	Closed
13Jun2002	7.50	Operating
13Jun2002	23.50	Closed
14Jun2002	7.50	Operating
16Oct2002	8.50	Closed
19Oct2002	8.00	Operating

Table 4-3 Temporary barrier operations schedule for the calibration period.

Barrier	Spring Installation	Spring Removal	Fall Installation	Fall Removal
ROLD046	15Apr2002	–	–	29Nov2002
Old River at Head	15Apr2002	25May2002	04Oct2002	23Nov2002
RMID023	15Apr2002	–	–	21Nov2002
Grant Line Canal	07Jun2002* 16Jun2002**	–	–	25Nov2002

* flap gates tied open
** flap gates begin operating

Table 4-4 Montezuma Slough salinity control gate operation schedule for the calibration period.

Date	Gate Status	Flashboard Status
01Jan2002	Operating	In
17Jan2002	Open	In
06May2002	Open	Out
28Sep2002	Operating	In
31 Dec2002	Operating	In

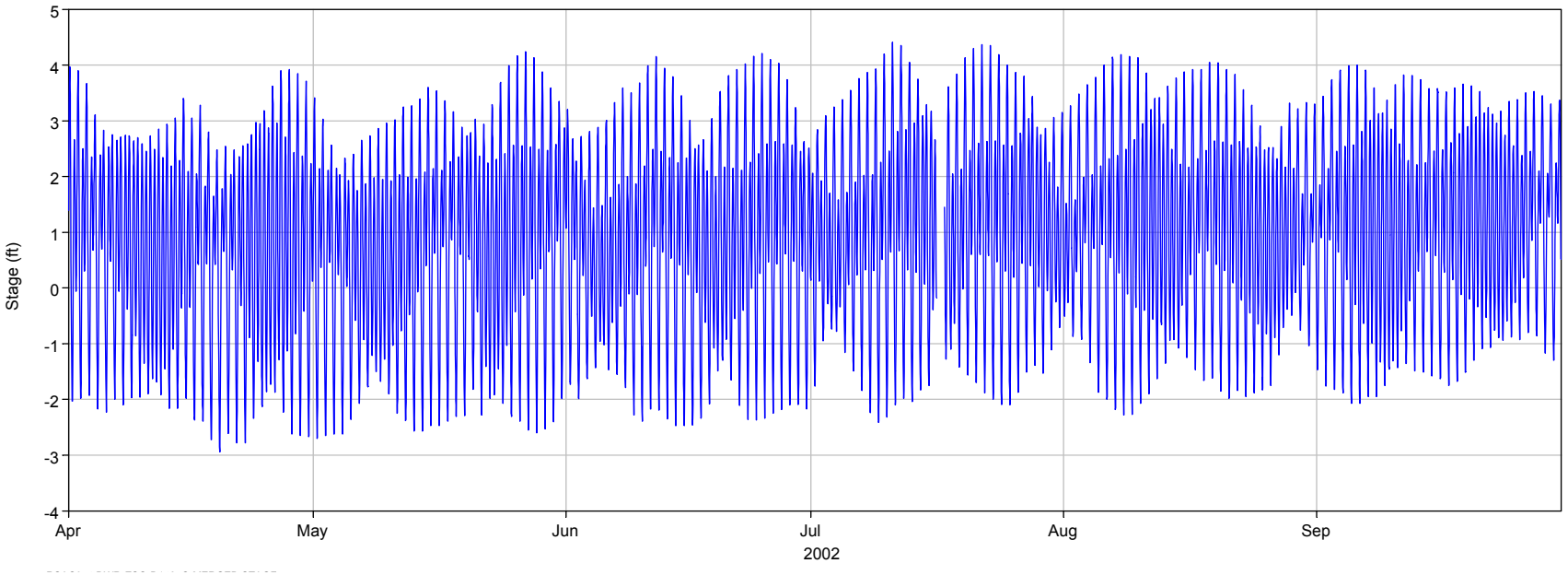

Figure 4-1 Calibration period stage at Martinez.

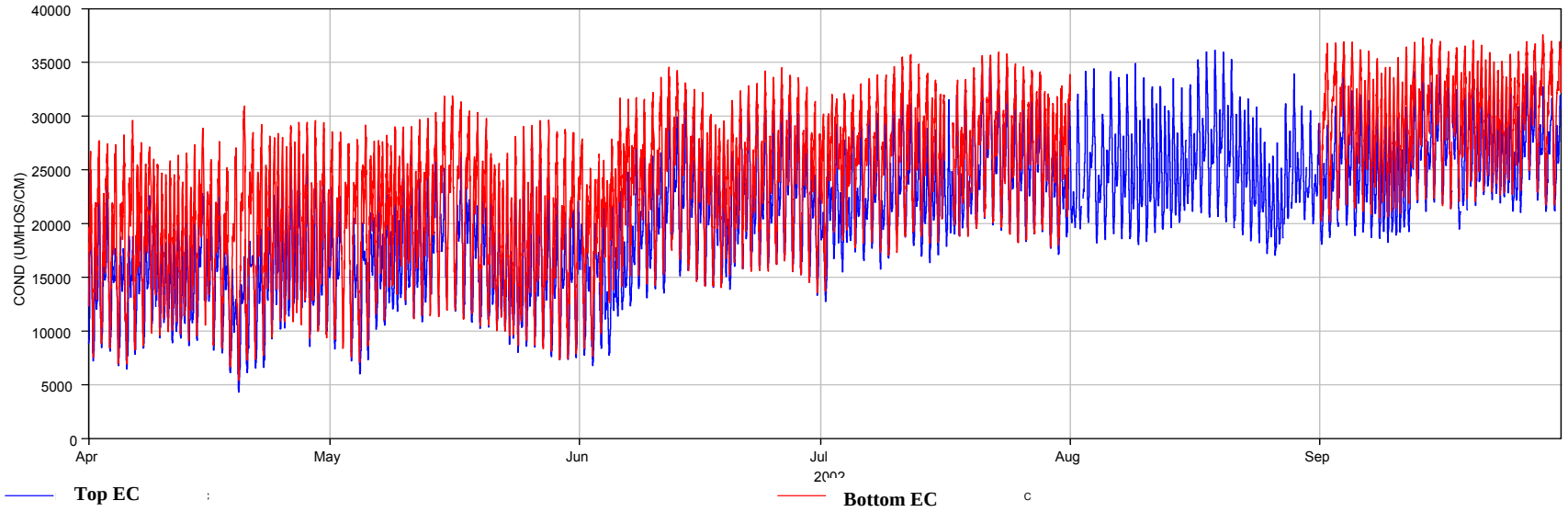

Figure 4-2 Top and bottom EC at Martinez during the calibration period.

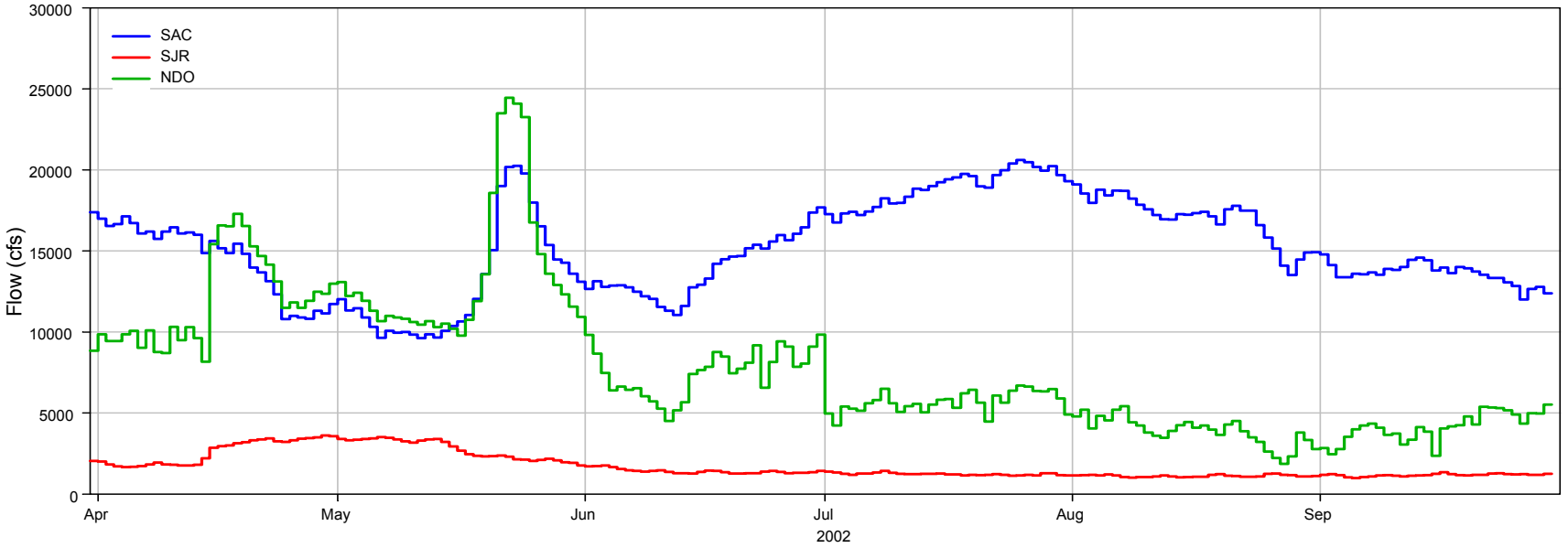

Figure 4-3 Calibration period river flows and Net Delta Outflow.

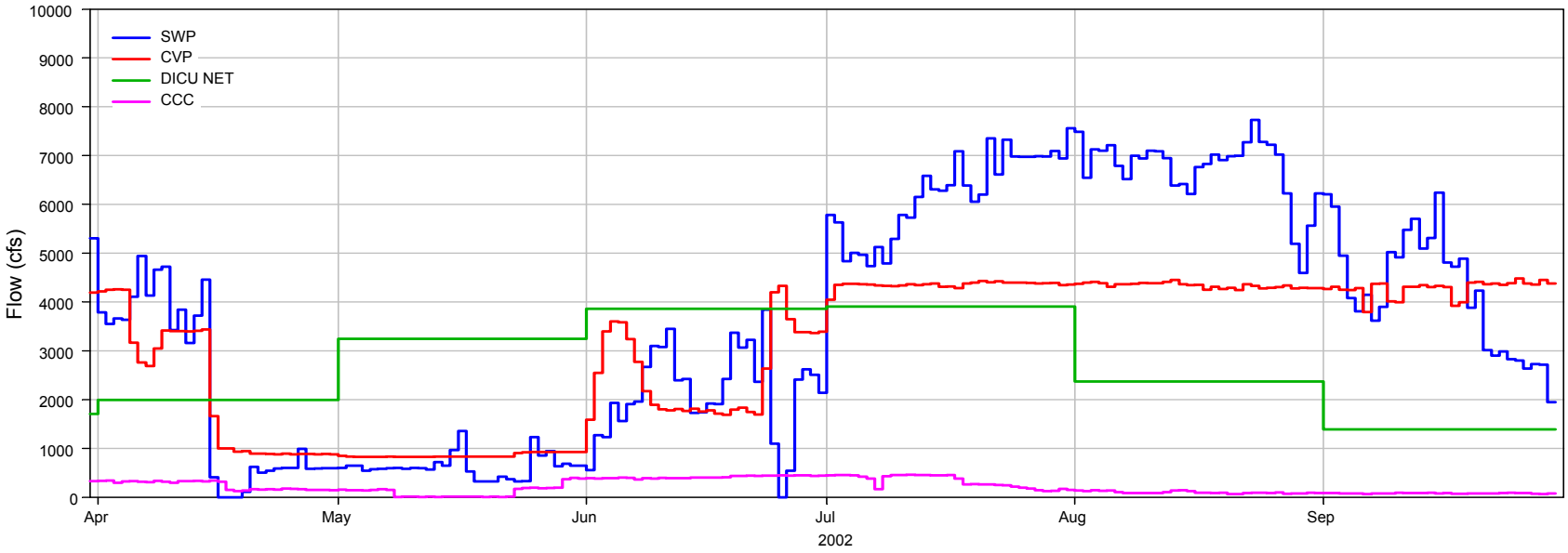

Figure 4-4 Calibration period exports and DICU flows.

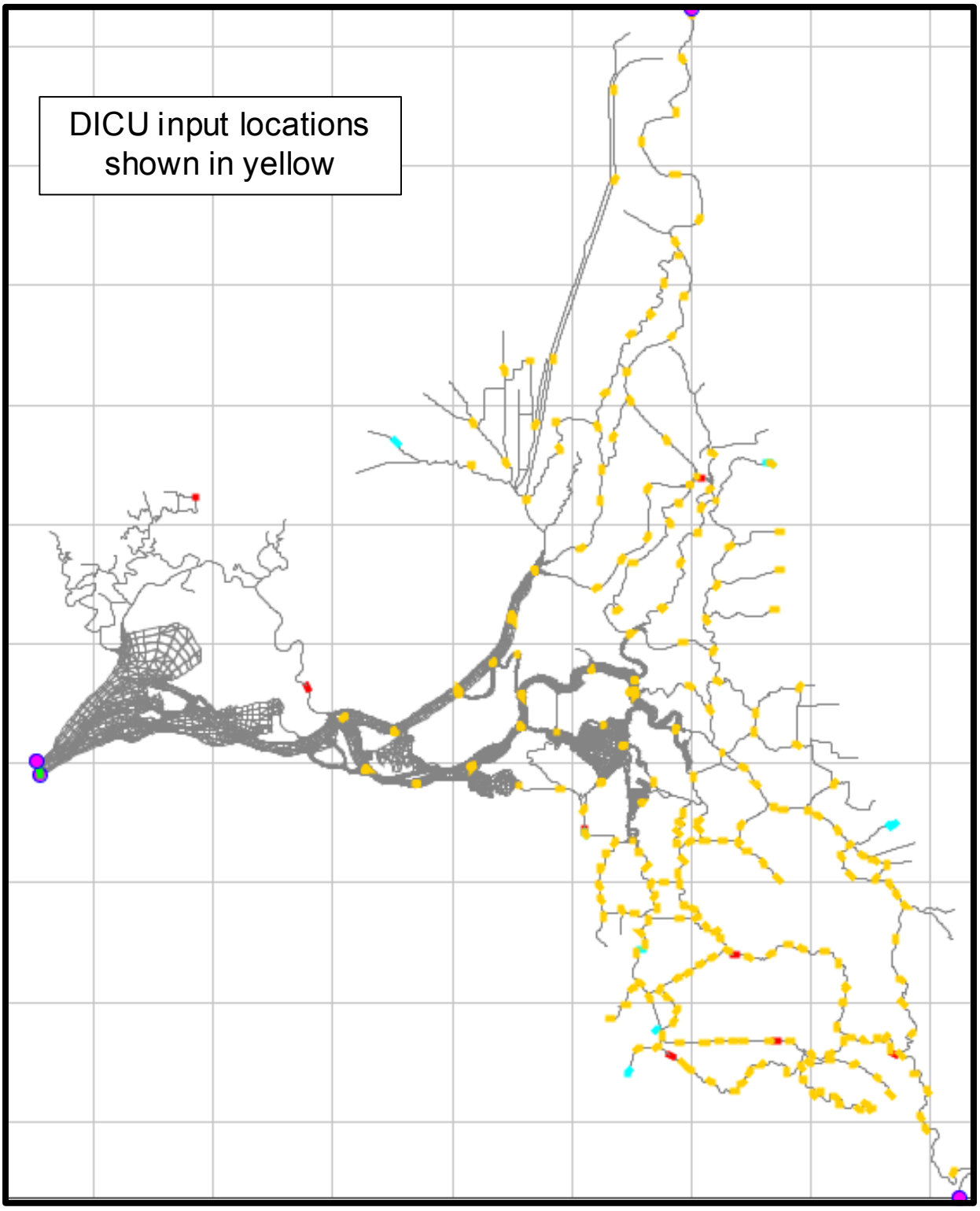

Figure 4-5 DICU input locations.

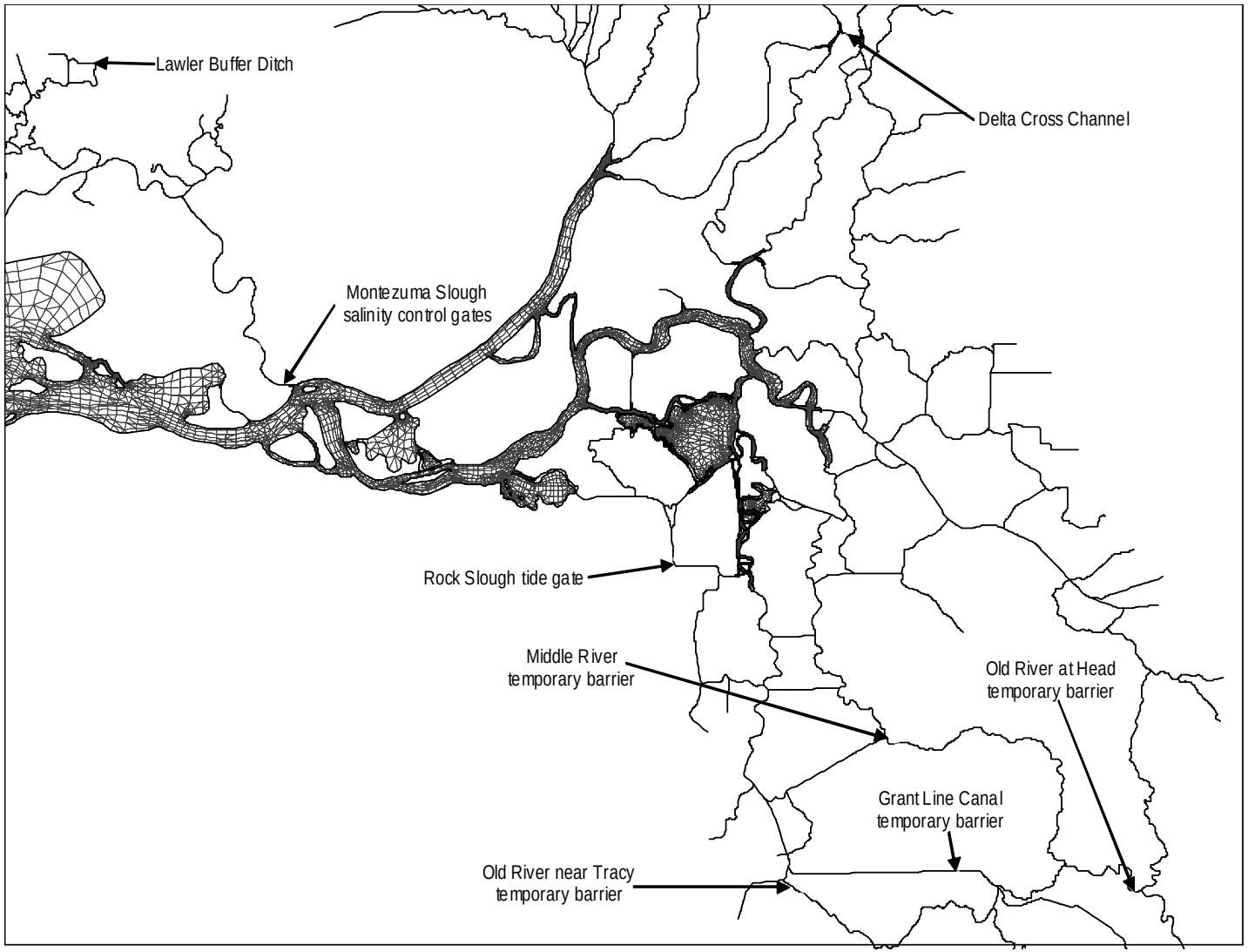

Figure 4-6 Control structure locations.

5 STAGE CALIBRATION

5.1 OVERVIEW

The tidal stage boundary condition is applied at Martinez. An important measure of performance of the model is how well the tidal signal is propagated upstream through the Delta considering phase, amplitude, and absolute stage. Propagation of the tidal signal is principally influenced by channel geometry, bed friction, and the operation of flow control structures. An excellent match between computed and observed stage has been achieved throughout the Delta with regard to amplitude and phase. Agencies collecting stage data in the Delta have not yet fully reconciled the datum at all stations, which makes calibration to absolute stage height problematic. In general the model matches reported absolute stage within 0.05 to 0.25 feet, while at a few station the difference is as large as 0.5 to 0.7 ft. Performing coupled hydrodynamic and salinity simulation helped to improve the stage calibration overall in the Delta. Further effort calibrating for absolute stage is not warranted until uncertainties in the individual station datums have been resolved.

5.2 MONITORING STATIONS

Stage is calibrated to data collected at the monitoring stations shown in Figure 5-1 including San Andreas Landing, Jersey Point, Old River near Highway 4, Middle River at Bacon Island, and Grant Line Canal.

5.3 COMPUTED AND OBSERVED STAGE PLOTS

The quality of fit between computed model results and observed data in a tidally driven system is typically presented in the form of time series plots of dynamic and tidally averaged values. In addition to this visual representation, statistics can be derived to quantify the differences between computed and observed tidal signals. Four types of statistics have been selected for presentation in this report.

Mean	Comparison of simple mean value of the computed and observed time series.
Phase Shift	The average shift in time between the computed and observed tidal signals.
Amplitude Ratio	Comparison of the tidal range, which ideally would be equal to 1. This value is evaluated after removing the phase shift between the computed and observed time series.
Scatter	The remaining difference between computed and observe tidal signals after phase and amplitude errors are removed. The better the model is at reproducing detailed variation of the observed tidal signal, the smaller the scatter will be. One measure of the scatter is the goodness of fit parameter, R2, from a linear regression performed on the observed and computed time series with phase error removed.

For each stage station shown in Figure 5-1, three plots of computed and observed stage are provided: dynamic and tidally averaged time series plots, and a scatter plot of computed versus observed data with linear regression statistics. Results are plotted at the tidal time-scale for a one-month period from June 20 through July 20, 2002. Tidally averaged stage is plotted from May 1 through August 31, 2003. The scatter plot also shows data from the period of May 1, through August 31, 2002.

The scatter plot is produced by first running a cross-correlation between the observed data and model results to find the average phase lag over the entire record. The phase lag is removed from the computed record before creating the scatter plot and performing a linear regression analysis to find the best fit slope and offset. Details of the cross-correlation procedure are detailed in Appendix B. The statistics reported with the scatter plot include the following.

Mean Observed (ft)	Average value of observed stage from May 1 to August 31.

Mean Computed (ft)	Average value of computed stage from May 1 to August 31. The difference between mean observed and mean computed approximates the overall shift in absolute stage.
Lag (minutes)	Phase difference between observed and computed. A positive value indicates that the computed record lags behind the observed record.
Y = slope*X + offset (ft)	Best linear fit where Y is computed and X is observed. The slope value approximates the tidal amplitude ratio.
R2	Linear regression goodness of fit parameter.

Small location plots are also provided with each set of plots for convenient reference.

5.4 DETAILED COMMENTS

Moving up the Sacramento River to Rio Vista (Figure 5-2) and above the Delta Cross Channel (Figure 5-3) the model propagates the tidal signal slightly faster (9 minutes) than the observed data indicates. The modeled tidal amplitude is about 4% low at Rio Vista and about 8% too large above the Cross Channel. The absolute stage is less than observed by 0.2 to 0.3 ft. Overall, the match is very good with R2 of 0.98 or greater at both stations.

Moving up the San Joaquin River to Jersey Point (Figure 5-4), San Andreas Landing (Figure 5-5), and into the Mokelumne River (Figure 5-6), the phase and amplitude match is excellent. The model phase leads the observed data by about 2 minutes and the tidal amplitude is within 2%. R2 ranges from 0.976 to 0.99. The absolute stage match at Jersey Point is off by 0.7 ft (the largest difference at any station) while the match at San Andreas Landing is within 0.1 ft. This is almost certainly due to a datum error. Given the overall comparison between computed and observed stage, the datum error is most likely in the Jersey Point stage data.

Farther up the San Joaquin at Rindge Pump and at Stockton (Figures 5-7 and 5-8) the model phase lags the slightly (4 minutes) and the amplitude error increases to 5.6%. This is still an excellent overall match with R2 values of 0.98 at both stations. The

average model stage is low at these stations by approximately 0.45 ft. The calibration at these stations will be revisited when new station datums are available.

The stage comparison is excellent at all three stations on Old River west of the south Delta barriers (Figures 5-9 to 5-11). Lag is 4 minutes or less, tidal amplitude is within approximately 2%, average absolute stage is within 0.2 ft. The R2 for these stations is 0.976 and greater.

Matching stage precisely is more difficult in the interior of the south Delta due to the presence of the south Delta barriers. Phase lag is estimated to be from 15 to 24 minutes at Middle River near Bacon Island, Grant Line Canal, and Old River at Head (Figures 5-12 to 5-14). For the Middle River station, examination of the observed data records indicate the times may have been shifted 15 minutes, and may largely account for the apparent phase error. The tidal amplitude is within 1%, 5%, and 14% at Grant Line Canal, Middle River, and Old River at Head, respectively. R2 values range from 0.98 at Middle River to 0.93 for Old River at Head. Absolute stage at Grant Line Canal and Middle River are within 0.2 ft of observed. The average model stage at Old River at Head is almost 0.7 ft below the observed record. This difference may be a combination of a datum error and the model under-predicting the stage in the San Joaquin River near Stockton. This and the over-prediction of the tidal amplitude for this location may indicate the need to increase friction in the San Joaquin River or adjust some of the south Delta barriers.

5.5 TIDAL ANALYSIS OF OBSERVED AND COMPUTED STAGE

Another method for evaluating the dynamics of the computed and observed stage is through tidal analysis. The tidal constituents for observed and computed stage were analyzed using the "Tidal Heights Analysis Computer Program" developed by Foreman (1977). The program uses a least-squares method of analysis to evaluate the amplitude and phase of the standard set of tidal constituents. Differences in model and observed amplitude and phase for the primary semi-diurnal (M2) and diurnal (K1) tidal constituents are presented in Table 5-1 for a number of Delta stage stations. For comparison, the table also lists the computed/observed amplitude ratio and the

computed/observed phase difference as determined from the cross-correlation analysis. The time of analysis was a 28-day period from July 7 to August 4, 2002. This is a shorter analysis period than used in section 5.4, so the mean values and cross-correlation statistics will vary somewhat from the values presented in the earlier section.

Table 5-1 shows that the computed/observed amplitude ratio and phase lag are fairly similar for M2 and cross-correlation. Comparison of the K1 and M2 amplitudes indicate the K1 tidal constituent is a significant component of the Delta tidal stage. The analysis shows the computed/observed amplitude ratio for M2 stage is usually near 1.0 while the K1 amplitude ratio is always higher, and that there is a greater lag in the computed K1 tidal phase vs. the computed M2 tidal phase.

Overall, the computed stage reproduces observed stage in the central Delta in terms of amplitude and phase. The one exception is the -17 minute phase lag at the RMID015 station. Examination of the observed data records indicate the times may have been shifted 15 minutes, and may largely account for the apparent phase error. The computed tide slightly lags the observed record further into the south Delta (ROLD034 and CHGRL009), while the computed tidal signal is too fast for the Sacramento River near the Delta Cross Channel. Differences in mean computed and observed stage vary from station to station. Efforts are underway to better establish exact elevation datums for the Delta water surface gage stations. On average, the computed mean stage under-predicts the observed Delta mean stage.

Table 5-1 Computed and observed stage and tidal analysis statistics summary for the period of July 7 to August 4, 2002.

Location	Mean Obs Stage (ft)	Mean Comp. Stage (ft)	Cross-correlation		Tidal Analysis					
			Amp Ratio	Phase Lag (min)	Obs Amp M2 9ft)	Amp Ratio M2	Phase Lag M2 (min)	Obs Amp K1 (ft)	Amp Ratio K1	Phase Lag K1 (min)
RSAN018 - Jersey Point	2.47	1.75	1.02	1	0.93	0.99	1	0.82	1.06	7
RSAN032 - San Andreas Landing	1.81	1.79	1.02	0	0.92	1.00	0	0.81	1.08	5
RSAN063 - SJR at Stockton	2.16	1.80	1.06	4	1.08	1.05	3	0.79	1.13	7
ROLD024 - Old River at Bacon Is	1.90	1.72	1.04	-4	0.99	1.02	-4	0.81	1.10	0
ROLD034 - Old River nr HWY 4	1.34	1.34	1.04	-2	0.92	0.99	-1	0.77	1.13	2
RMID015 - Middle Rvr at Bacon Is	1.56	1.70	1.05	-17	1.01	1.04	-17	0.82	1.10	-13
CHGRL009 - Grant Line Canal DS	1.17	0.88	1.01	7	0.80	0.96	14	0.69	1.18	7
RSAC101 - Sac R at Rio Vista	2.27	1.86	0.96	8	1.17	0.93	8	0.92	1.01	14
RSAC128 - Sac River above DXC	2.46	2.38	1.09	-12	0.73	1.10	-11	0.67	1.14	-12

Table Notes

Amp Ratio: Computed/Observed amplitude ratio

Phase Lag: Positive value indicates Computed stage lags Observed stage

ID Code	Name
CHGRL009	Grant Line Canal DS
RMID015	Middle R at Bacon Is
RMID023	Middle R nr Hwy 4
ROLD024	Old River at Bacon Is
ROLD034	Old River nr Hwy 4
ROLD046	Old R DS of DMC Barrier
ROLD074	Old River at Head
RSAC101	Rio Vista
RSAC128	Sac River above DXC
RSAN018	Jersey Pt
RSAN032	San Andreas Landing
RSAN052	SJR at Rindge Pump
RSAN063	SJR at Stockton
SLGE019	Georgiana Slough
SLTRM004	Three Mile Slough

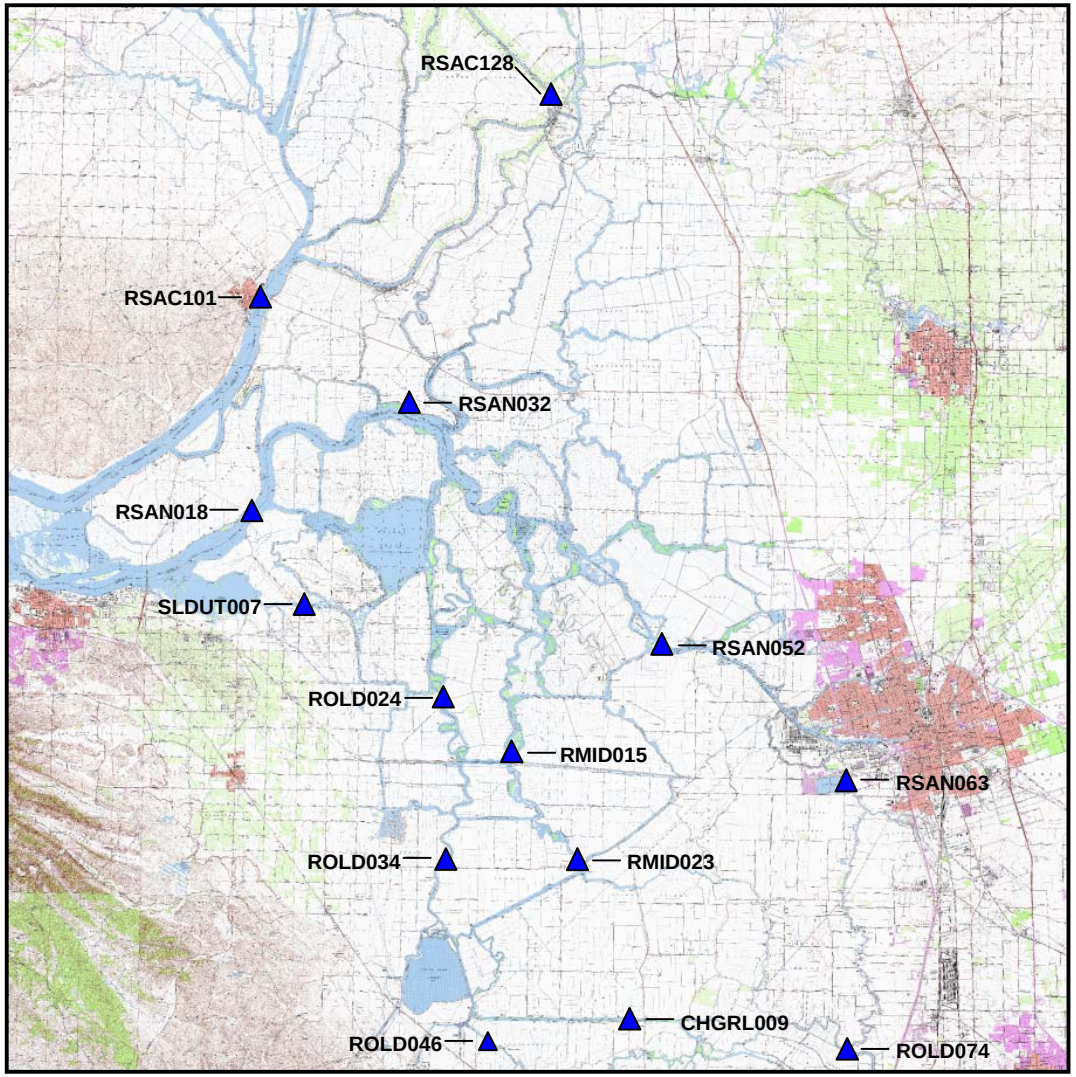

Figure 5-1 Stage monitoring stations.

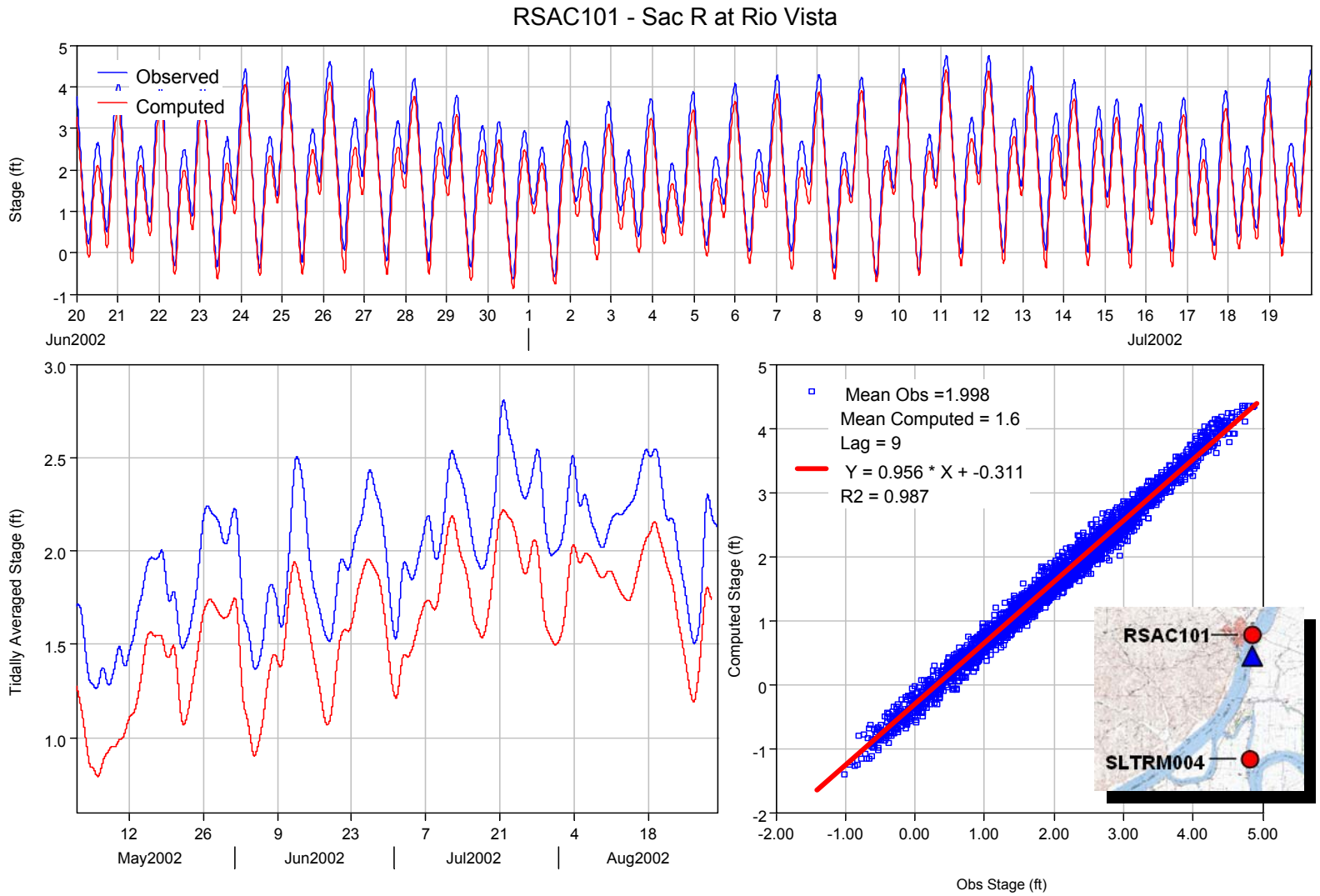

Figure 5-2 Computed and observed stage in Sacramento River at Rio Vista.

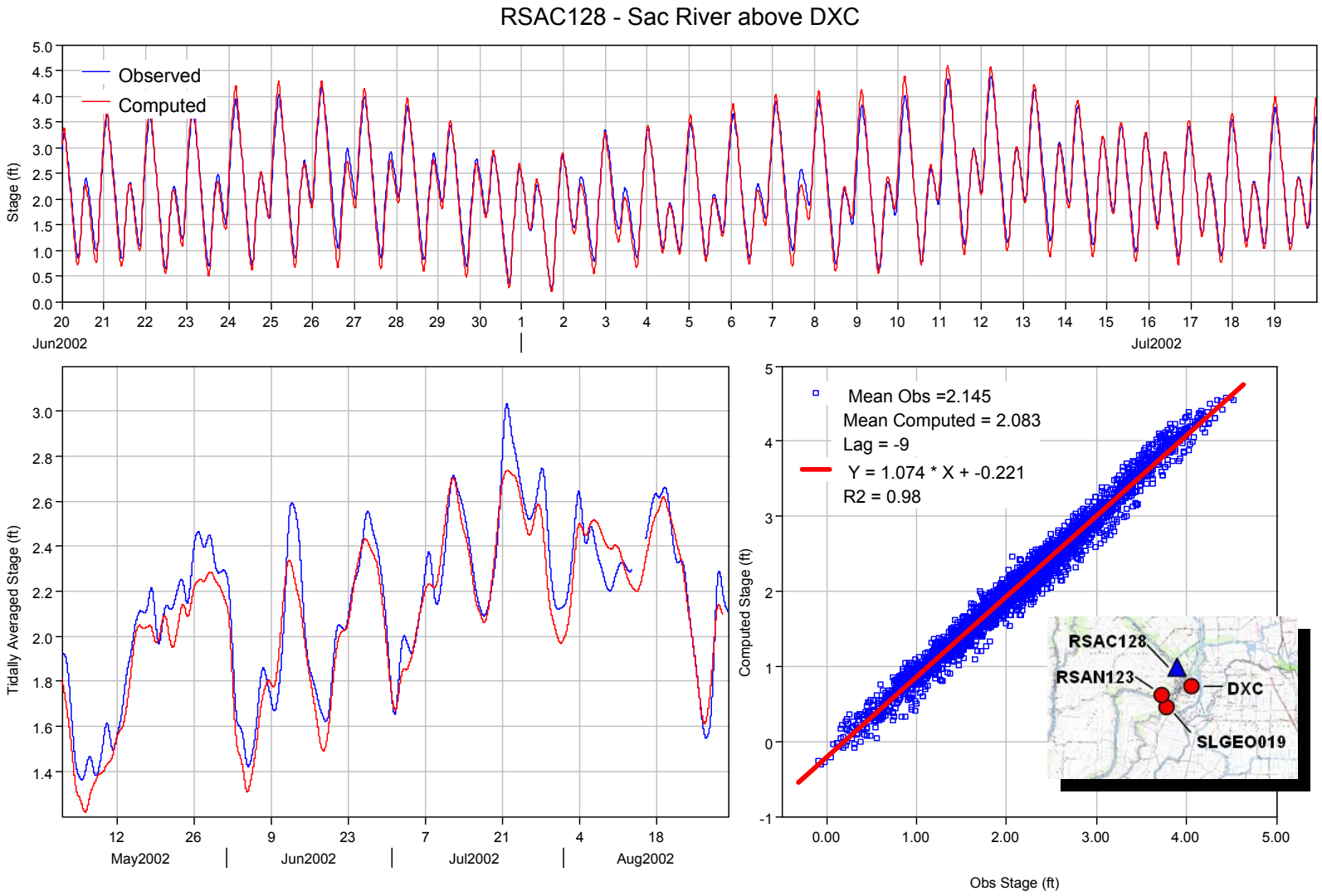

Figure 5-3 Computed and observed stage in Sacramento River above DXC.

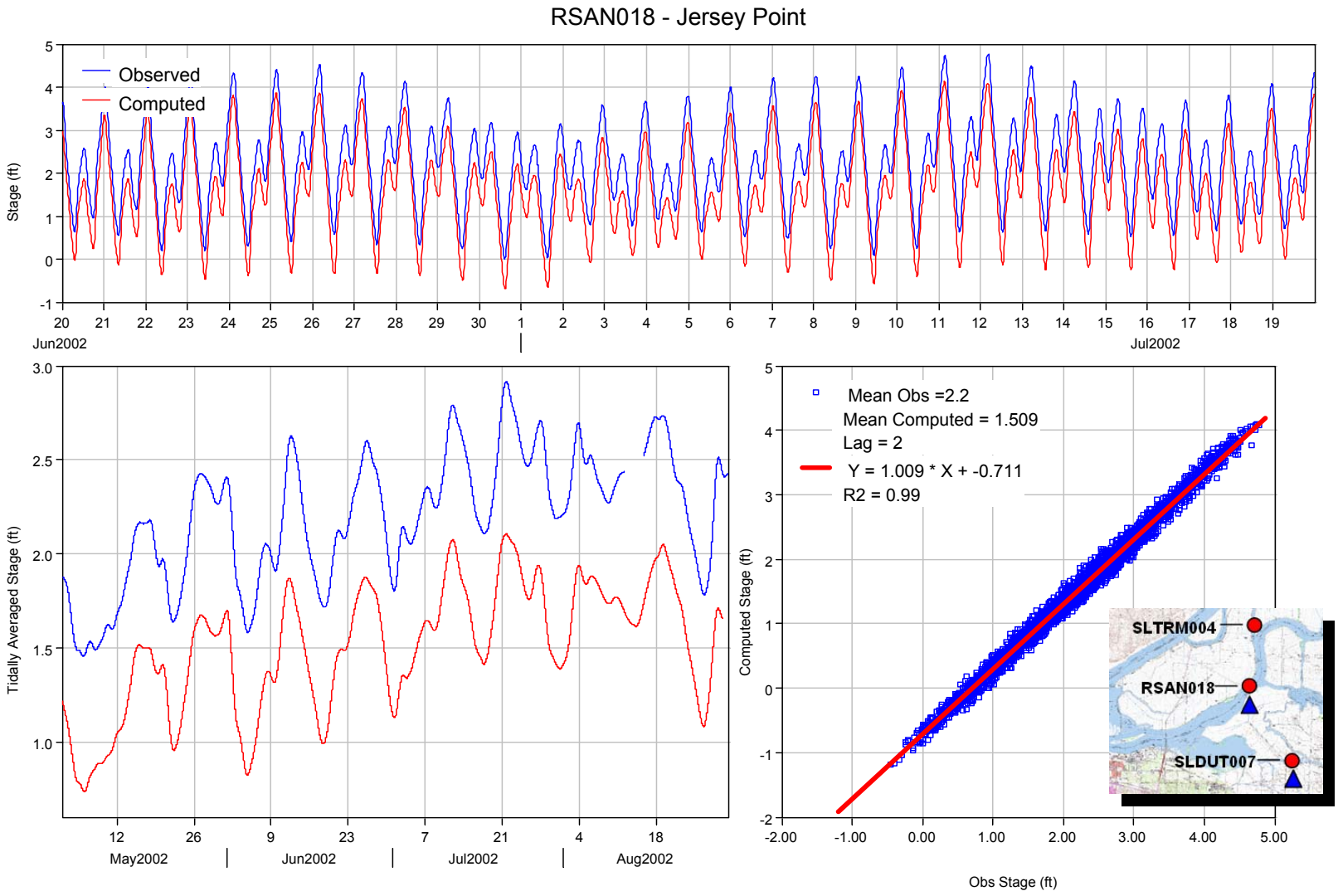

Figure 5-4 Computed and observed stage at Jersey Point.

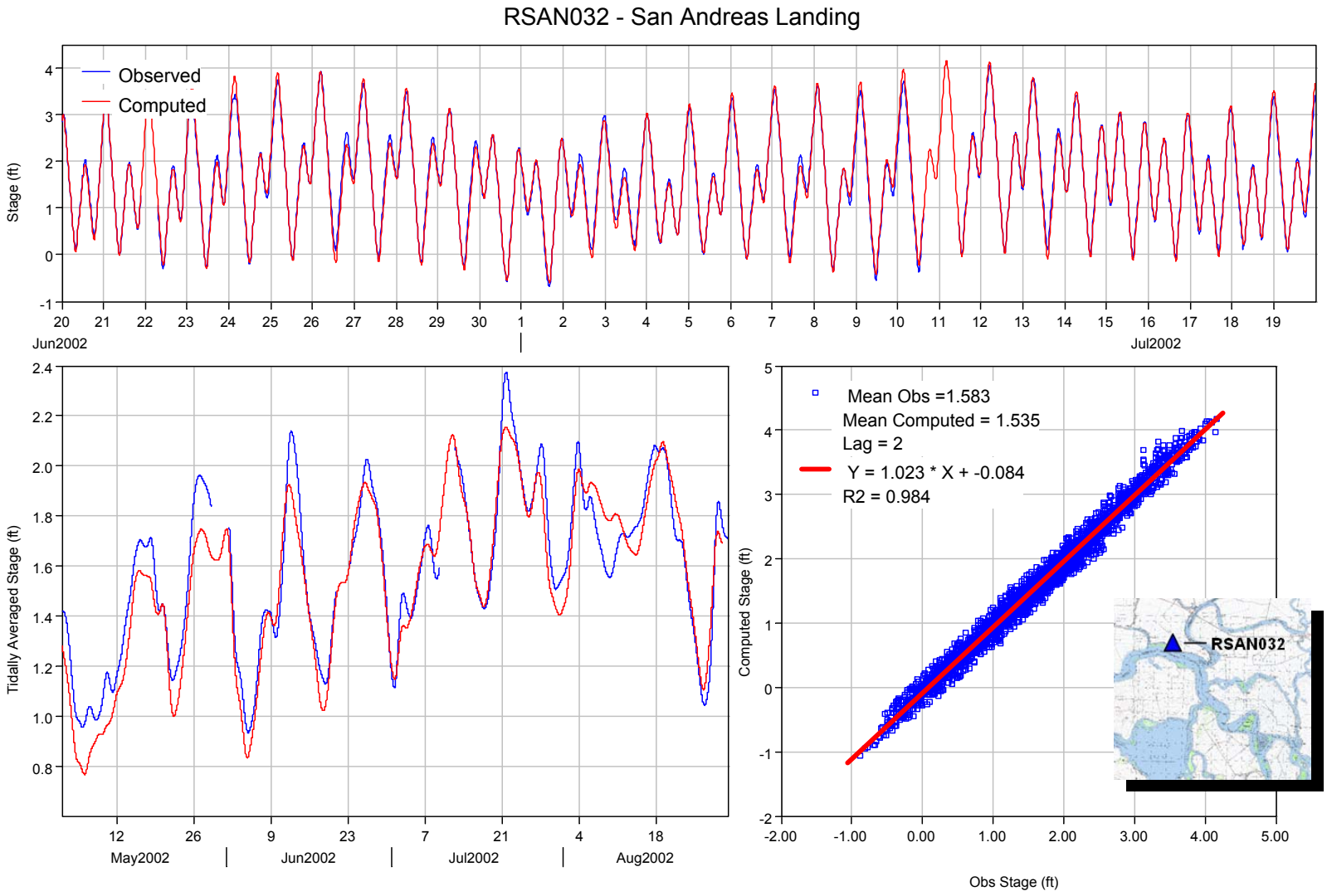

Figure 5-5 Computed and observed stage at San Andreas Landing

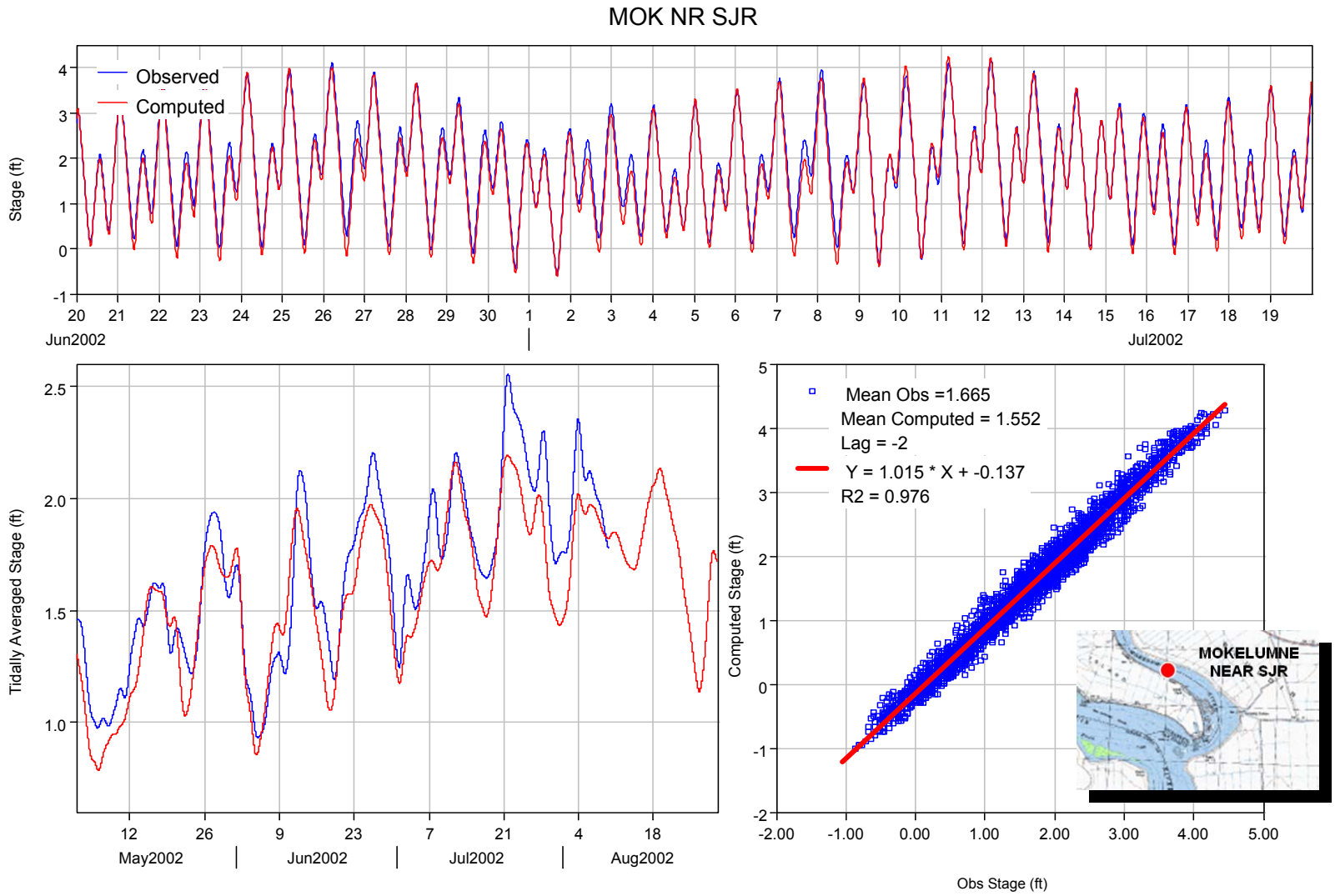

Figure 5-6 Computed and observed stage in Mokelumne River near San Joaquin River.

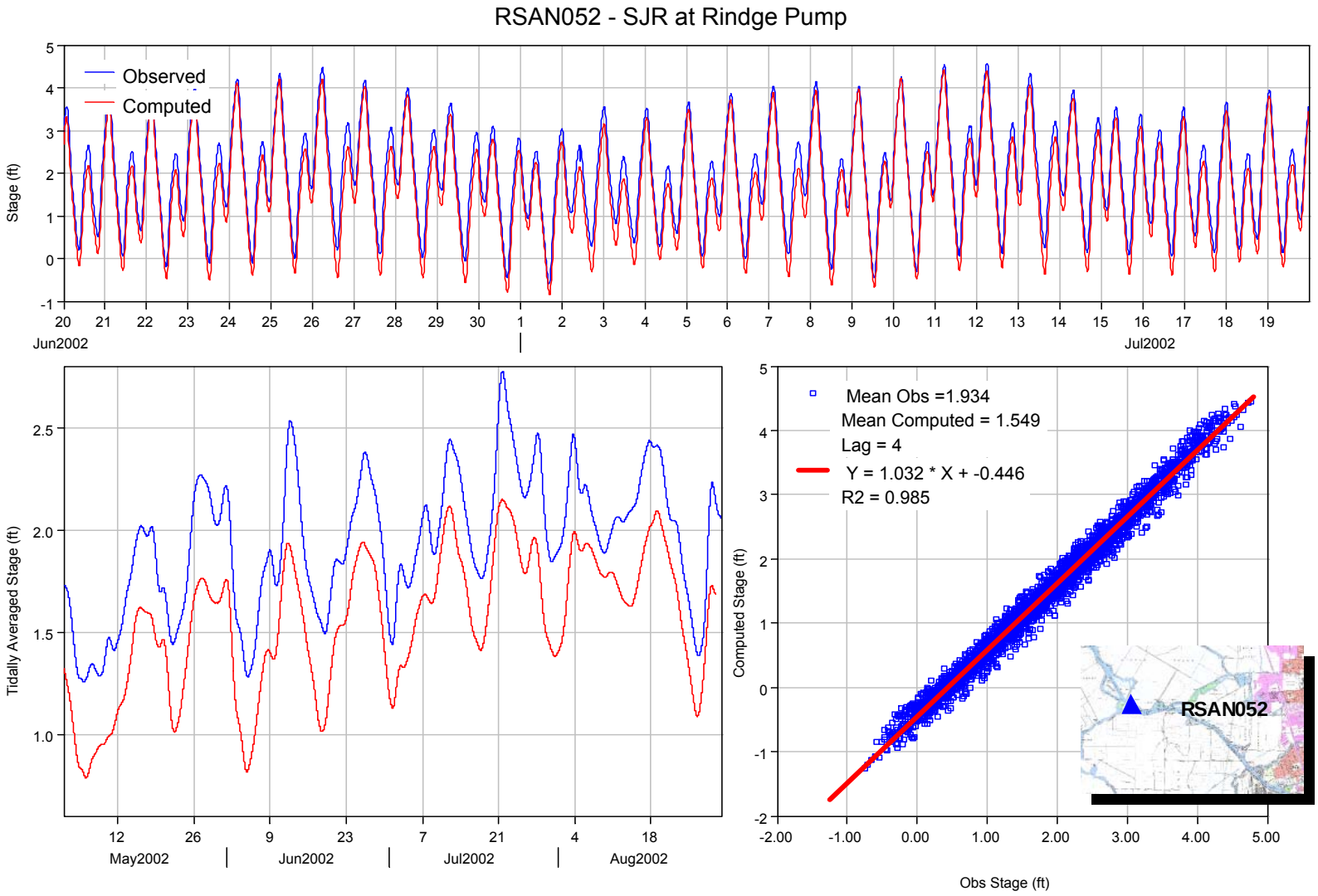

Figure 5-7 Computed and observed stage in San Joaquin River at Rindge Pump.

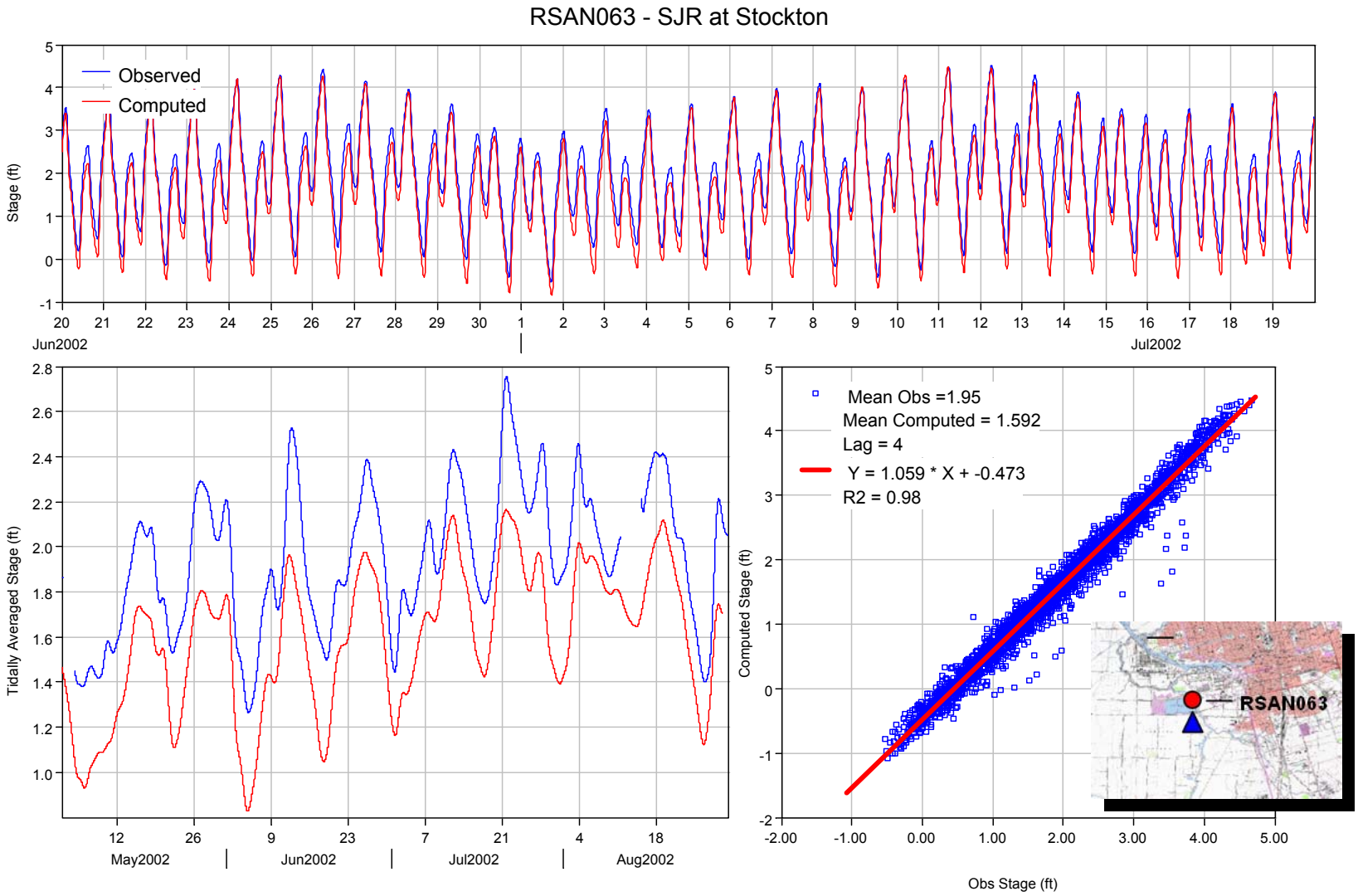

Figure 5-8 Computed and observed stage in San Joaquin River at Stockton.

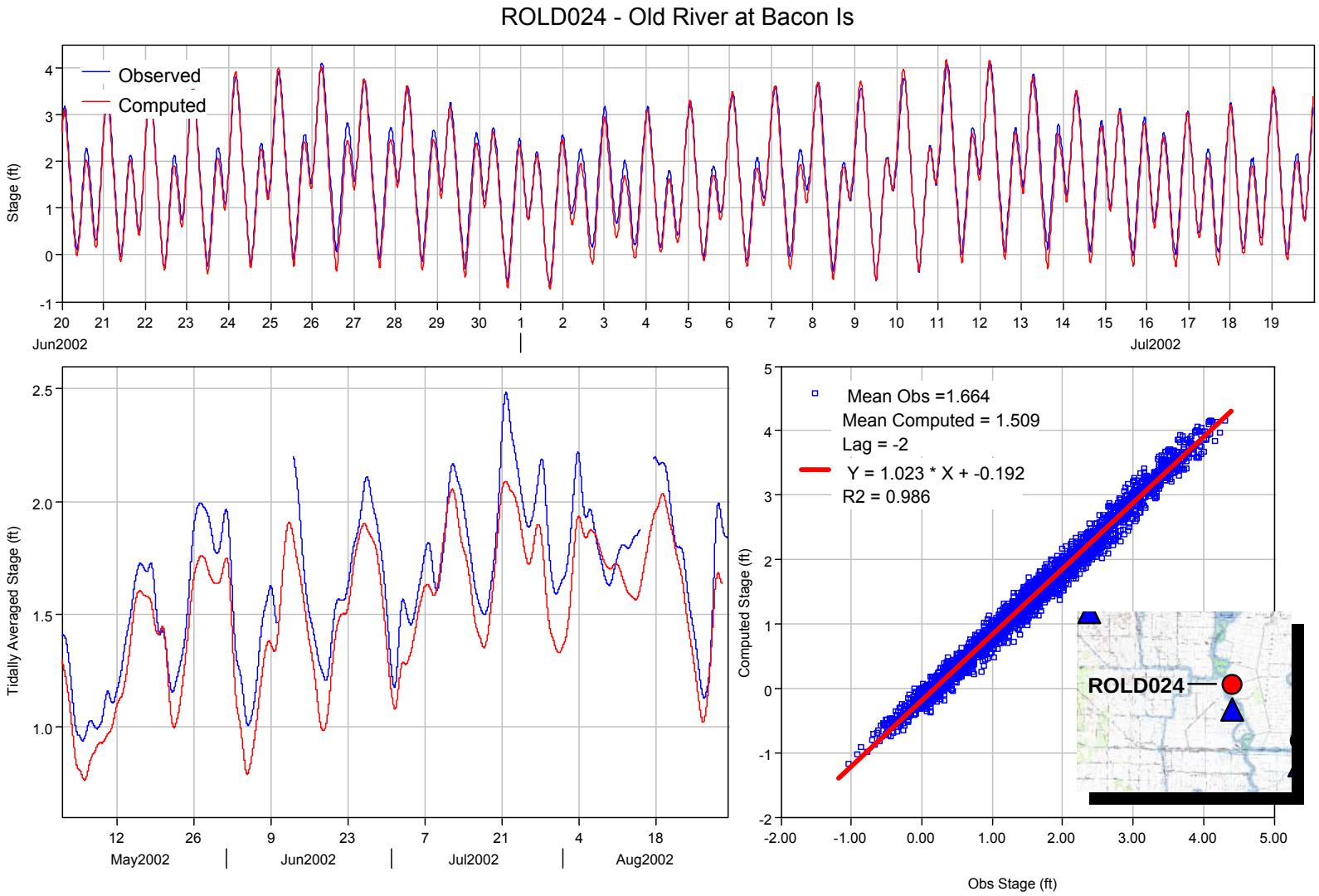

Figure 5-9 Computed and observed stage in Old River at Bacon Island.

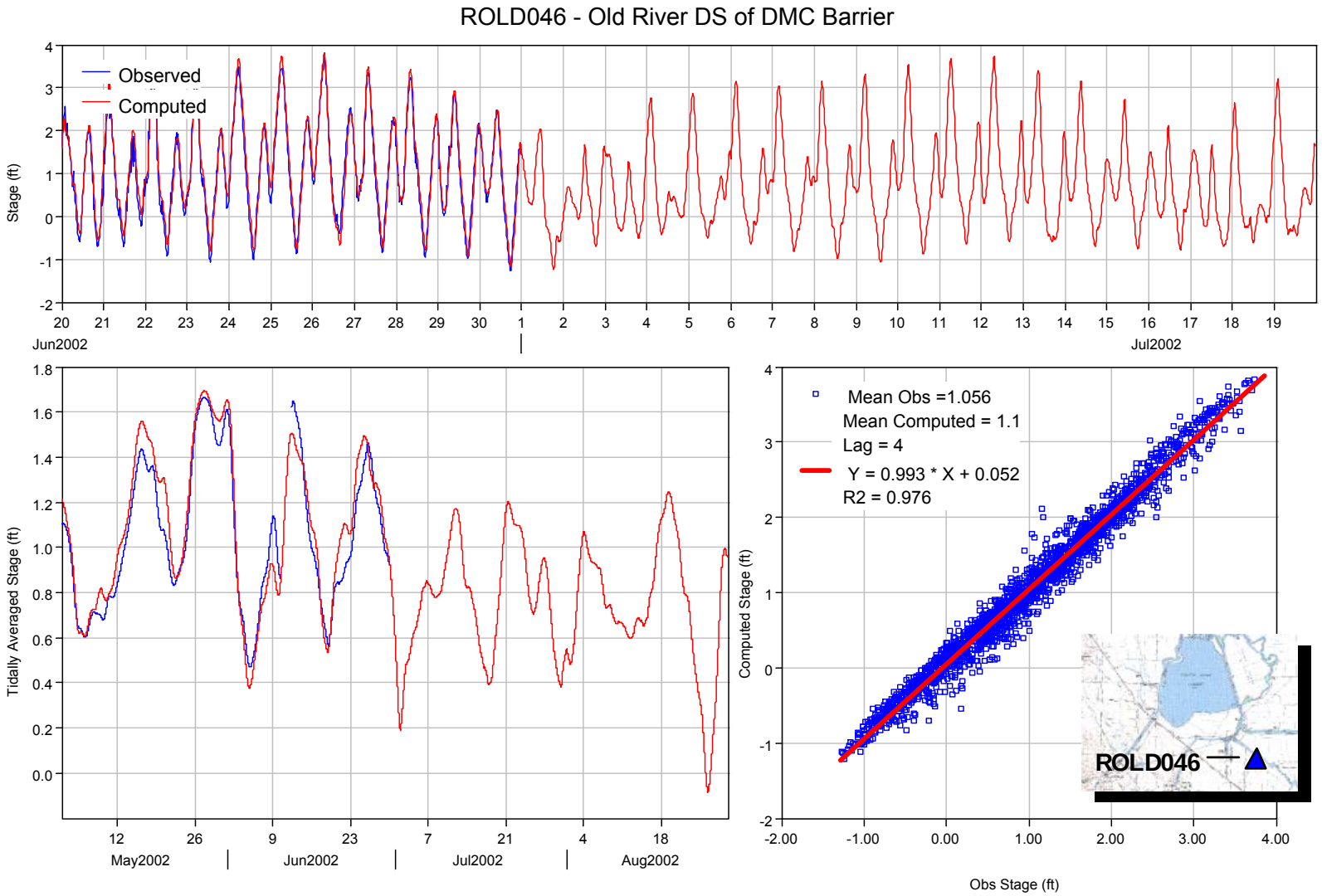

Figure 5-10 Computed and observed stage in Old River downstream of DMC Barrier.

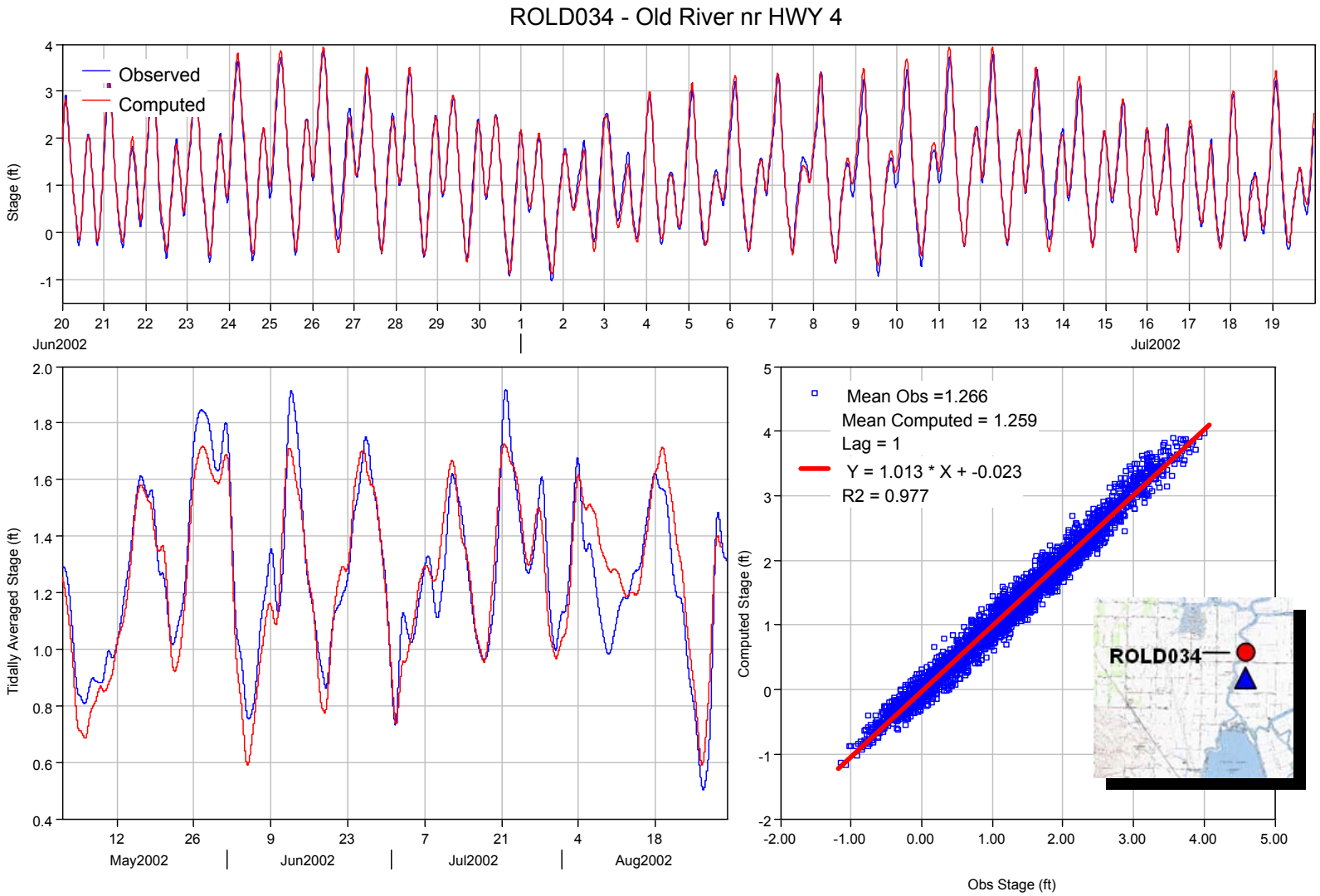

Figure 5-11 Computed and observed stage at ROLD034 - Old River near Highway 4.

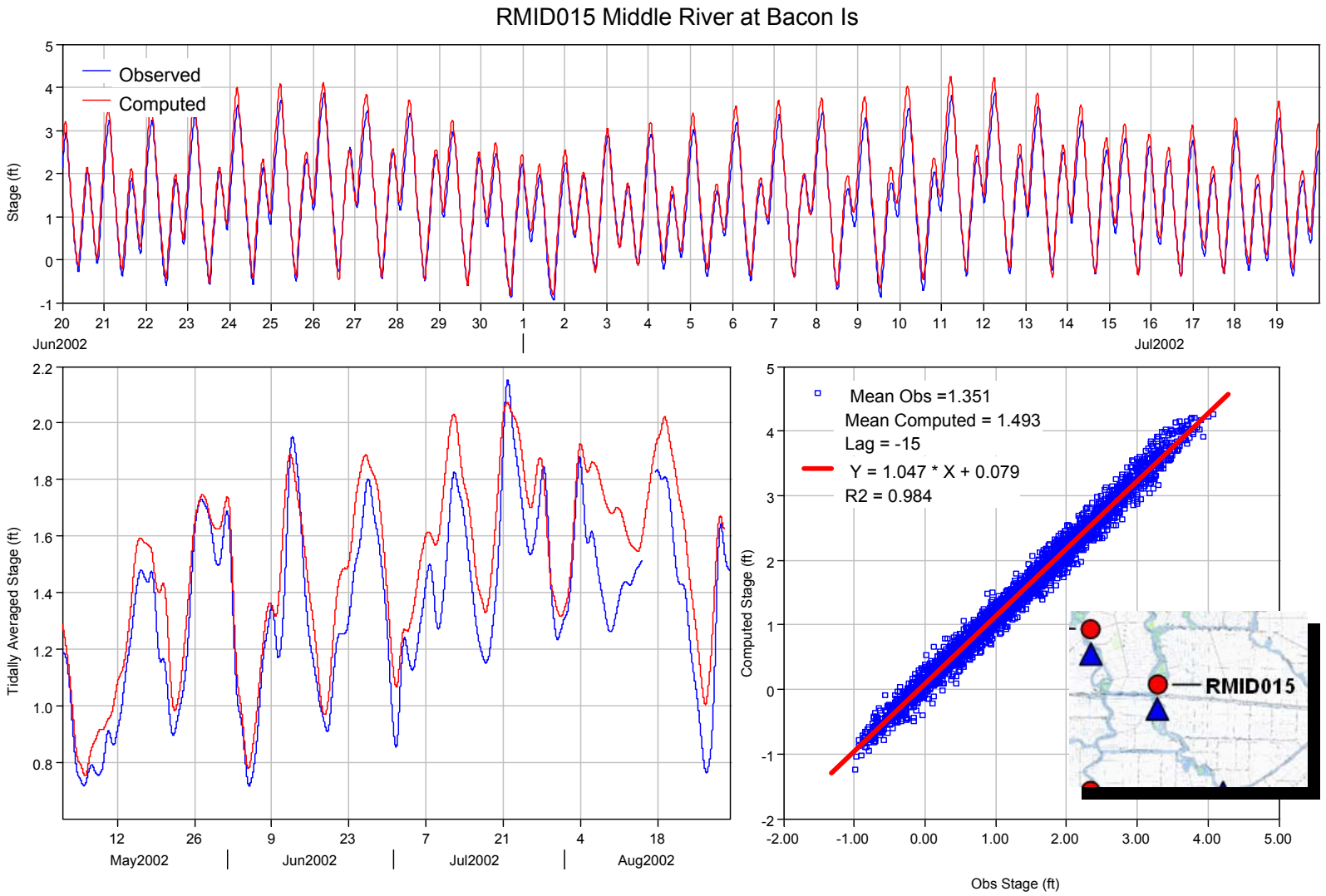

Figure 5-12 Computed and observed stage at RMID015 - Middle River at Bacon Island.

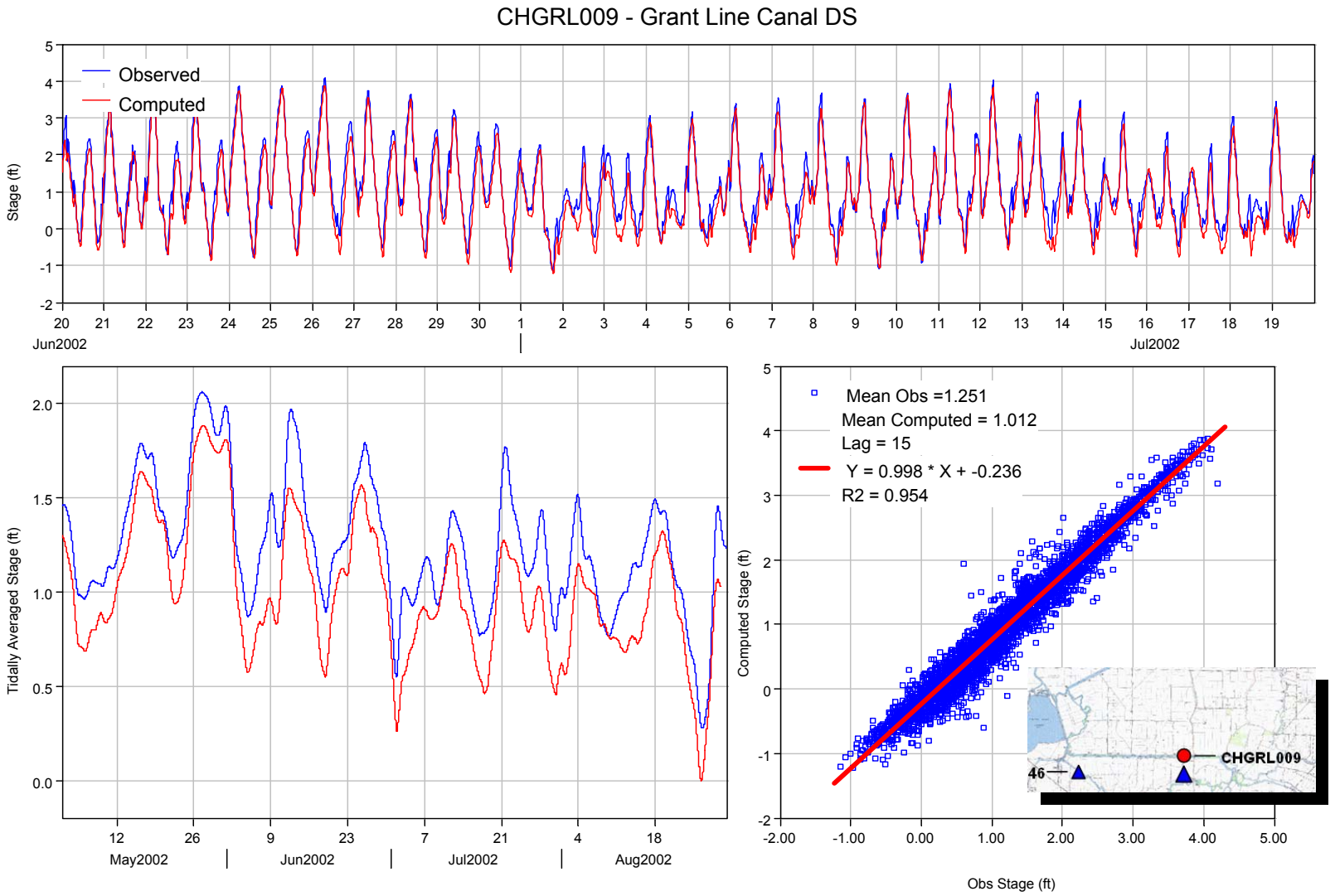

Figure 5-13 Computed and observed stage at CHGRL009 - downstream Grant Line Canal.

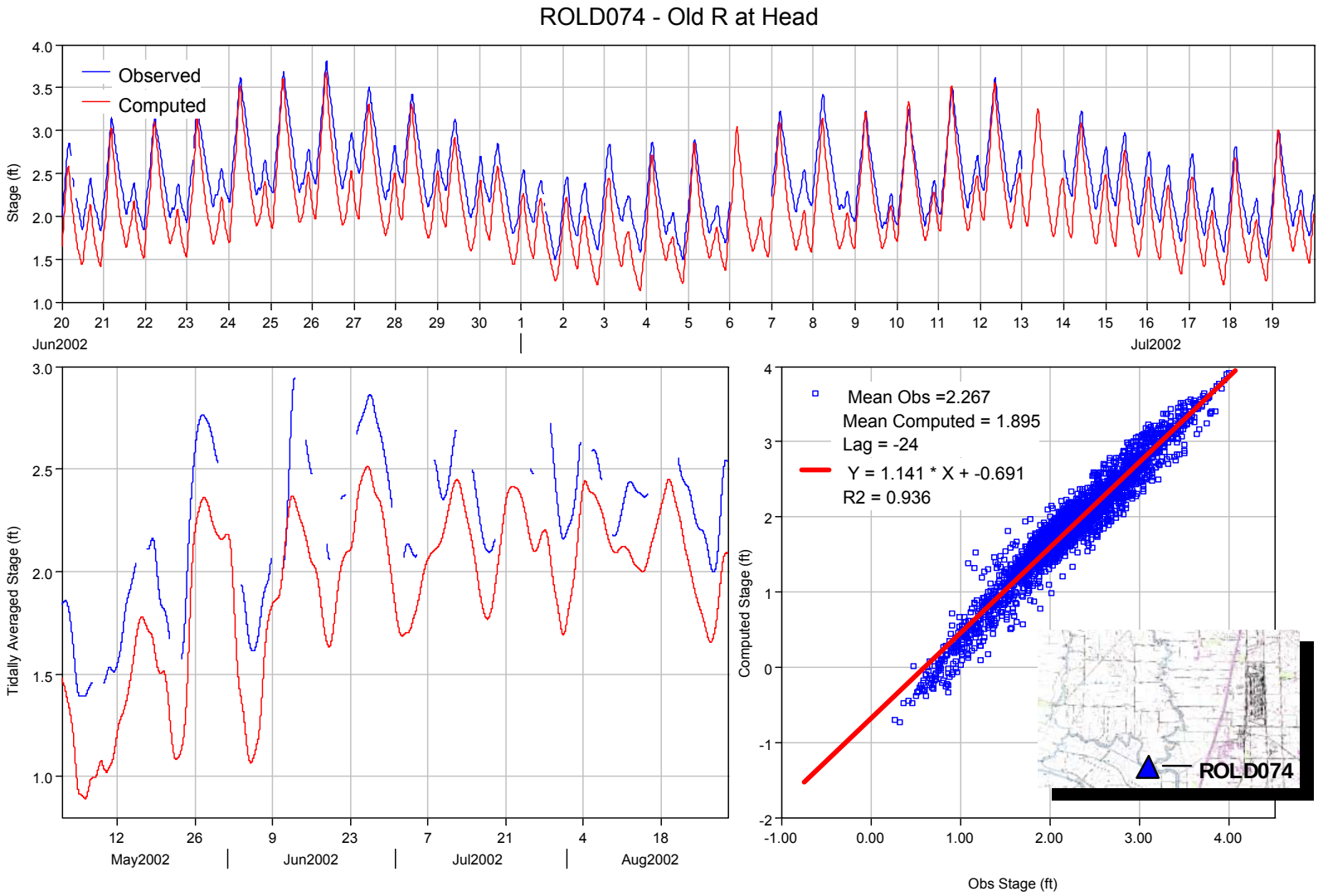

Figure 5-14 Computed and observed stage in Old River at Head.

6 FLOW CALIBRATION

6.1 OVERVIEW

Flow in the model is a function of the tidal flood and ebb driven by the rise and fall of the stage boundary at Martinez, boundary inflows such as the Sacramento River and San Joaquin Rivers, internal diversions and returns associated with Delta Island Consumptive Use, water exports, and control structure operations. The Delta is a tidally driven system and flows exhibit a sinusoidal pattern of ebb and flood similar to the rise and fall of the stage record. Thus the primary measure of the quality of calibration is how well the model reproduces the phasing and amplitude of flows measured on the tidal time scale at key channel cross sections. Also of critical interest is the tidally averaged flow, or net flow, as the net flow plays an important role in salt transport. Matching net flows is more difficult because the net flows are typically very small relative to the tidal flow at any given station. Net flow values derived from observed tidal flow also have a significant level of uncertainty for the same reason, especially in very large channels such as the Sacramento River at Rio Vista. Model parameters that influence flow calibration include channel geometry, tidal prism (channel volume above lower low water), bed friction coefficients, and momentum exchange coefficients (eddy viscosity). Flow calibration for the model is very good overall. Excellent results have been achieved in False River, San Joaquin River at Jersey Point and at the Old and Middle River UVM stations. Some improvement is still needed to match net flows in Fisherman's Cut, Old River between Franks Tract and the San Joaquin, Mokelumne River near the San Joaquin, the Delta Cross Channel, and in Three Mile Slough.

6.2 MONITORING STATIONS

Flow is calibrated to data collected at the monitoring stations shown in Figures 6-1 and 6-2 including, Jersey Point, False River, Fisherman's Cut, Three Mile Slough, Rio Vista, Sacramento River below the Delta Cross Channel, in the Delta Cross Channel, Georgiana Slough, Mokelumne River near the San Joaquin River, Old River near the San

Joaquin River, Holland Cut, Old River near Mandeville Island, Dutch Slough, Old River at Bacon Island, Old River near Highway 4, Middle River at Bacon Island, and San Joaquin River near Stockton.

6.3 COMPUTED AND OBSERVED FLOW PLOTS

For each flow station shown in Figure 6-1 and 6-2, three plots of computed and observed flow are provided: dynamic and tidally averaged (net flow) time series plots, and a scatter plot of computed versus observed data with linear regression statistics. Results are plotted at the tidal time-scale for a one-month period from June 23 through July 10, 2002. Tidally averaged flow is plotted from May 1 through August 31, 2003. The scatter plot also shows data from the period of May 1, through August 31, 2002. Positive flow is in the ebb (downstream) direction.

The scatter plot is produced by first running a cross-correlation between the observed data and model results to find the average phase lag over the entire record. The phase lag is removed from the computed record before creating the scatter plot and performing a linear regression analysis to find the best fit slope and offset. Details of the cross-correlation procedure are detailed in Appendix B. The statistics reported with the scatter plot include the following.

Mean Observed (cfs)	Average value of observed flow from May 1 to August 31.
Mean Computed (cfs)	Average value of computed flow from May 1 to August 31. The difference between the mean observed and mean computed provides an overall estimate of the error in net flow.
Lag (minutes)	Phase difference between observed and computed. A positive value indicates that the computed record lags behind the observed record.
Y = slope*X + offset (cfs)	Best linear fit where Y is computed and X is observed. The slope value approximates the variation in flow amplitude.
R2	Linear regression goodness of fit parameter.

Small location plots are also provided with each set of plots for convenient reference.

6.4 DETAILED COMMENTS

In the north Delta, flow from the Sacramento River splits into Steamboat Slough, then again into Georgiana Slough and the Cross Channel (Figures 6-3 to 6-5). Unlike most Delta channels, flows in the Sacramento River above the Cross Channel (Figure 6-6) and in Georgiana Slough near the Cross Channel show tidal variation but do not reverse directions during summer export period. Computed flows at these stations and in the Sacramento River below the Cross Channel (Figure 6-7) matched observed data very well, net flows are within a few percent. When the Cross Channel is open, the net flow through the Cross Channel is about 200 to 300 cfs lower than observed.

At Rio Vista on the Sacramento River (Figure 6-8) the tidal flows are very large, peaking at more than 110,000 cfs, while net flows during the summer are on the order of 5,000 to 15,000 cfs. The model matches the tidal flows within approximately 3%, but the net flow generally too low by 1,800 cfs. As will be discussed in the following section, this discrepancy in net flow may, in part, be attributable to measurement error at the Rio Vista station or error in the boundary inflow from the Yolo Bypass.

On the San Joaquin River at Jersey Point (Figure 6-9), the model provides an excellent match to observed data. Flow amplitude is within approximately 3% and the R2 value is greater than 0.98.

Three Mile Slough (Figure 6-10) is an important connection between the Sacramento and San Joaquin Rivers. The model matches flow amplitude in Three Mile Slough within 1.5% of observed with an R2 value greater than 0.99. However, the computed record has as a general shift in net flow of 1,100 cfs toward the San Joaquin River. The reason for this shift is still under investigation. One of the possible explanations is the presence of large bed forms which impose a directionally varying frictional resistance. Numerical tests applying a directionally dependent Manning's n value in the model shows that the net flow error can be corrected, however this will not be incorporated in to the model without further field data analysis.

On the Mokelumne River near the San Joaquin (Figure 6-11), the model matches the ebb flow very precisely, but the flood flow is less than observed. This results in a net flow shift of the computed record of 1,100 cfs toward in the downstream direction. The model still does a good job matching the tidal flow with overall amplitude within 8% and an R2 value of 0.98. The reason for the ebb flow bias is not yet determined. It may be related to conveyance capacity in Little Potato Slough and/or other channels west and north of the Mokelumne, perhaps as far up the system as Snodgrass Slough. Additional bathymetric and flow data collection will be needed to guide further calibration.

Flows in channels surrounding Franks Tract are critical to salt transport in the Delta. These channels include False River, Fisherman's Cut, Dutch Slough, Holland Cut, Old River near Mandeville Island, and Old River near the San Joaquin (Figures 6-12 through 6-17). The model does an excellent job matching observed data at the west side stations in False River and Dutch Slough where tidal flow amplitude is within 4% and R2 values are greater than 0.99. The southeast side stations on Holland Cut, and Old River near Mandeville Island are also good with R2 values greater than 0.98.

The model does not do as well at Fisherman's Cut or Old River near the San Joaquin. The tidal flow through Fisherman's cut is very small (peak flood is on the order of 2,000 cfs) but there is a consistent shift in the computed net flow of 900 cfs toward the San Joaquin. At Old River near the San Joaquin, the model does an excellent job matching the magnitude and detailed pattern of flood flows, but under-predicts the ebb flow, resulting in a net flow bias of 800 cfs towards Franks Tract from the San Joaquin. Essentially, flow entering through False River is incorrectly entering the San Joaquin through Fisherman's Cut rather than passing through Franks Tract and moving into the San Joaquin through Old River. While 800 cfs is small relative to the tidal range of 10,000 to 15,000 cfs flood and ebb flow in Old River, this error in net flow is important in terms of salt transport through Franks Tract into Old River. Many numerical tests were performed with the model looking for the means to correct this discrepancy. It appears that, like Three Mile Slough, there is an asymmetry in the frictional resistance to flow in and out of Franks Tract near the main jet connecting Franks Tract to False River. Application of directionally dependent Manning's n in that region was able to correct the net flow bias in Old River near the San Joaquin. Additional field data collection is

recommended to identify the physical mechanisms that cause this asymmetry. Until the relevant physical mechanisms are identified, directional frictional resistance will not be used in the model.

South of Franks Tract in Old and Middle Rivers (Figures 6-18 through 6-20) the influence of the export pumps is clearly visible in the net flow record. Daily operation of the Clifton Court Gate is also visible in the dynamic tidal record as evidenced by dips and shoulders on the peak flows. The model does an excellent job matching the complexities of the tidal signal as well as the net flows with R2 values of 0.977 to 0.986 at these three stations.

Influence of the export pumps is also seen in San Joaquin River near Stockton (Figure 6-21). Here the model does a very good job overall, matching flow amplitude within less than 1% and average net flow within 80 cfs. There is, however, more variability at this station with an R2 value of 0.969.

6.5 NET FLOW SPATIAL PLOTS

The spatial distribution of net flows is show in two sets of figures illustrating periods with and without significant export pumping. Observed and computed averaged net flows for the period of May 5 to May 19, 2002 are shown in Figures 6-22 and 6-23. The difference between the observed and computed average net flows (observed minus computed) is shown in Figure 6-24. A second set of net flow spatial plots for the period of July 20 to August 4, 2002 is shown in Figures 6-25 to 6-27. Each plot shows the average of daily net flows over the period rounded to the nearest 10 cfs.

During early May, south Delta exports are low and the Delta Cross Channel is closed. Net flows in the San Joaquin River at Jersey point and in False River are seaward. Net flow through Franks Tract is relatively low. Net flows in Old and Middle River are small and toward the export pumps. Net flow in the San Joaquin near Stockton is in the downstream direction.

During late July, export pumping is high and the Cross Channel is open. Net flow in the San Joaquin River and False River is reversed. There is a strong net flow southward through Franks Tract toward Old River and the export pumps. Net flows in

Old and Middle Rivers are strongly toward the pumps. Net flow in the San Joaquin is still downstream, but very small.

The same general trends are seen in the observed and computed net flow discrepancy plots for both periods. In the Sacramento River at Rio Vista, discrepancies between computed and observed net flow are 2,530 cfs in May and 1,900 cfs in July. While these numbers are small compared to peak tidal flows on the order of 110,000 cfs, they merit further consideration. Because net flow discrepancies upstream of Rio Vista do not indicate that this flow is being lost elsewhere (for example in Georgiana Slough), the discrepancy at Rio Vista is likely due to a data error. Either the boundary flows at Sacramento River and/or Yolo Bypass are too low, or the measured flow data at Rio Vista are high.

The net flow differences in Three Mile Slough, the Mokelumne River, False River, and Old River and the San Joaquin are likely the result of the flow biases in the model as discussed in section 6.4 above.

Net flows in and out of Franks Tract (including False River, Fisherman's Cut, Old River, Holland Cut and Dutch Slough) should sum to approximately zero. In the model, flows into Franks Tract sum to -10 cfs in May and 60 cfs in July. The observed data, however, sum to -1090 cfs in May and -930 cfs in July, indicating some error in the flow data. This could possibly explain the relatively large discrepancy between observed and computed net flows in Holland Cut.

In examining the net flow differences (observed minus computed) for May in Figure 6-24, the computed downstream flow for the San Joaquin River near Stockton is 310 cfs too high. The tidally averaged flow time series for this location (Figure 6-21) shows the computed downstream flow is higher than observed flow until late May 2002. This time coincides with the presence of the Old River Barrier at Head, and with high San Joaquin River flow. Further examination during a different simulation year may be needed to determine if the flow error is related to the temporary barrier model parameters or the model representation of the San Joaquin River. Figure 6-21 shows after late May, the computed tidally averaged flow for the San Joaquin River near Stockton closely matched the observed values, until July 1, 2002 when both the tidal and tidally averaged

computed net downstream flow suddenly falls below the observed data. This is reflected in the net flow difference plot for July (Figure 6-27) as an error of 190 cfs. The apparent model error in the net flow in San Joaquin River near Stockton (Figure 6-24 and 6-27) may account for much of the flow error in the opposite direction for the Old River and Middle River. Other sources of error for the south Delta flow locations may be related to the estimate of the south Delta agricultural diversions.

6.6 TIDAL ANALYSIS OF OBSERVED AND COMPUTED FLOW

The dynamics of the computed and observed Delta flow are evaluated using tidal analysis. A least-squares tidal analysis program, developed by Foreman (1977), was used to derive the primary semi-diurnal (M2) and diurnal (K1) tidal components for computed and observed stage (see Section 5.5). However, the input format of this program did not readily allow for the use of this method for the tidal analysis of Delta flow. Instead M2 and K1 amplitude and phase were computed using Fourier analysis. A comparison of stage time series computations using the Fourier method and the Foreman least-squares program shows the two methods produce identical results for amplitude and phase for M2. The K1 tidal amplitude determined by the Fourier analysis however is 5% higher than the value determined by the least-squares analysis and one minute off in phase.

The results of the tidal analysis of observed and computed flow time series for a number of Delta locations are presented in Table 6-1. For comparison, the table also lists the computed/observed amplitude ratio and the computed/observed phase difference as determined from the cross-correlation analysis. The time of analysis was a 28-day period from July 7 to August 4, 2002. For three of the stations, the observed record had significant missing data during this time. Therefore, as noted in the table, a different 28-day time period was used at these locations. Twenty-eight days is a shorter analysis period than used in section 6.4, so the mean values and cross-correlation statistics will vary somewhat from the values presented in the earlier section.

Whereas the M2 and K1 amplitudes for stage were roughly equal, the K1 flow amplitude is approximately half the M2 flow amplitude. Since tidal flow is related to the

change in stage with time, the M2-K1 flow difference is likely due to the two-times higher frequency of the M2 tidal component.

Generally the cross-correlation computed/observed amplitude ratio and phase lag are similar to those for the M2 tidal constituent. Much of the discussion of Section 6.4 regarding the ability of the model to predict tidal flow at the various Delta locations applies here also. For some locations, such as at Georgiana Slough and the Sacramento River above the Delta Cross Channel, the variation in the tidally averaged flow over the 28 days is about the same order of magnitude as the variation in the tidal flow. Because of the difficulty in correlating the varying flow time series with a sinusoidal wave when computing the statistics, the M2 and K1 tidal statistics can be skewed unfavorably, and may not accurately reflect the quality of the model results. In these instances, if the tidally averaged flow were removed from the time series before performing a tidal analysis, the statistics might be more meaningful. However, it was deemed most appropriate to keep the computation method consistent for all locations.

Computed phase error for the cross-correlation analysis and M2 tidal component is generally -6 to -16 minutes. That is, the computed tidal signal is 6 to 16 minutes fast relative to the observed. The phase error for the stations near the Delta Cross Channel is -28 to -30 minutes. Computed tidal flow amplitude is about 21% high for the Sacramento River above the Delta Cross Channel and 25% low for the Cross Channel. Computed tidal flows for the Sacramento River below the Cross Channel are near the observed values.

Table 6-1 Computed and observed flow and tidal analysis statistics summary.

Location / dates	Mean Obs (cfs)	Mean Computed (cfs)	Cross-correlation		Tidal Analysis					
			Amp Ratio	Phase Lag (min)	Obs Amp M2 (cfs)	Amp Ratio M2	Phase Lag M2 (min)	Obs Amp K1 (cfs)	Amp Ratio K1	Phase Lag K1 (min)
July 7 - August 4										
RSAN018 - Jersey Point	-592	-662	1.04	-7	119,077	1.03	-6	57,687	1.08	1
False River	-1,605	-1,647	1.04	-6	44,729	1.03	-5	20,146	1.06	-5
SLTRM004 - Three Mile Slough	-1,630	-2,709	1.02	-6	22,790	1.02	-5	11,044	1.06	-9
Fishermans Cut	-860	135	1.20		797	1.61	-81	405	1.78	7
Holland Cut	-2,668	-2,098	1.13	-7	13,737	1.13	-6	6,131	1.20	-6
Old River nr Mandeville Is	-2,799	-2,584	1.05	-12	13,140	1.06	-11	6,486	1.02	-14
Old River nr SJR	-2,053	-3,176	0.89	-6	9,440	0.86	-3	5,143	0.93	-12
Mokelumne nr SJR	3,960	5,183	0.93	-10	11,462	0.93	-10	5,792	0.94	-3
RMID015 - Middle River at Bacon Is	-6,603	-6,068	0.95	-21	9,022	0.95	-16	4,386	0.96	-17
ROLD024 - Old River at Bacon Is	-4,590	-4,661	1.00	-16	9,746	1.00	-16	4,815	1.07	-19
ROLD034 - Old River nr HWY 4	-7,126	-6,973	0.91	-10	4,471	0.92	-7	2,360	0.90	-20
RSAC101 - Sac R at Rio Vista	12,178	9,773	0.98	-11	93,413	0.97	-10	40,193	1.01	-4
RSAC128 - Sac River above DXC	12,359	12,482	1.21	-28	2,705	1.26	-28	2,061	1.18	-49
SLGEO19 - Georgiana Slough	3,051	3,054	0.93	-5	527	1.01	16	236	0.72	34
SLSBT039 - Steamboat Slough	2,593	2,843	0.83	-15	2,421	0.82	-13	1,422	0.89	-4
RSAN063 - SJR nr Stockton	398	210	0.95	-7	2,525	0.94	-7	1,368	1.02	1
July 9 - August 6										
RSAC123 - Sac River below DXC	4,230	4,144	1.02	-30	6,188	1.01	-30	3,428	1.06	-31
July 1 - July 29										
Delta Cross Channel	5,384	5,081	0.75	-30	3,503	0.74	-28	1,476	0.77	-17
August 1 - August 29										
SLDUT007 - Dutch Slough	-234	-49	1.01	-12	7,719	1.01	-11	2,961	0.99	-10

Table Notes

Amp Ratio: Computed/Observed amplitude ratio

Phase Lag: Positive value indicates Computed stage lags Observed stage.

ID Code	Name
CHGRL009	Grant Line Canal DS
DXC	Delta Cross Channel
RMID015	Middle R at Bacon Is
ROLD024	Old River at Bacon Is
ROLD034	Old River nr Hwy 4
RSAC101	Rio Vista
RSAN018	Jersey Pt
RSAN063	SJR at Stockton
RSAN123	Sac River below DXC
SLGE019	Georgiana Slough
SLDUT007	Dutch Slough
SLTRM004	Three Mile Slough

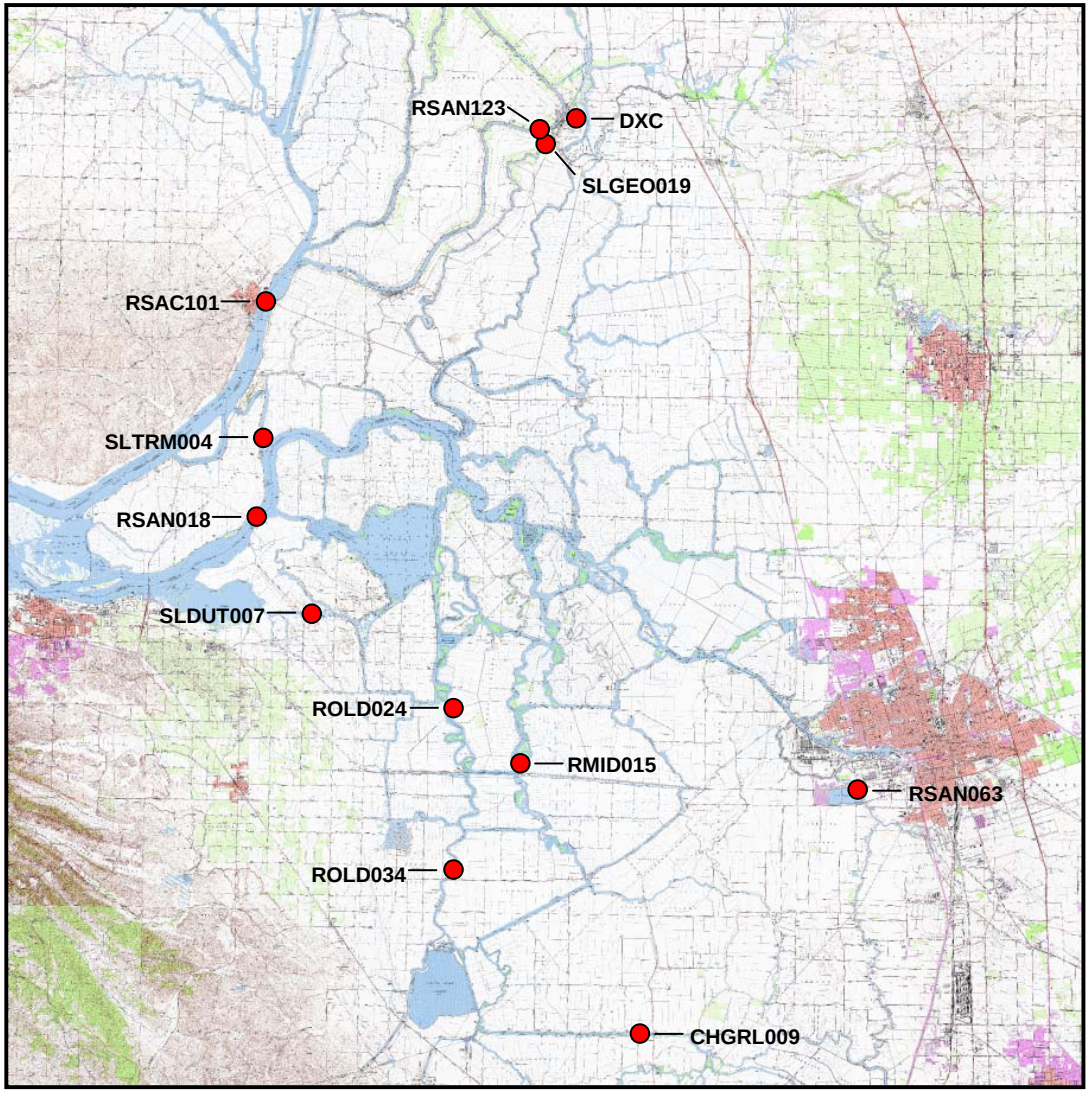

Figure 6-1 Flow monitoring locations.

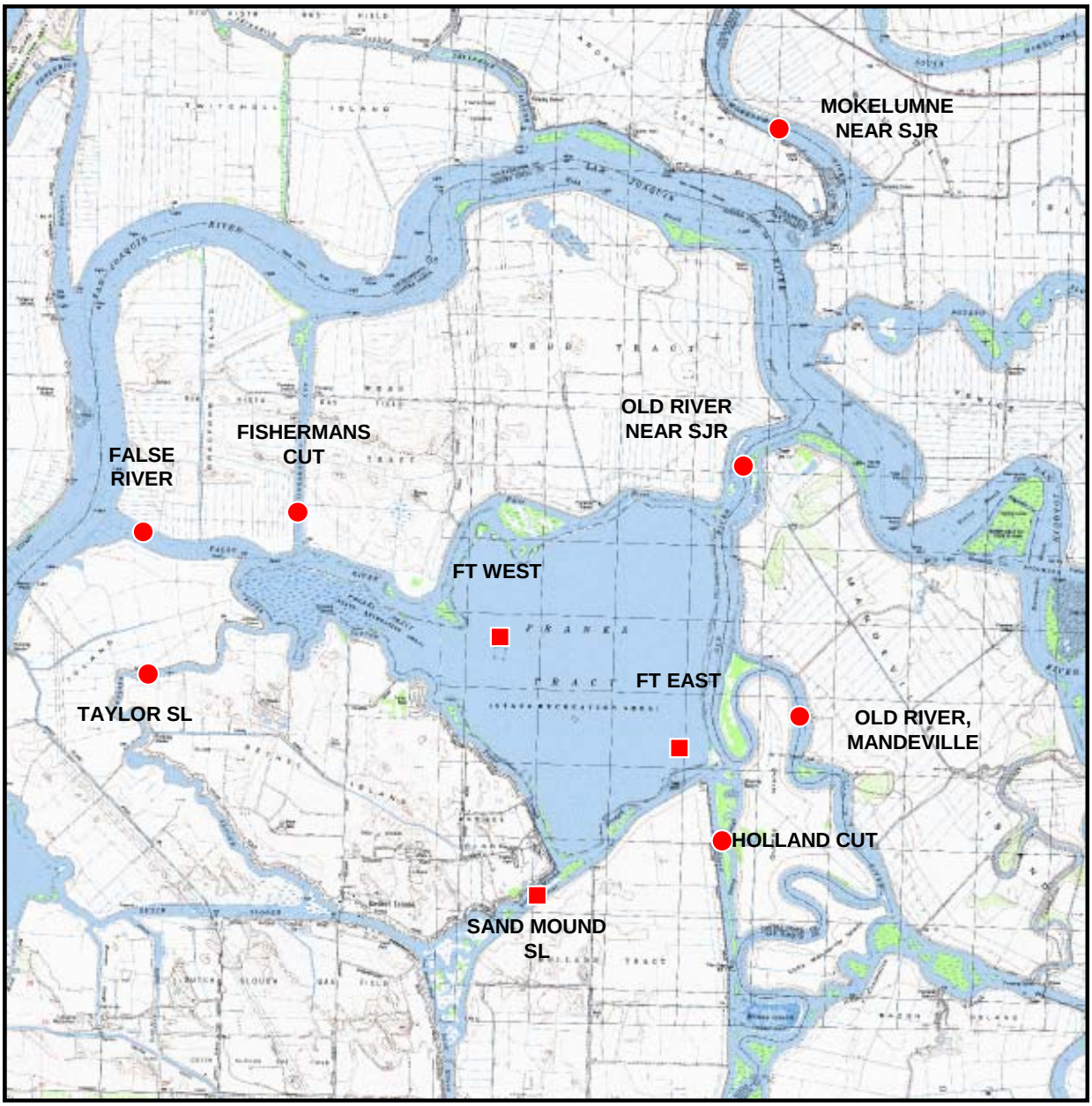

Figure 6-2 Franks Tract USGS monitoring locations.

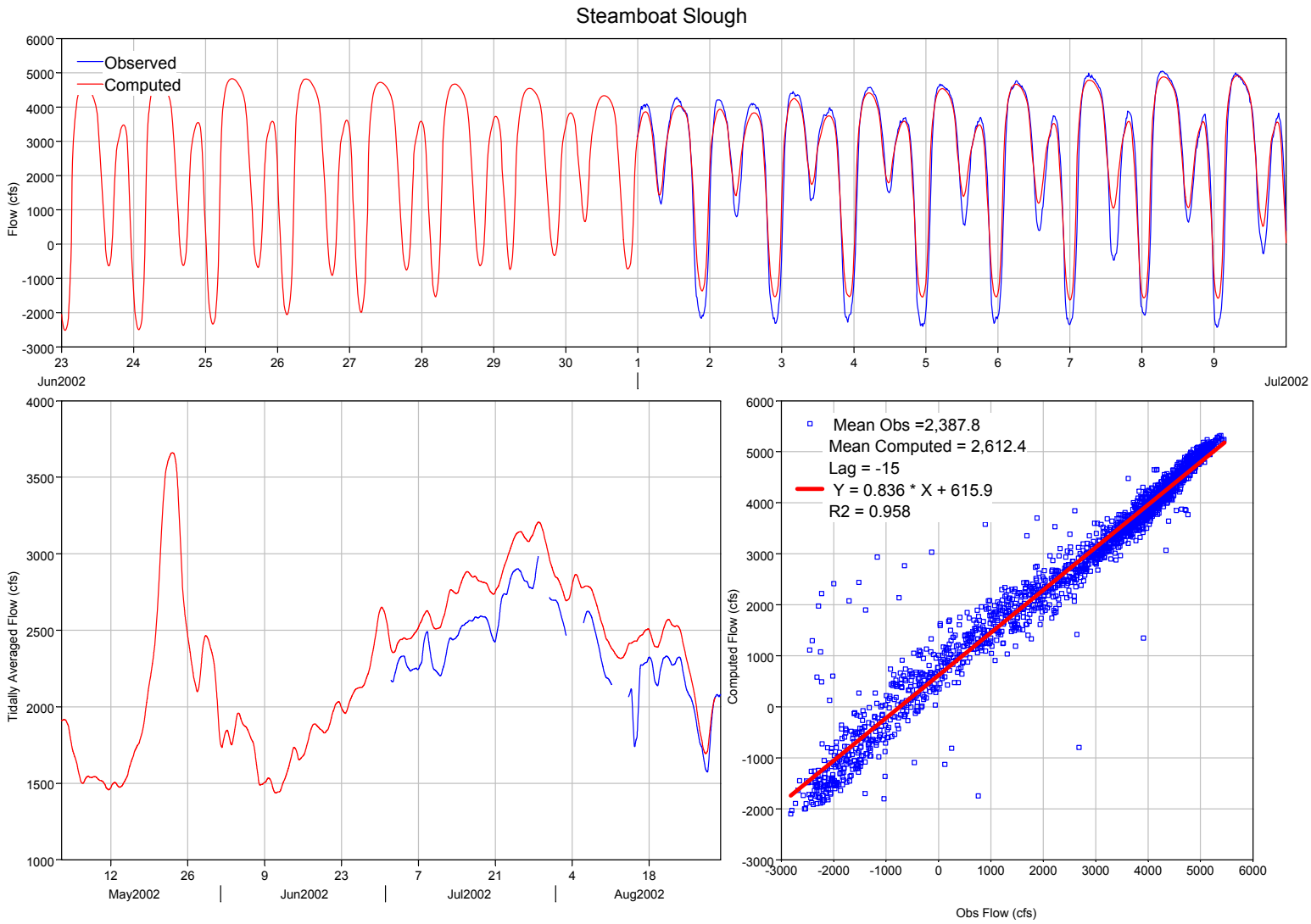

Figure 6-3 Computed and observed flow in Steamboat Slough.

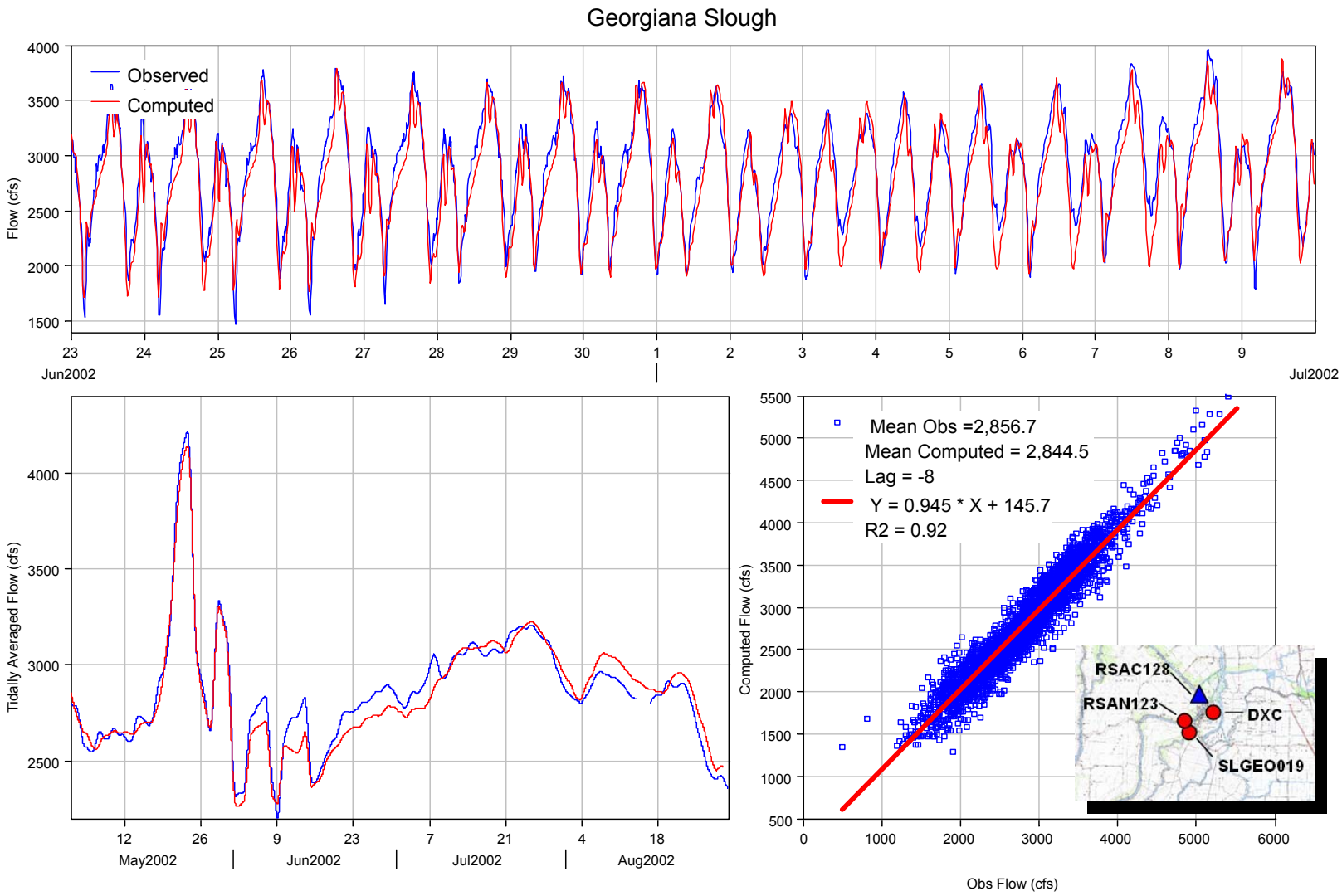

Figure 6-4 Computed and observed flow in Georgiana Slough.

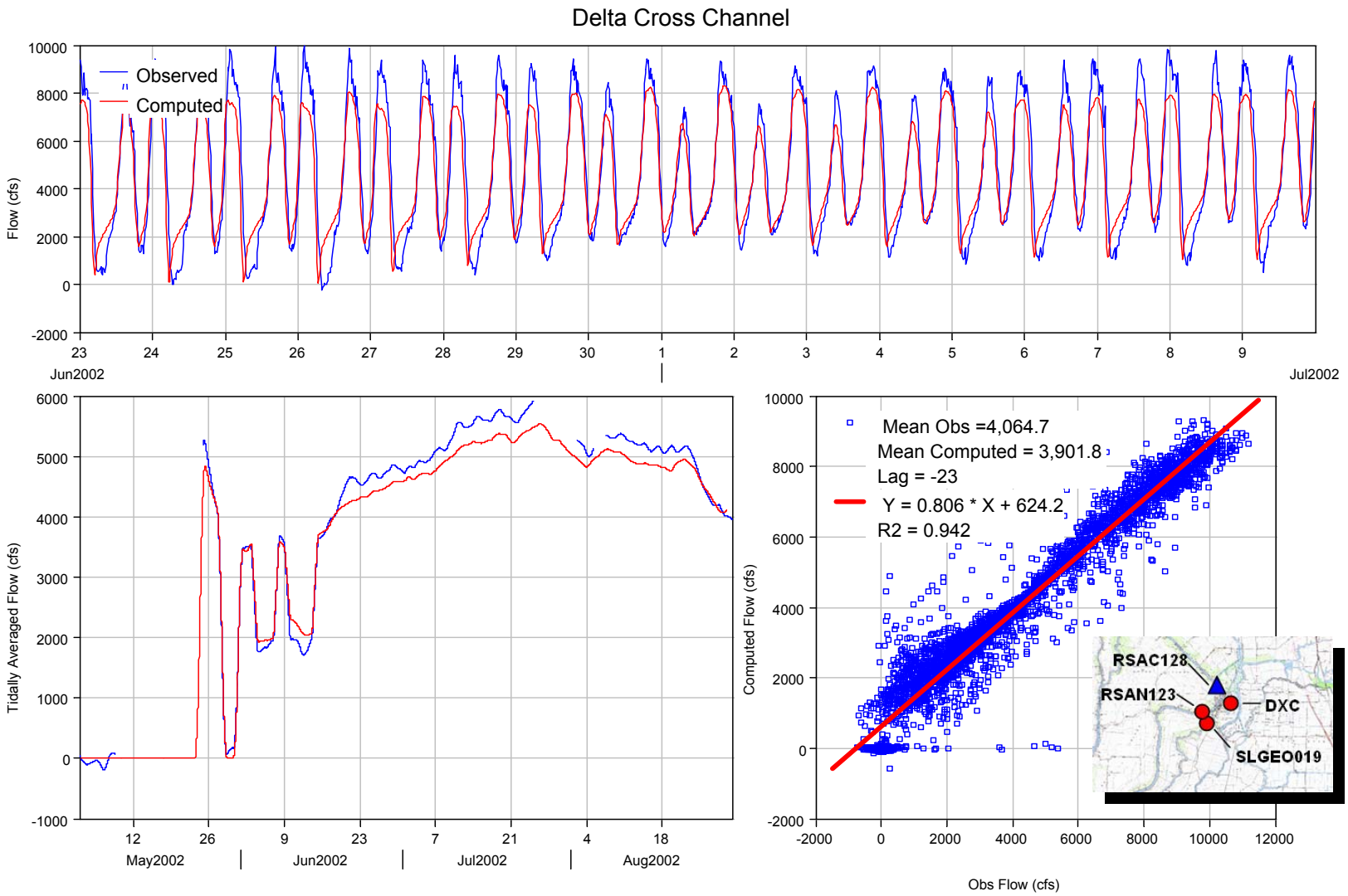

Figure 6-5 Computed and observed flow in the Delta Cross Channel.

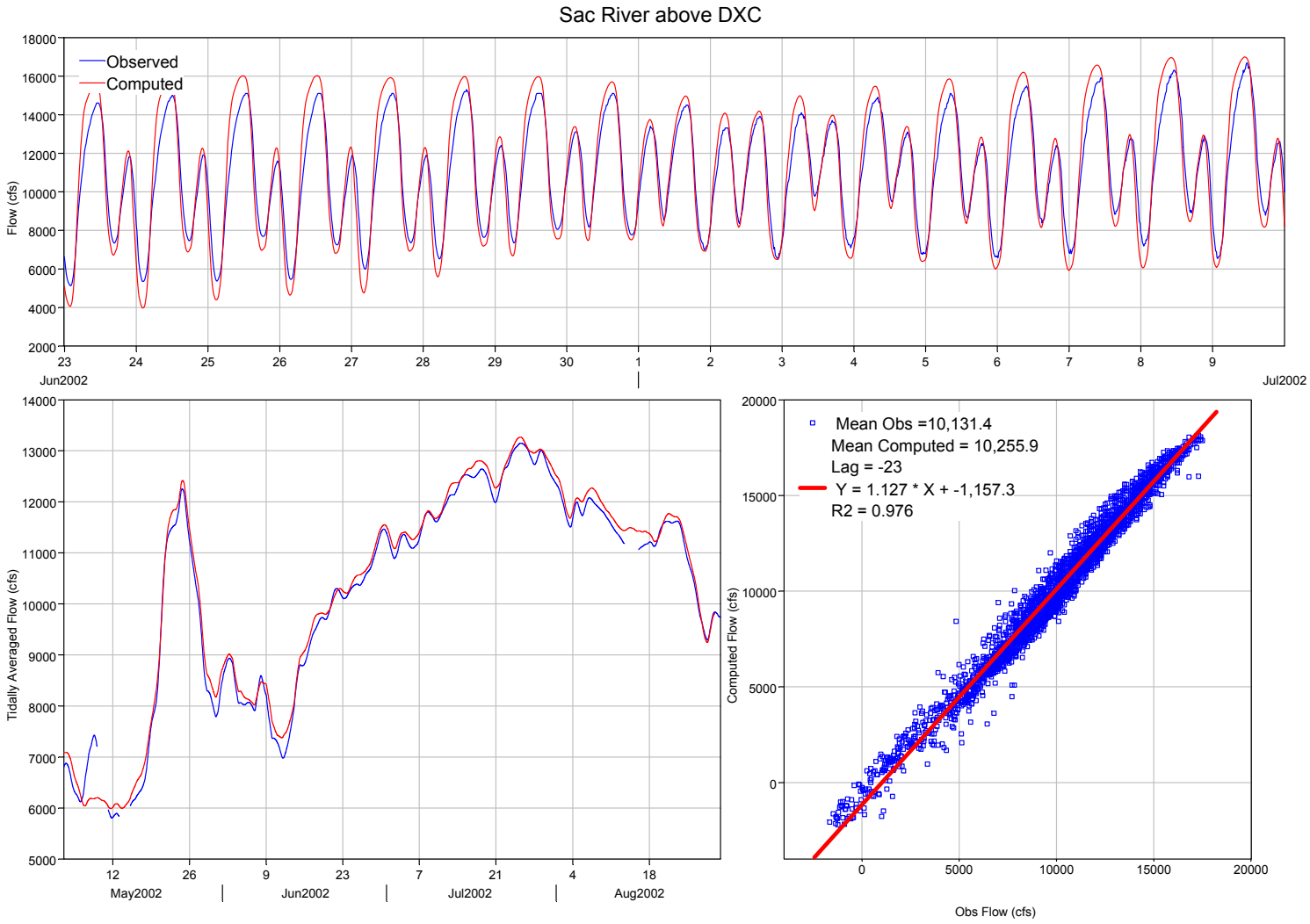

Figure 6-6 Computed and observed flow in Sacramento River above the Delta Cross Channel.

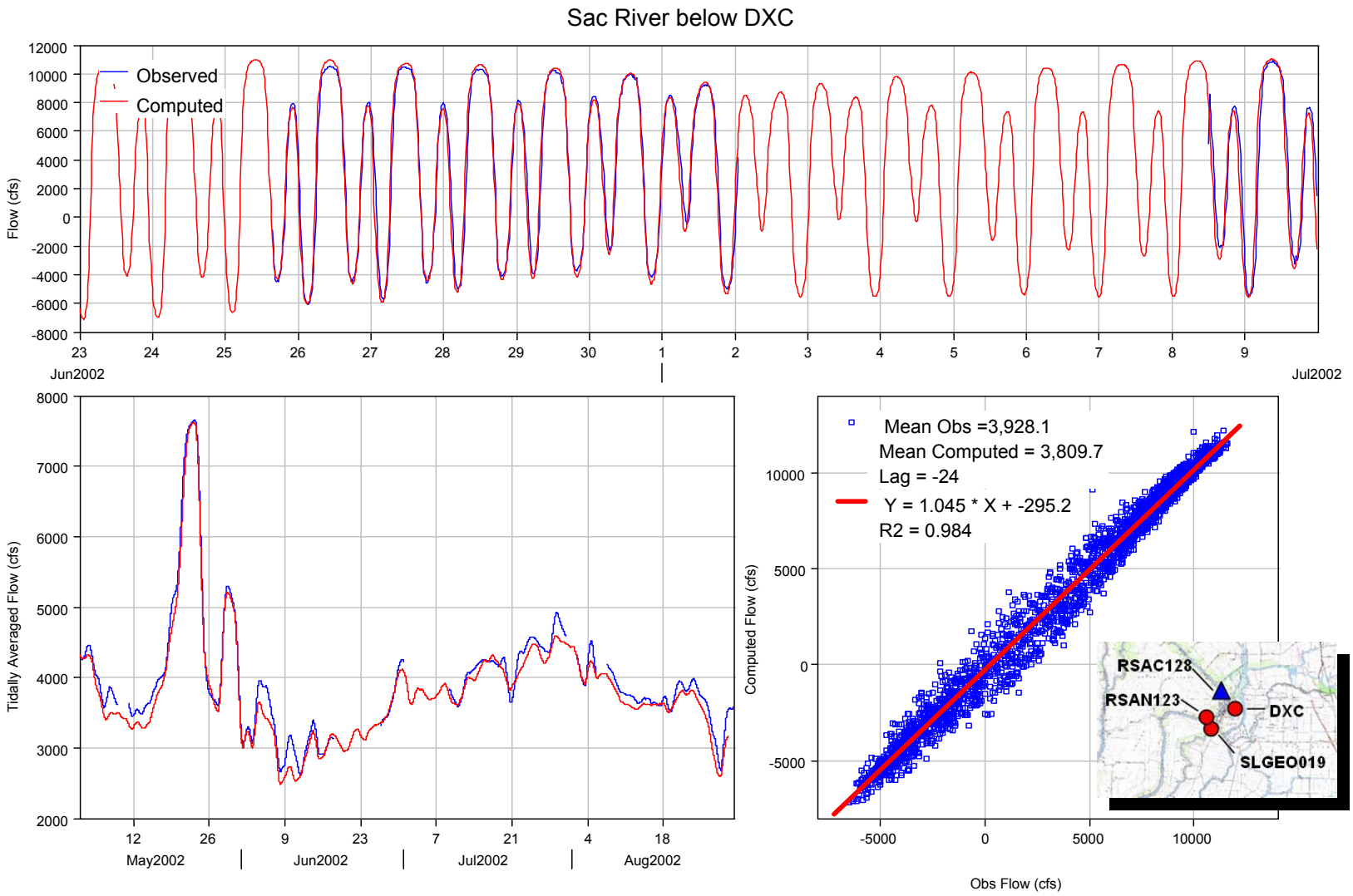

Figure 6-7 Computed and observed flow at RSAC123 - Sacramento River below the Delta Cross Channel.

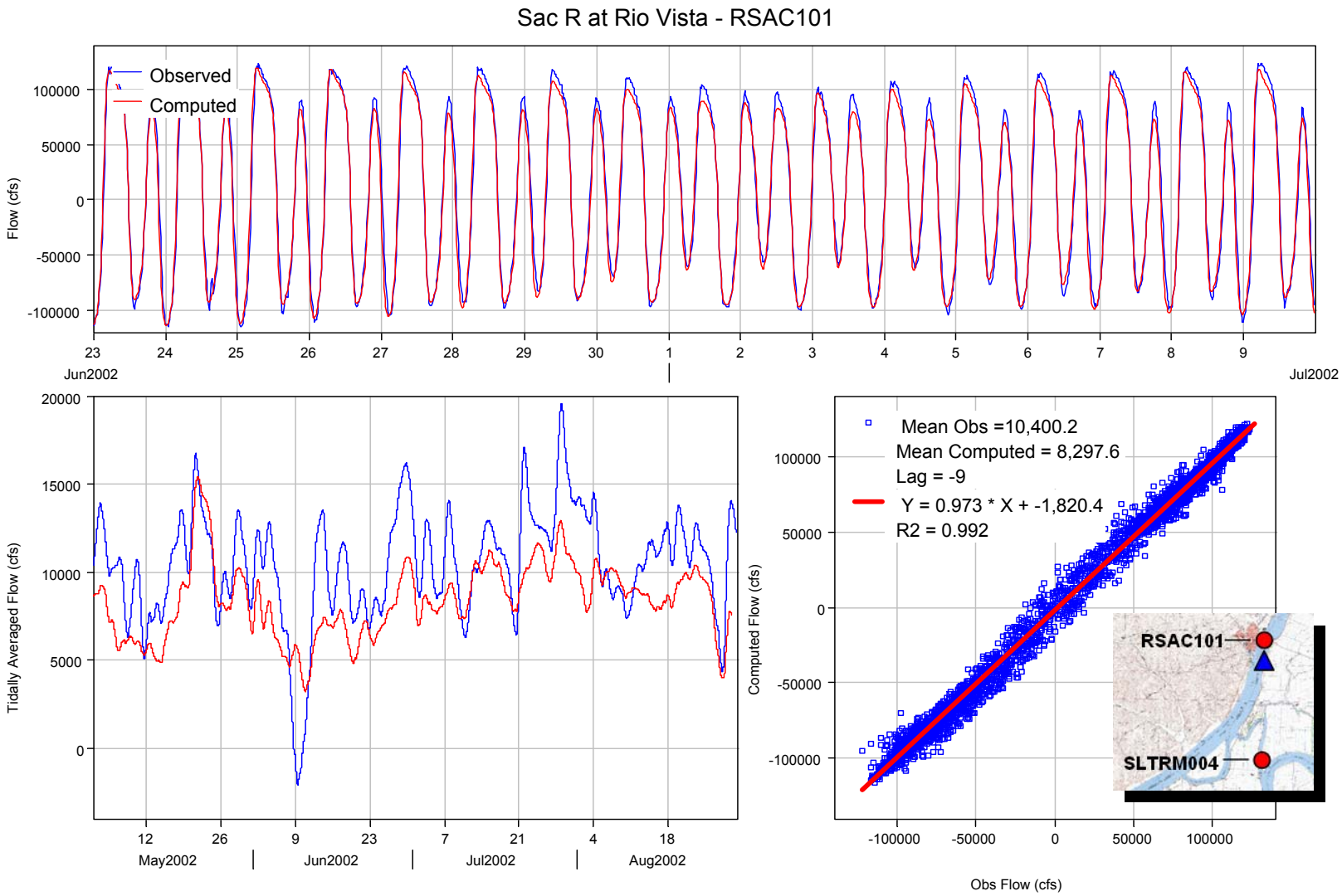

Figure 6-8 Computed and observed flow at RSAC101 - Sacramento River at Rio Vista.

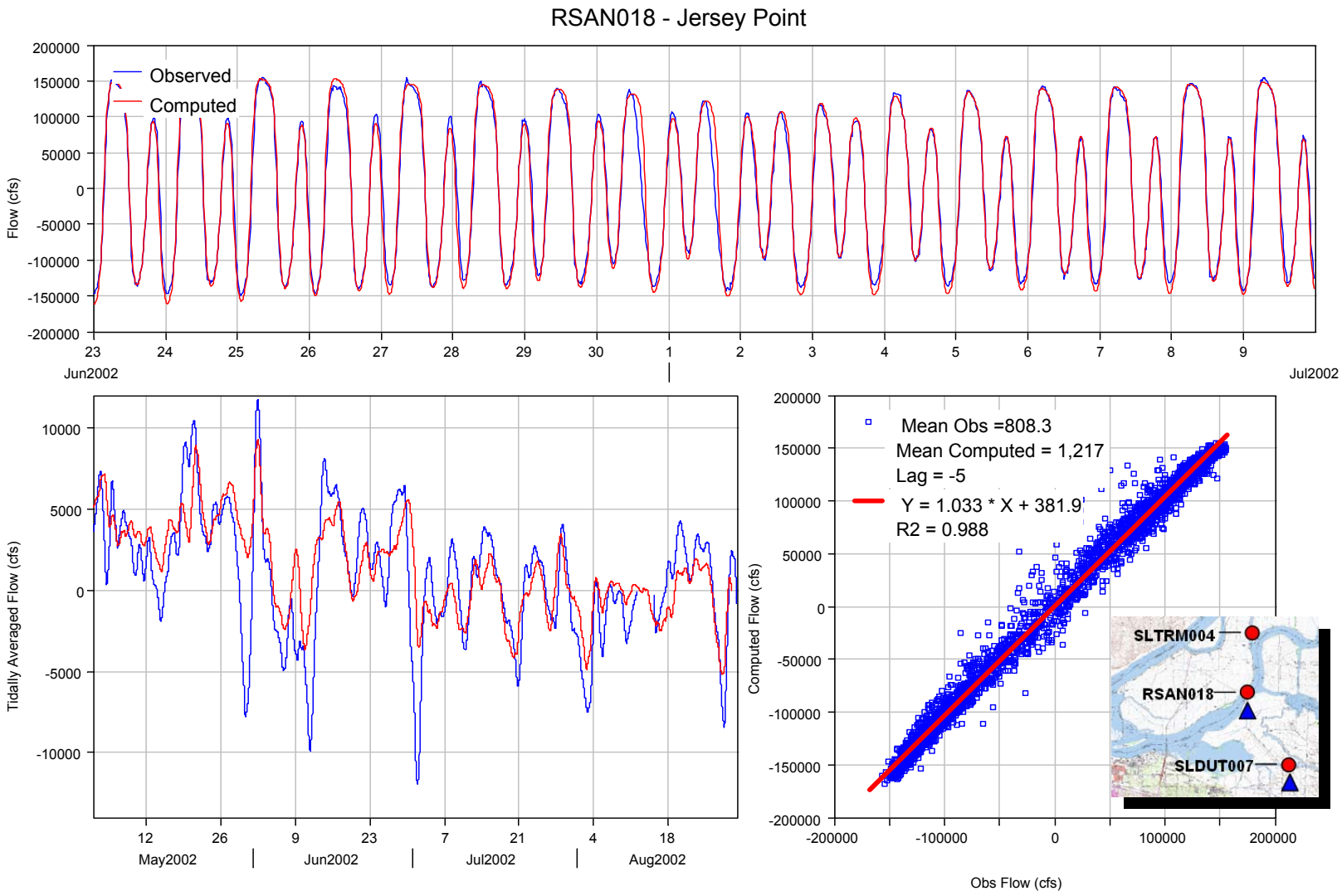

Figure 6-9 Computed and observed flow at RSAN018 - Jersey Point.

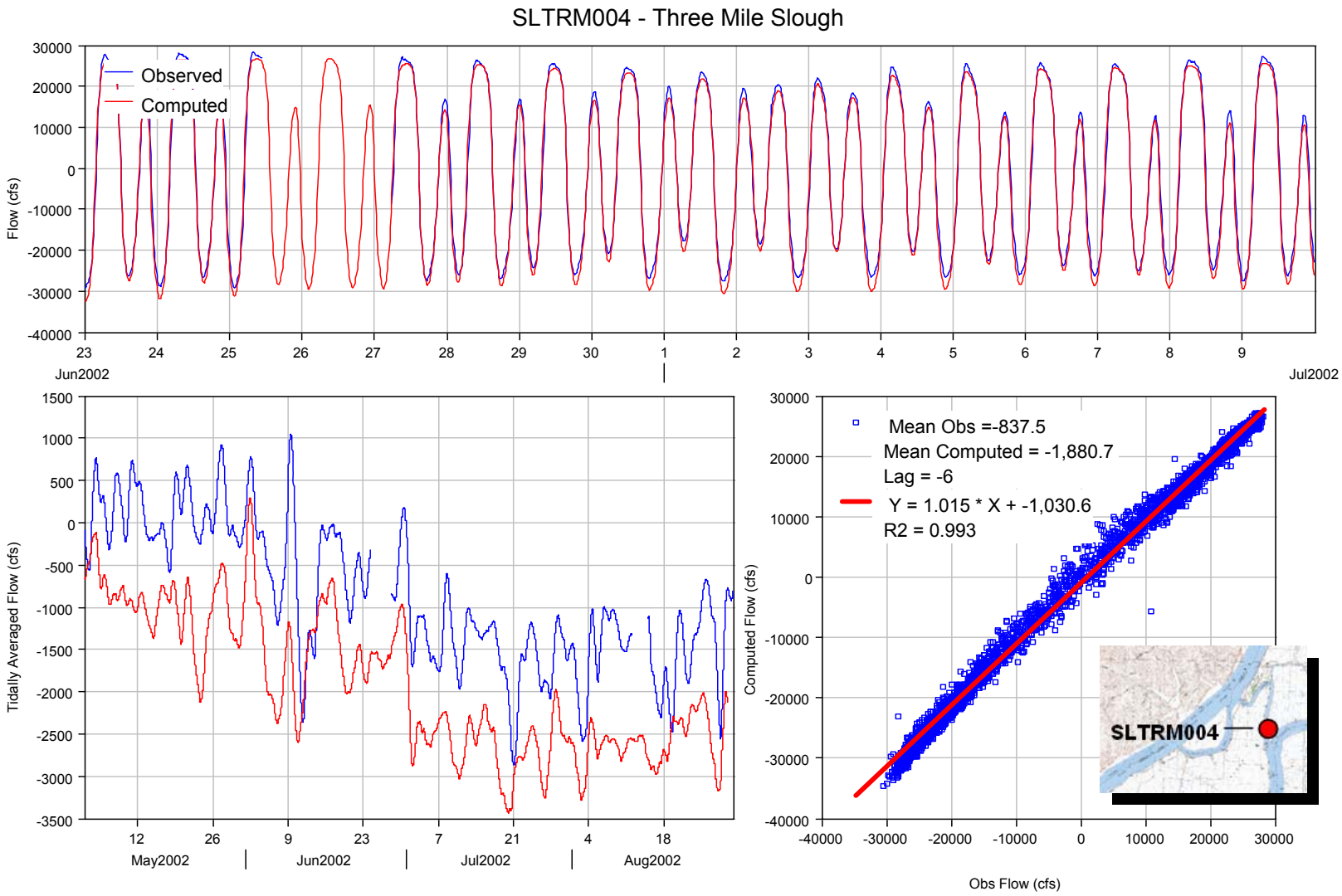

Figure 6-10 Computed and observed flow in Three Mile Slough.

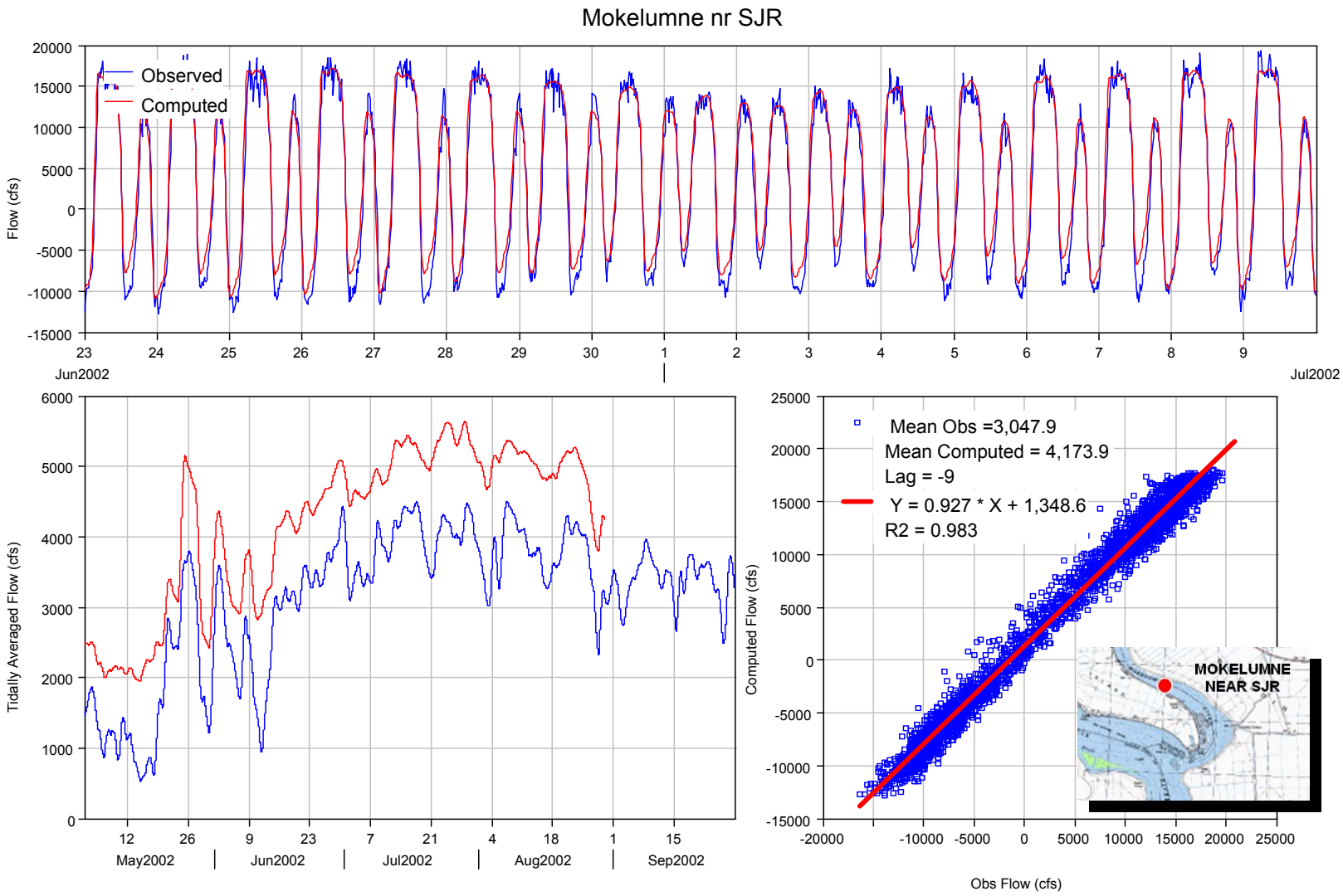

Figure 6-11 Computed and observed flow in Mokelumne River near San Joaquin River.

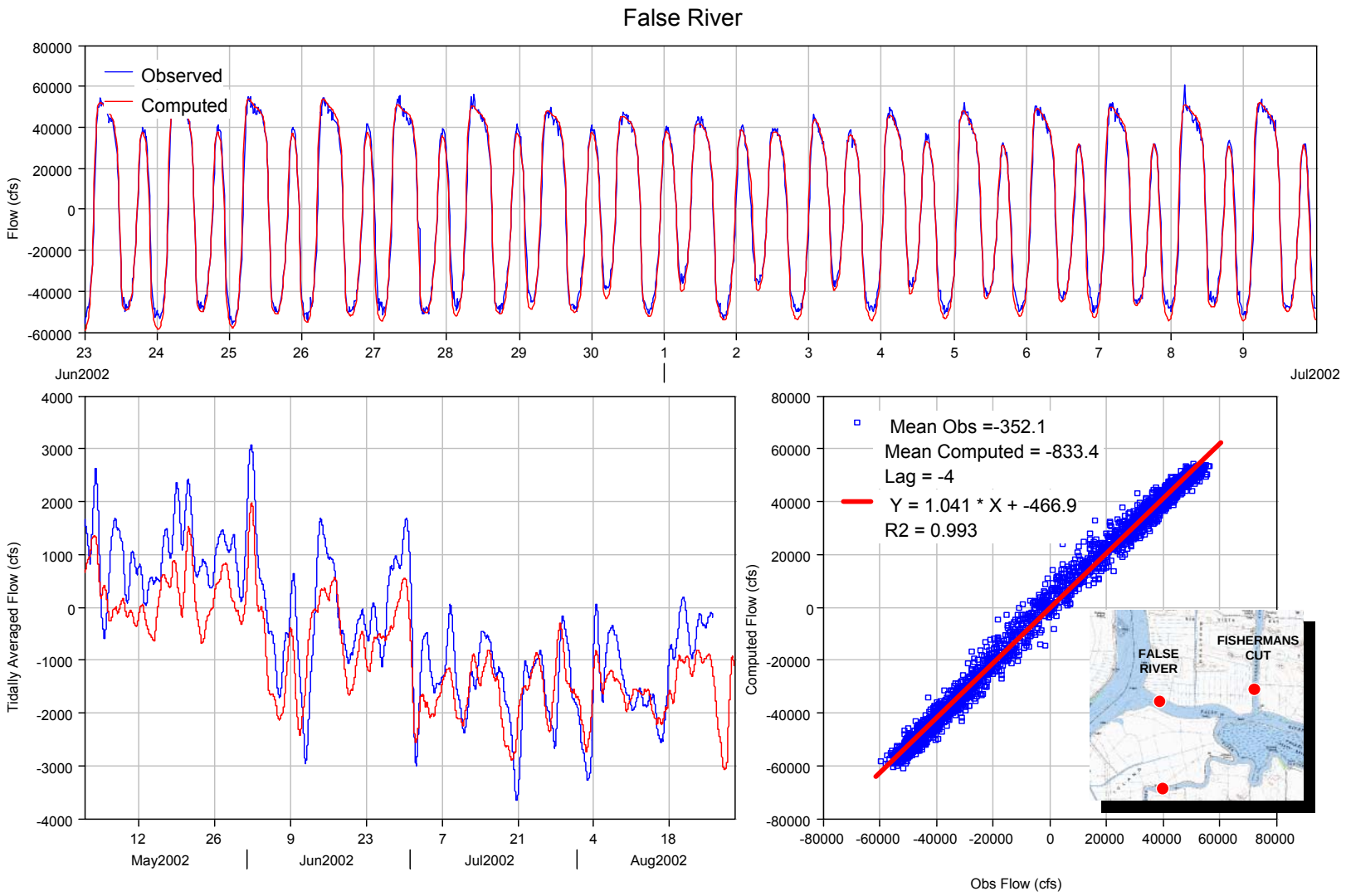

Figure 6-12 Computed and observed flow in False River.

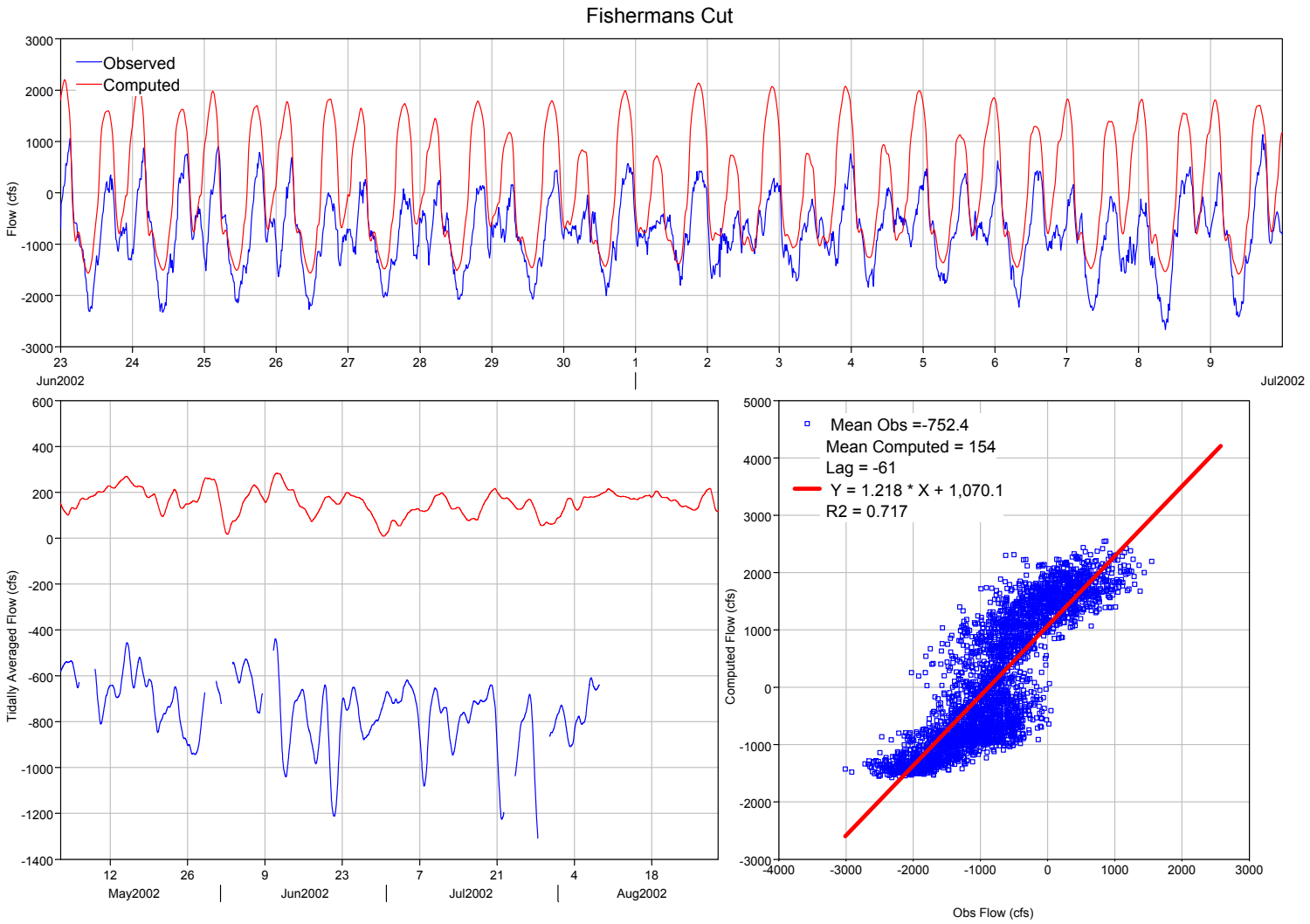

Figure 6-13 Computed and observed flow in Fisherman's Cut.

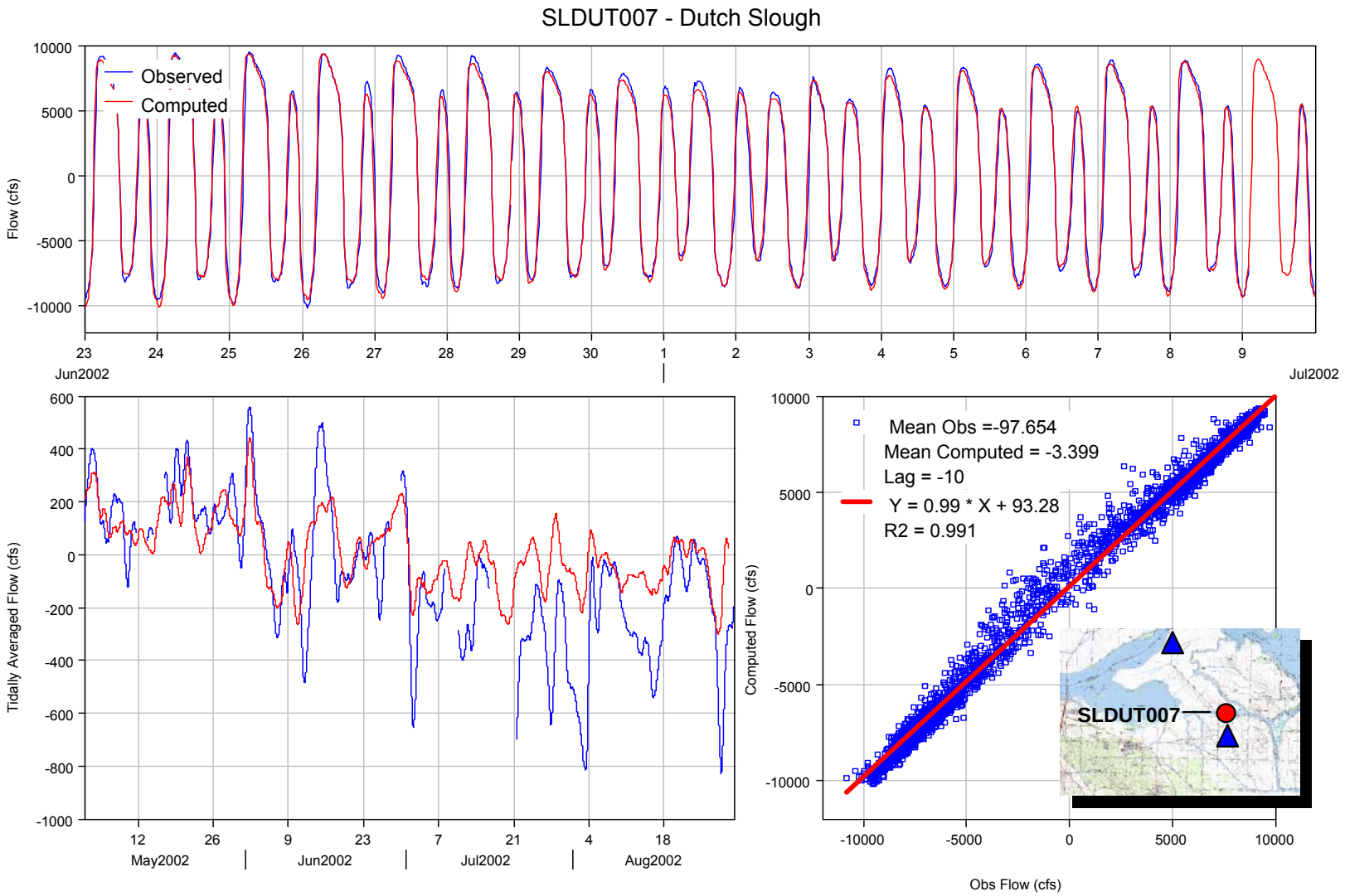

Figure 6-14 Computed and observed flow at SLDUT007 - Dutch Slough.

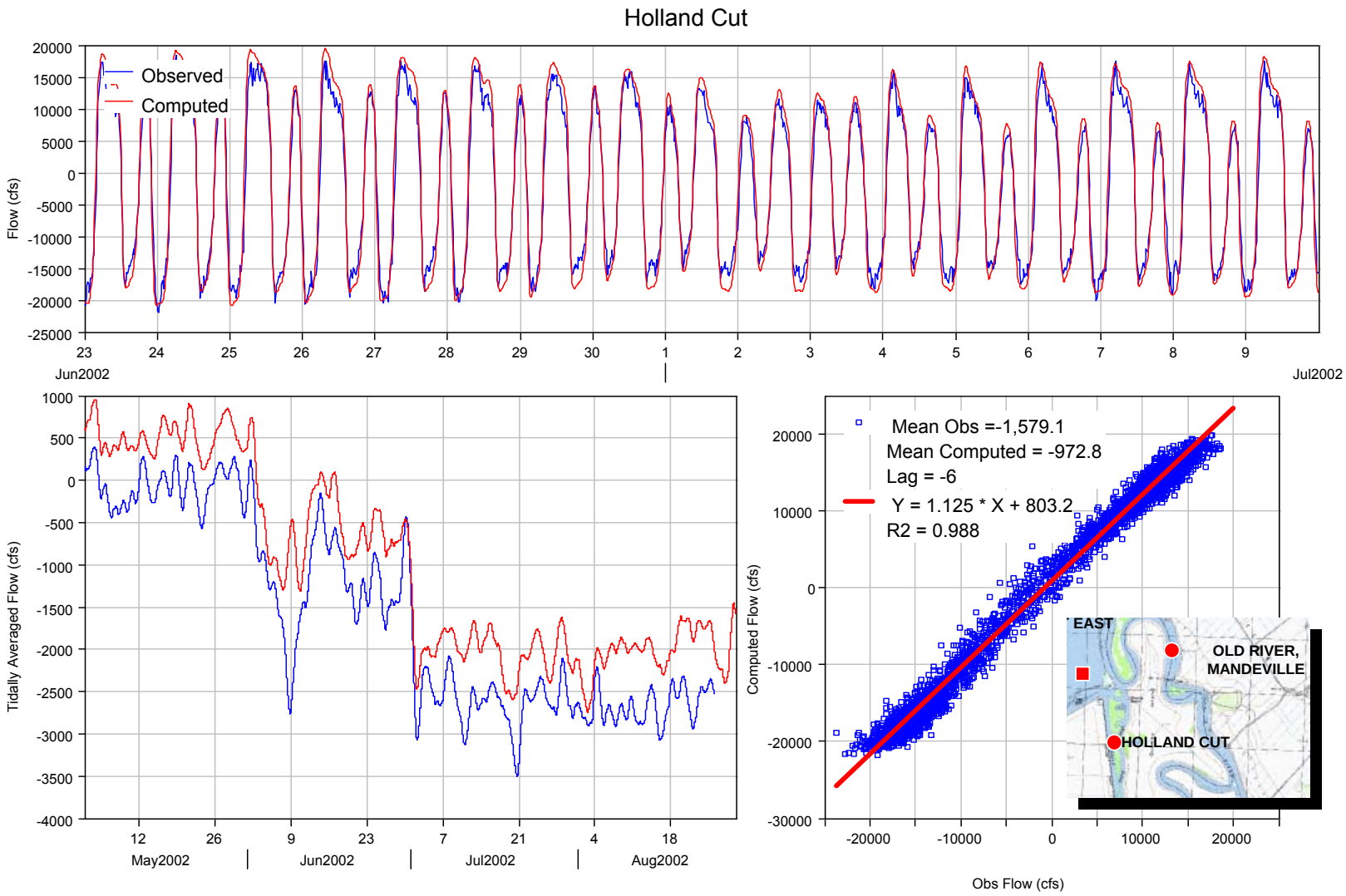

Figure 6-15 Computed and observed flow in Holland Cut.

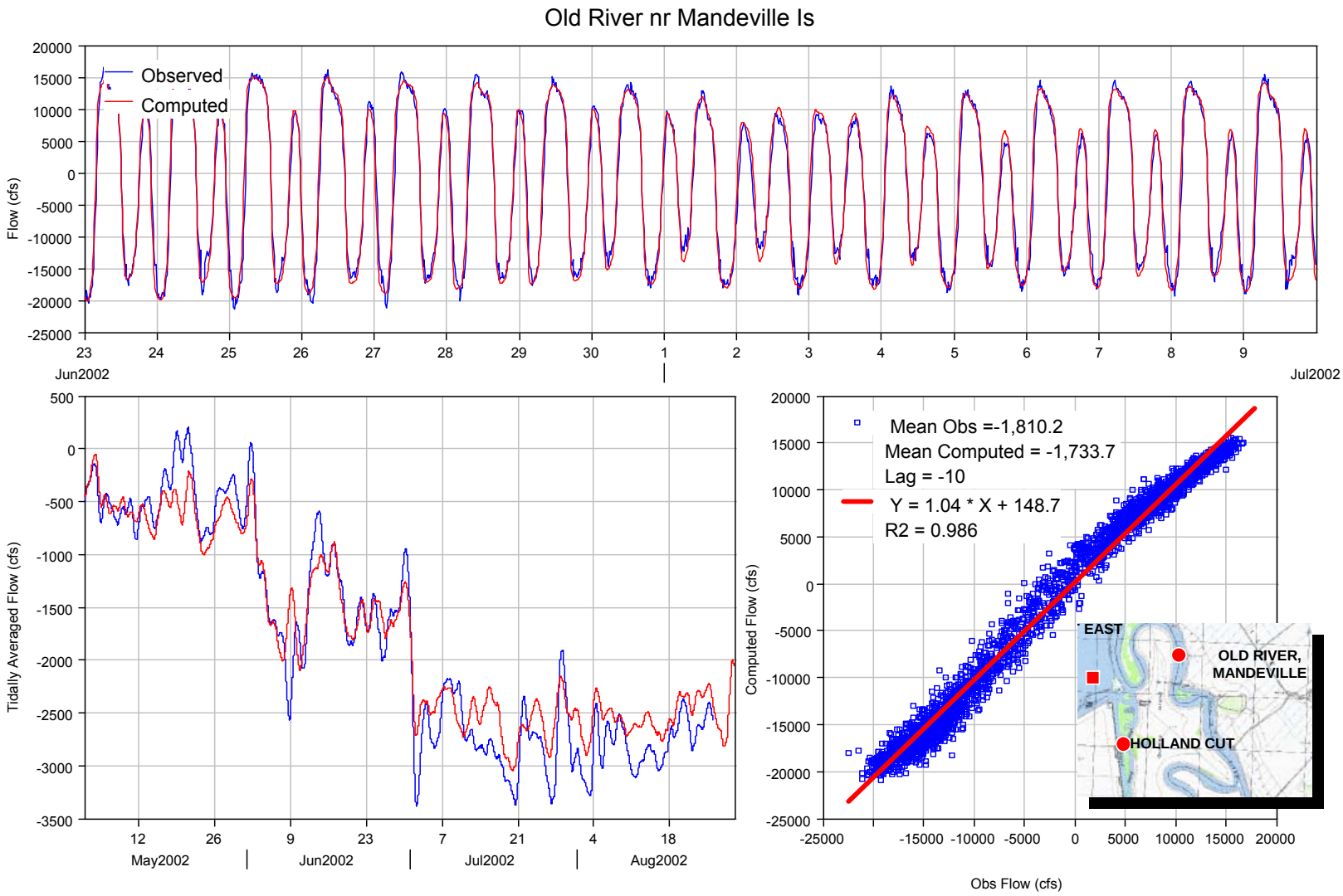

Figure 6-16 Computed and observed flow in Old River near Mandeville Island.

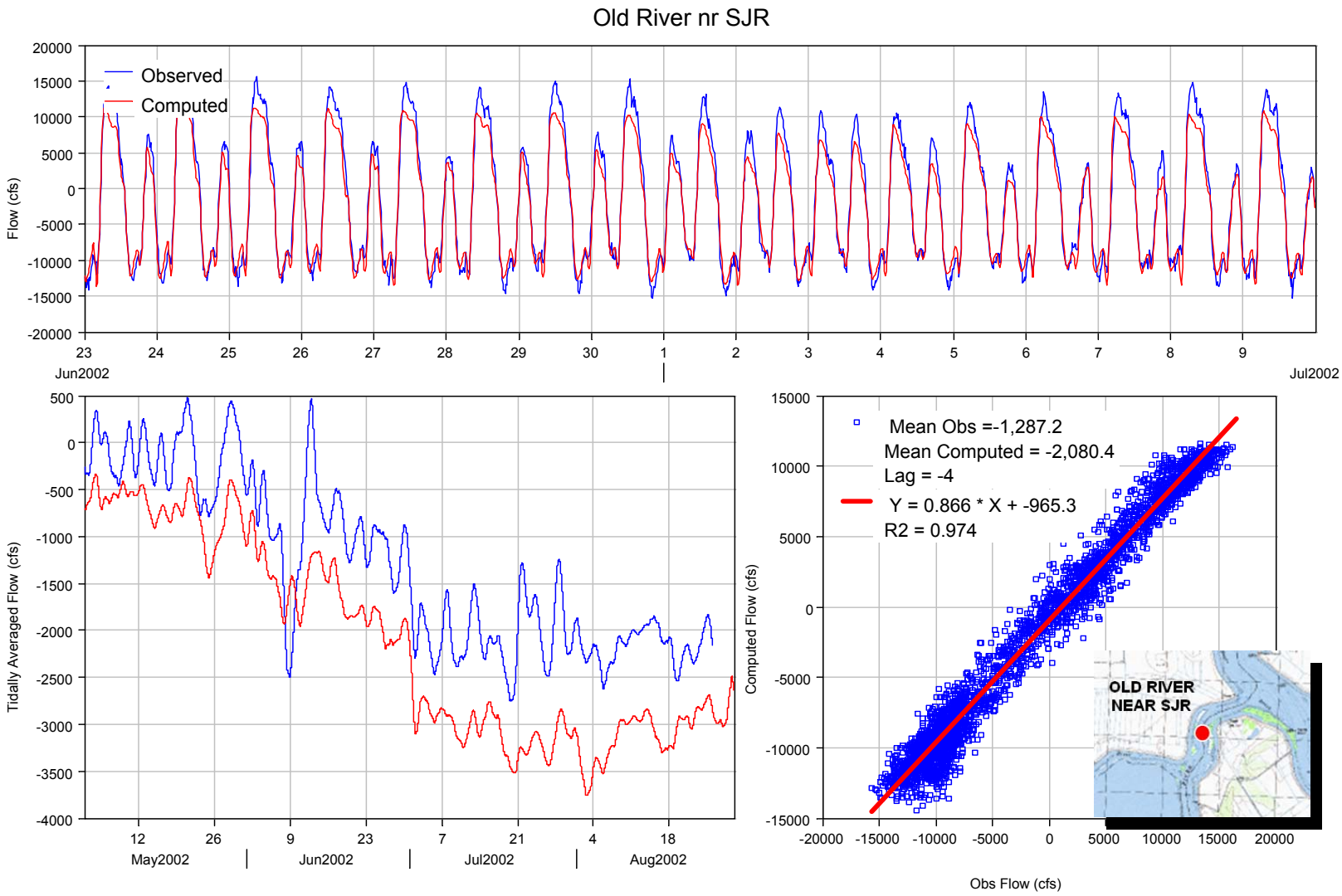

Figure 6-17 Computed and observed flow in Old River near San Joaquin River.

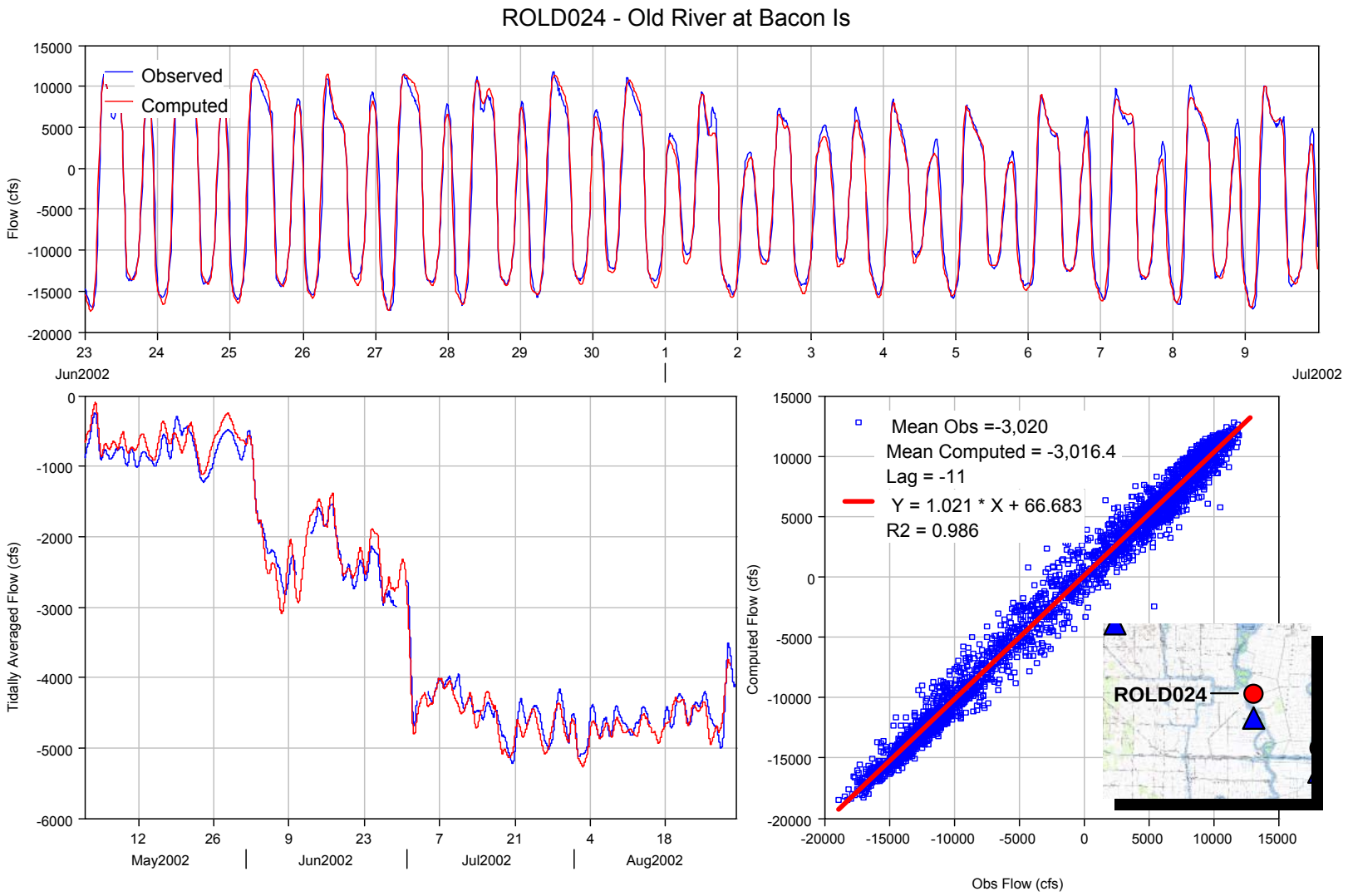

Figure 6-18 Computed and observed flow at ROLD024 - Old River at Bacon Island.

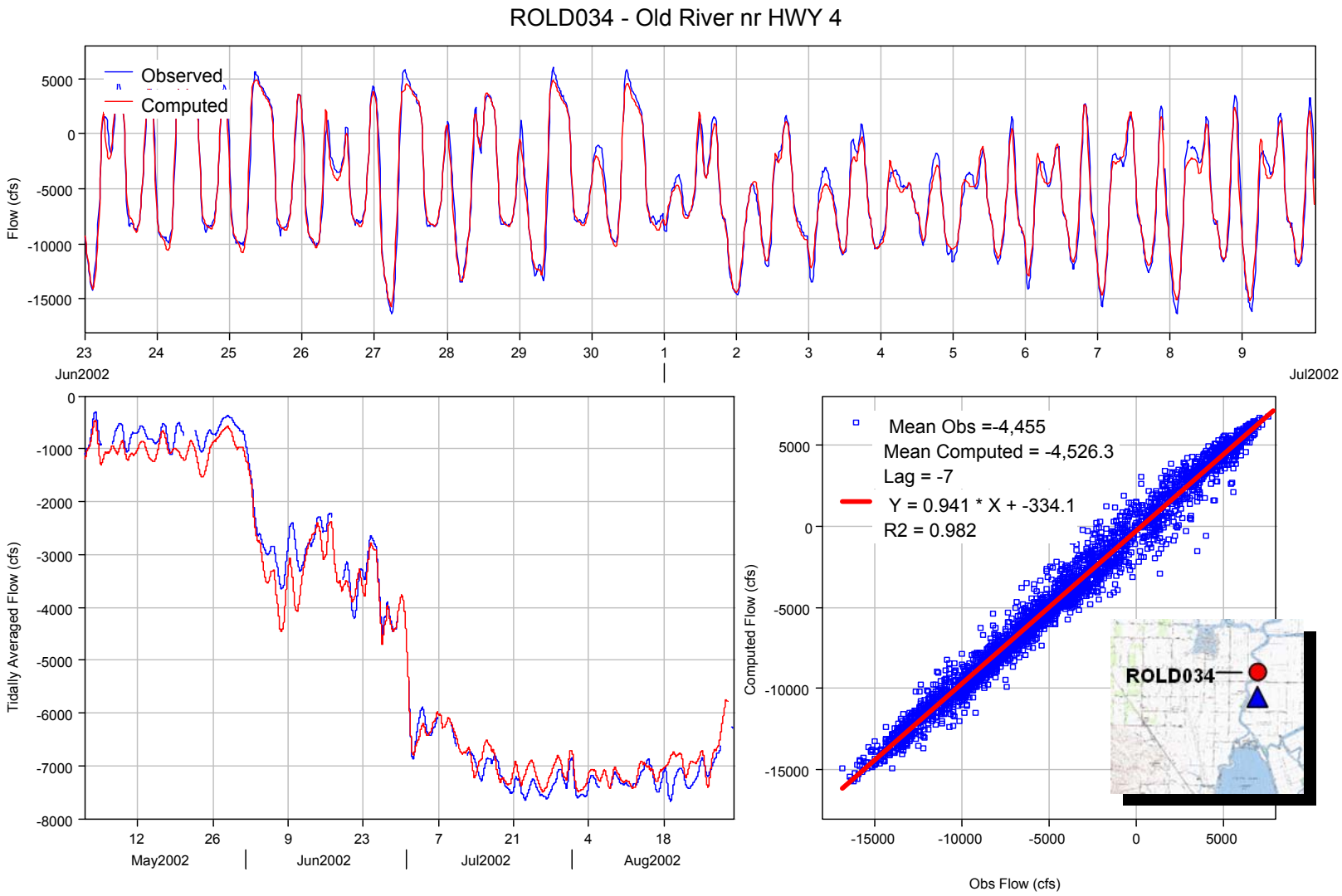

Figure 6-19 Computed and observed flow at ROLD034 - Old River near Highway 4.

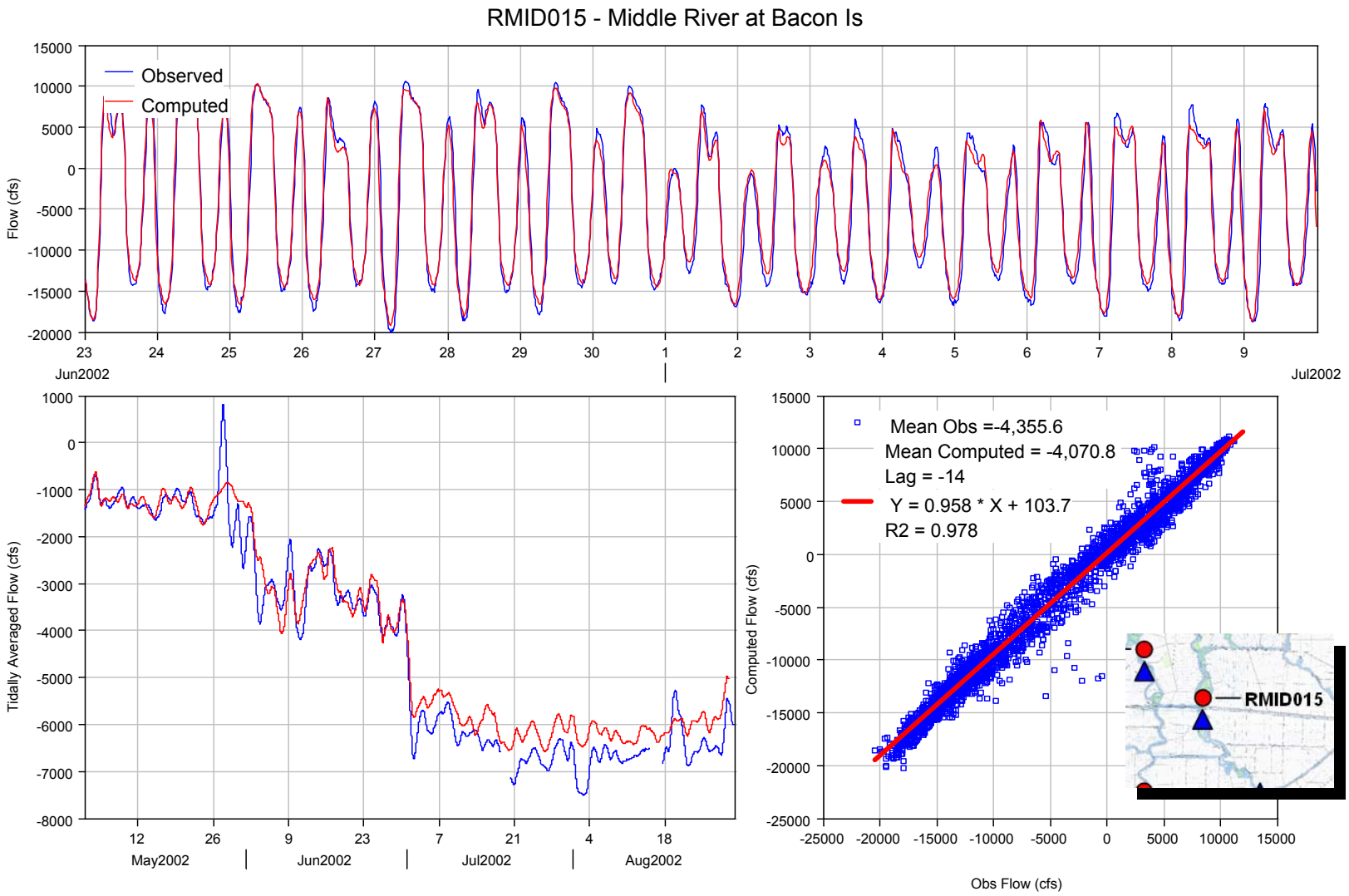

Figure 6-20 Computed and observed flow at RMID015 - Middle River at Bacon Island.

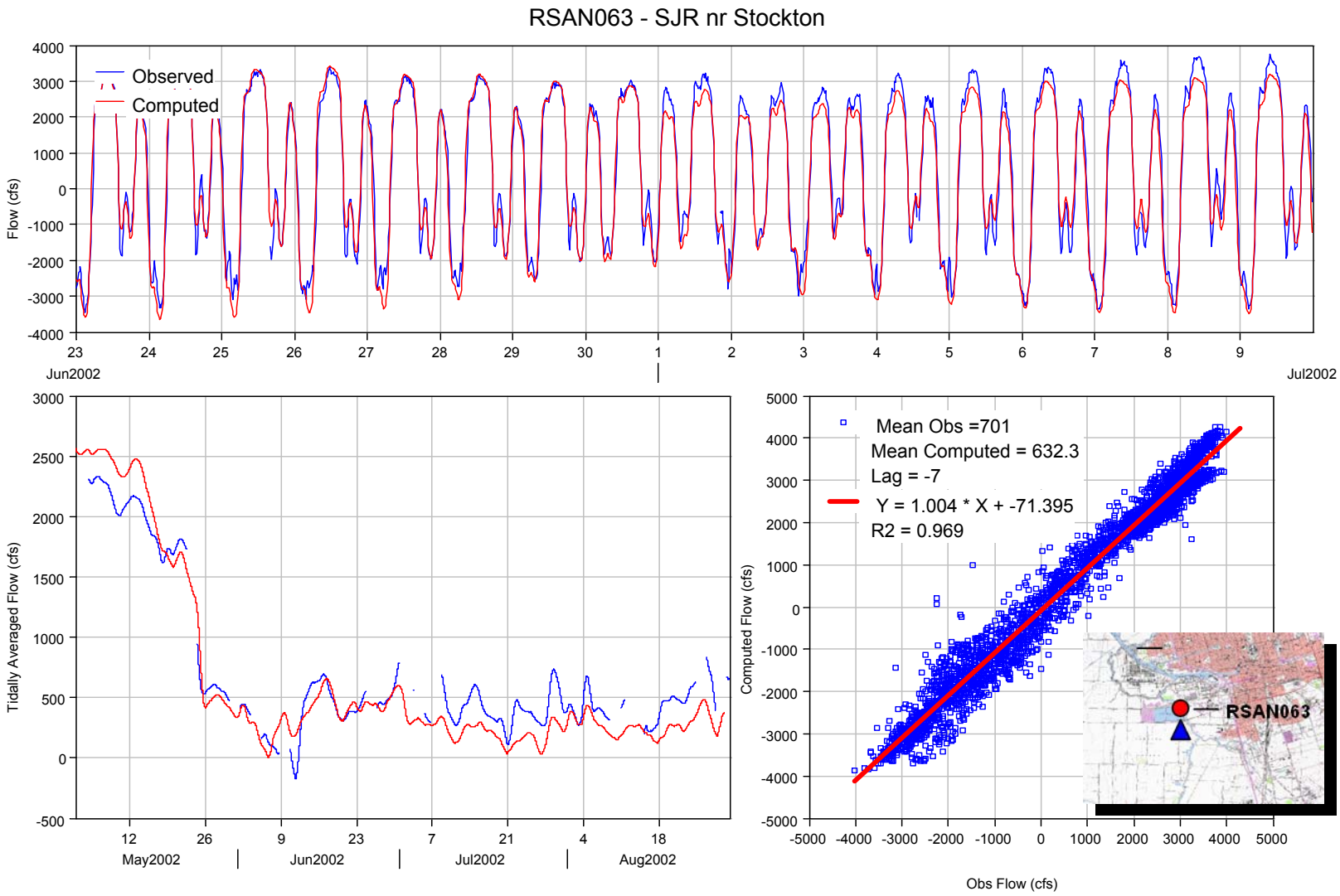

Figure 6-21 Computed and observed flow at RSAN063 - San Joaquin River near Stockton.

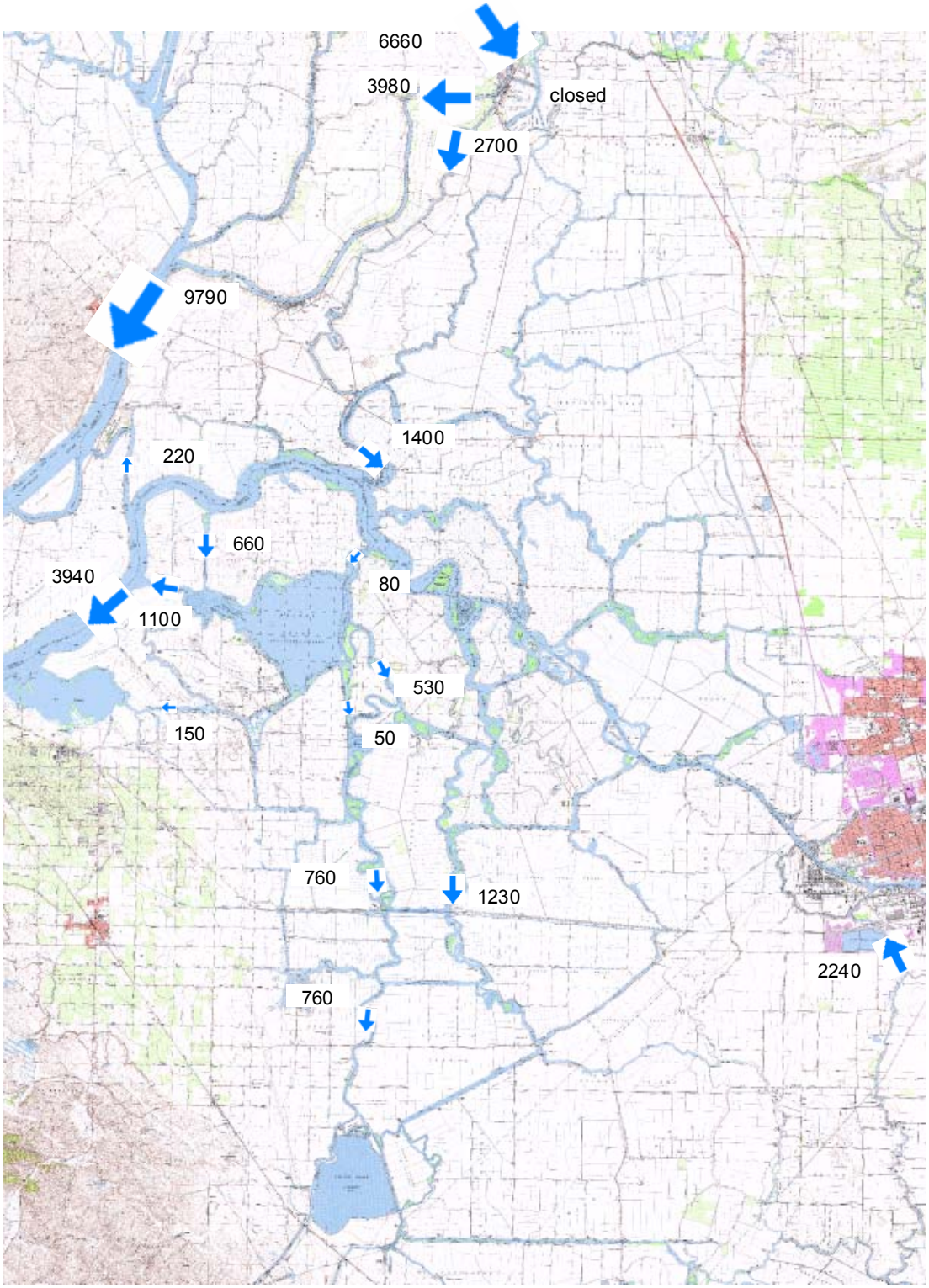

Figure 6-22 Average Observed Net Flow (cfs), May 5 to May 19, 2002.

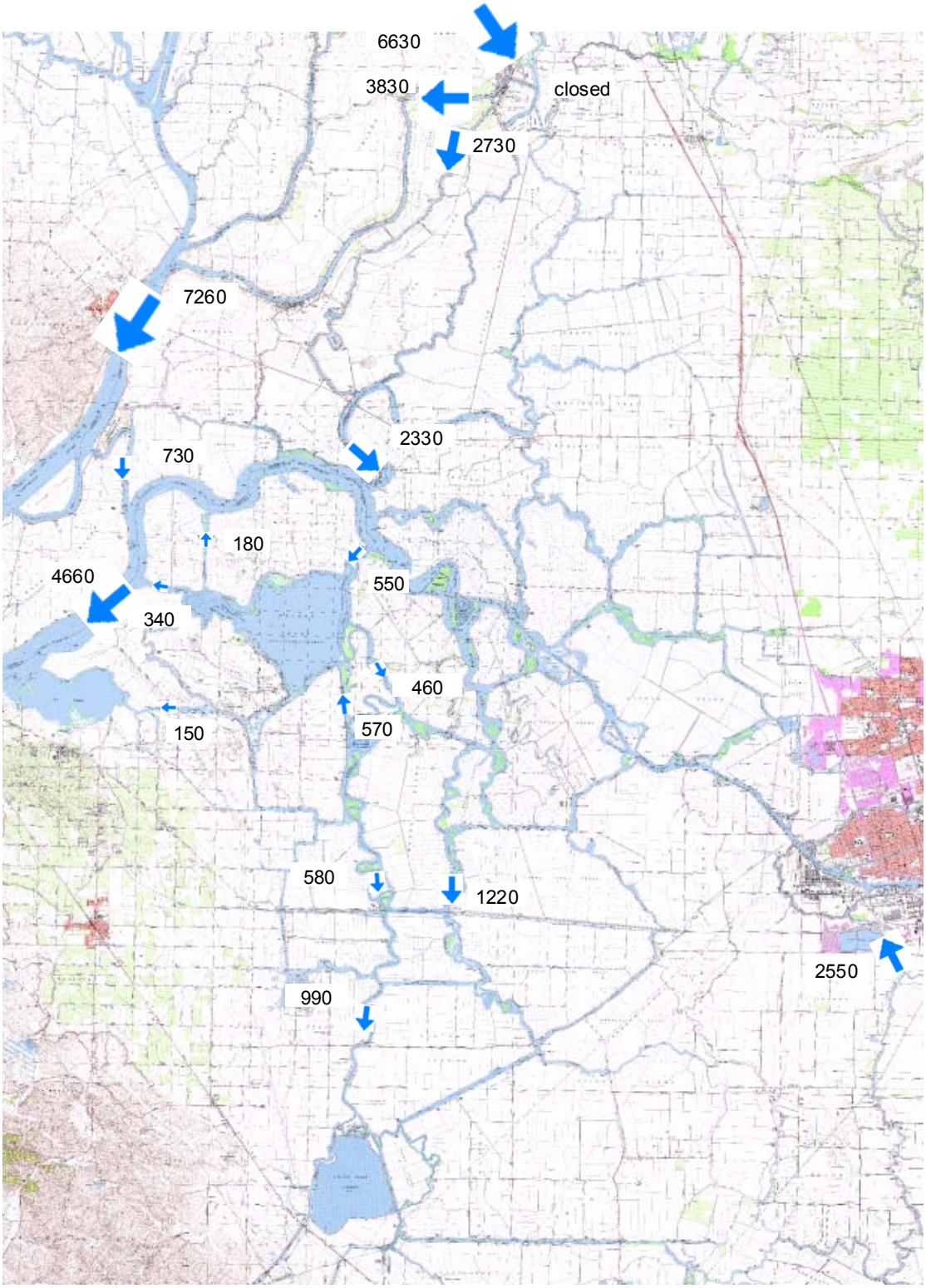

Figure 6-23 Average Computed Net Flow (cfs), May 5 to May 19, 2002.

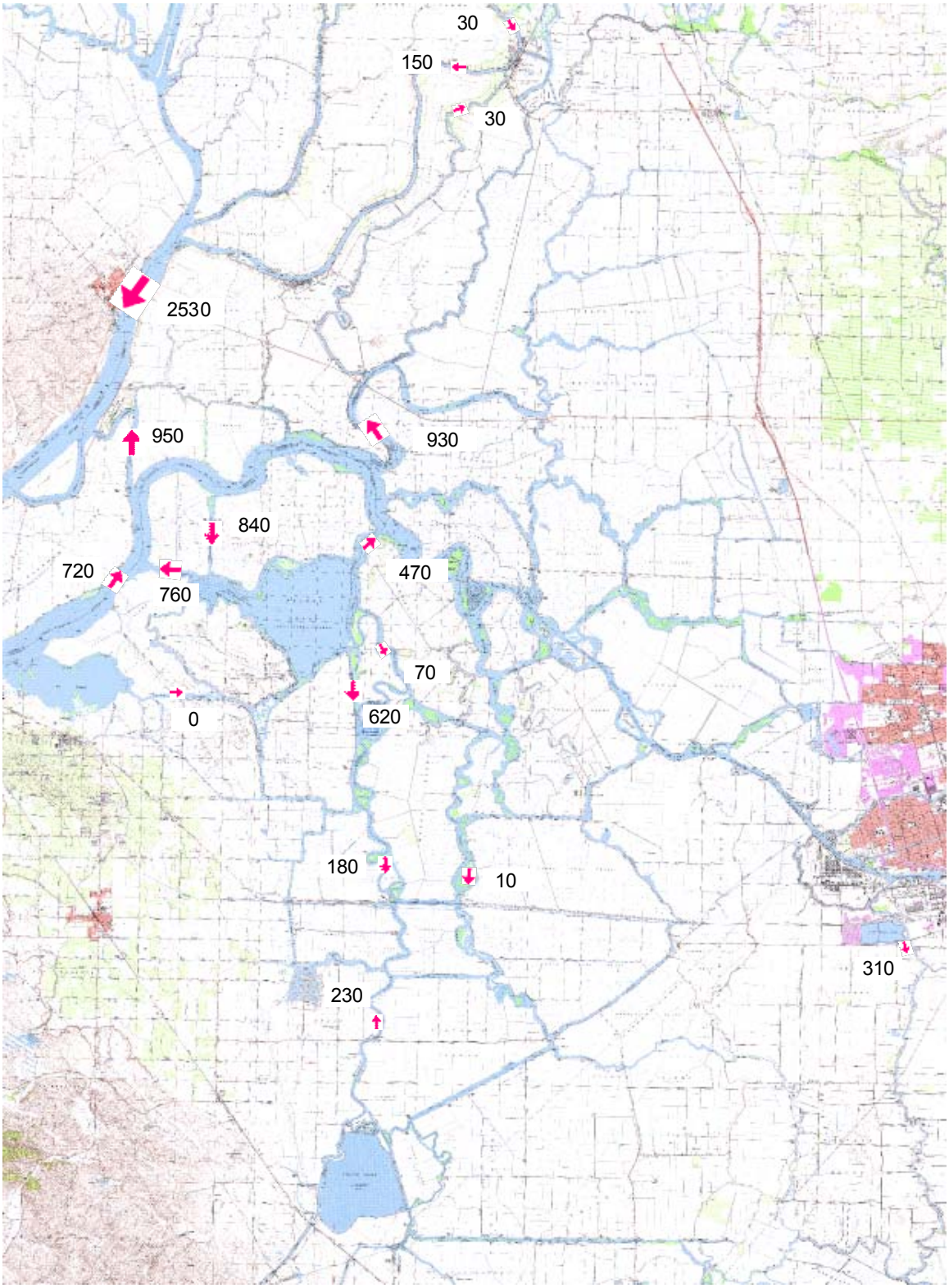

Figure 6-24 Average Observed minus Average Computed Net Flow (cfs), May 5 to May 19, 2002.

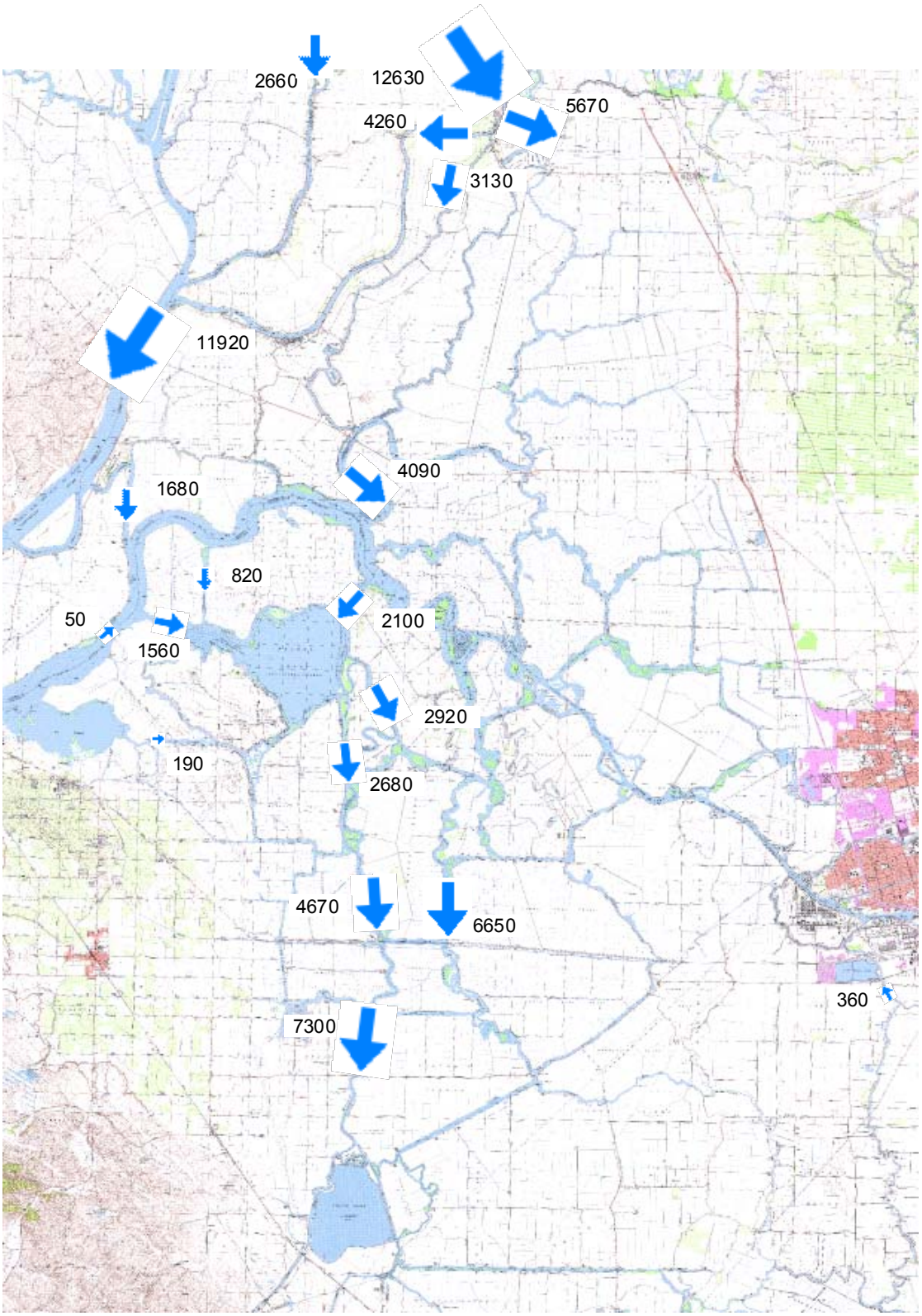

Figure 6-25 Average Observed Net Flow (cfs), July 14 to August 4, 2002.

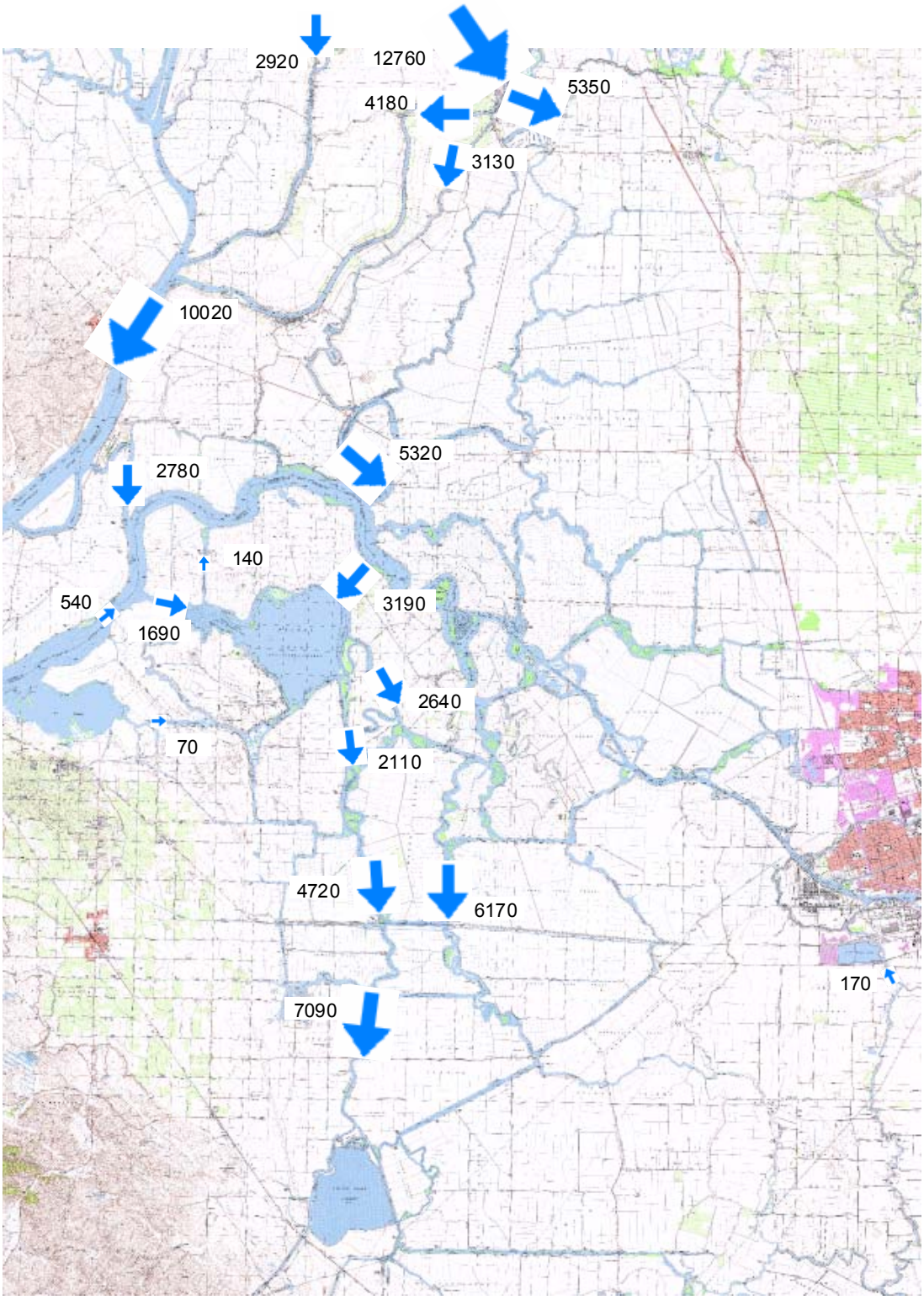

Figure 6-26 Average Computed Net Flow (cfs), July 14 to August 4, 2002.

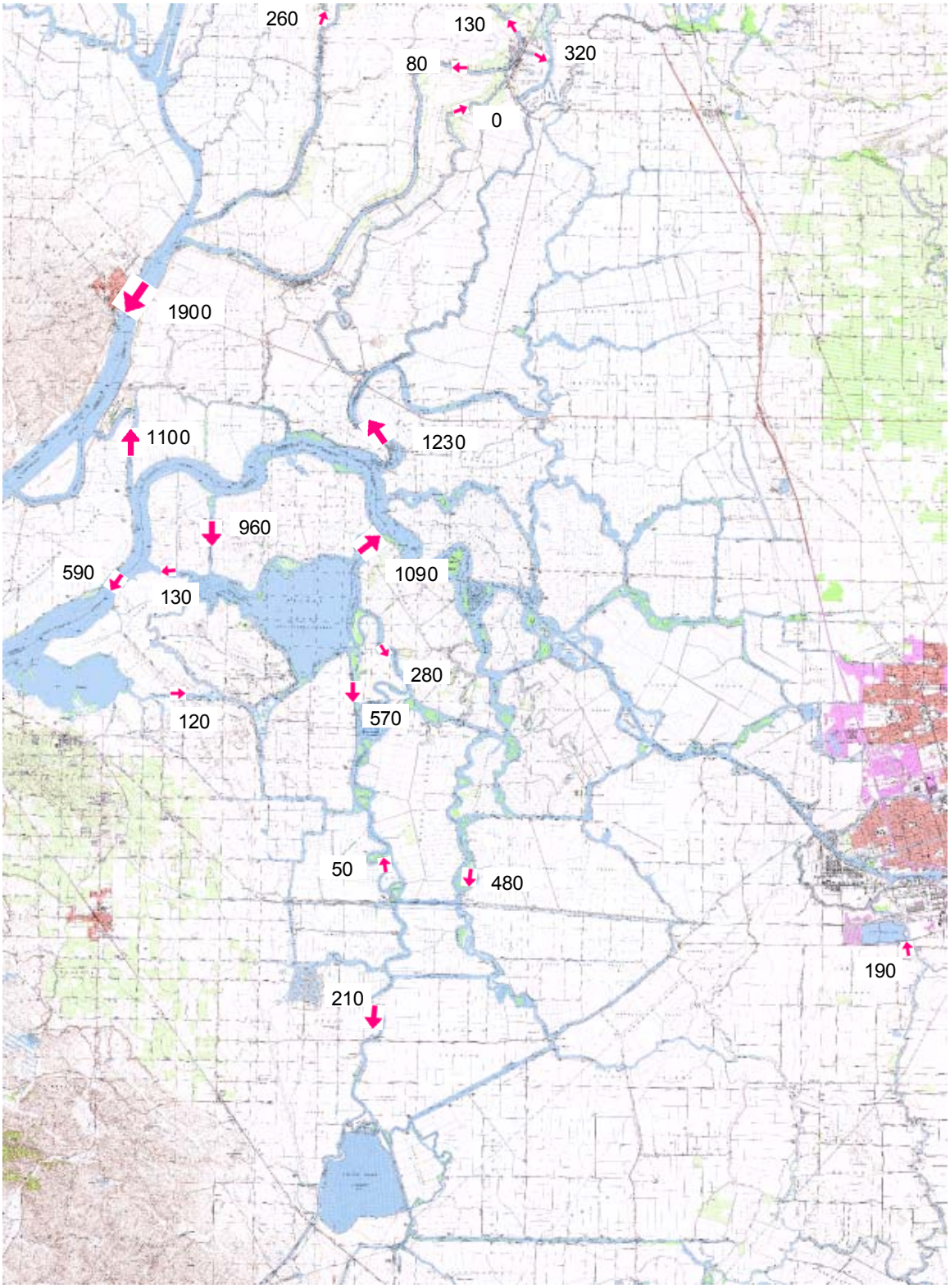

Figure 6-27 Average Observed minus Average Computed Net Flow (cfs), July 14 to August 4, 2002.

7 SALINITY CALIBRATION

7.1 OVERVIEW

Each year the Delta flushes with fresh water during the winter and spring. As spring flows recede (Net Delta Outflow is reduced), salinity begins to work its way upstream from San Pablo Bay, through Suisun Bay and into the western and central Delta. Salinity continues to increase in the Delta throughout the summer and fall period. In addition to the gradual increase in salinity through the dry period, the filling and draining of the Delta associated with spring and neap tidal cycles affects salinity. Larger tidal excursion during spring tides creates larger daily variations in salinity. Also, as the Delta fills during the spring tide, higher salinity water is pulled farther into the Delta causing a rise in the tidally averaged salinity. During the neap period, the Delta drains, resulting in a general reduction in tidally averaged salinity. Within the Delta, Delta Island Consumptive Use (DICU) acts as a salinity source by concentrating salts in return waters.

Modeling the transport of salt into the Delta requires that both the net flows and tidal flows be well represented by the hydrodynamic model. Model parameters affecting salinity transport are the longitudinal and transverse diffusion coefficients that represent sub-grid scale turbulent mixing. Salinity is primarily monitored using the surrogate observation of electrical conductivity (EC) measured in μmhos/cm. EC is a function of the balance of salts in the water column and not strictly conservative. However, the common approach to modeling salinity in the Delta is to simulate EC as a conservative constituent because of the lack of direct salinity measurements. The Department of Water Resources Delta Modeling section has found that EC is sufficiently conservative at the levels typically found in the Delta to warrant its use as a calibration parameter (DWR, 2001).

The salinity calibration is very good in the western Delta. The net flow errors in the Franks Tract region slow the transport of salt through Franks Tract, leading to a 10 to 15%

underestimation of tidally averaged EC late in the summer in Old River south of Franks Tract and subsequently at the SWP intake. Tidally averaged EC at the CVP intake matches observed data very closely.

7.2 MONITORING STATIONS

EC is calibrated to data collected at the monitoring stations shown in Figures 7-1 and 7-2 including, Antioch, Jersey Point, False River, Taylor Slough, Sand Mound Slough, Franks Tract West, Franks Tract East, Old River near San Joaquin River, San Andreas Landing, Mokelumne River near San Joaquin River, Old River at Holland Tract, Old River at Bacon Island, Middle River at Victoria Island, San Joaquin River near Stockton, SWP and CVP.

7.3 COMPUTED AND OBSERVED EC PLOTS

For each EC station shown in Figure 7-1 and 7-2, three plots of computed and observed flow are provided: dynamic and tidally averaged time series plots, and a scatter plot of computed versus observed data with linear regression statistics. Time series and scatter plots cover the period of May 1 through September 30, 2002. In reviewing the EC calibration, the tidally averaged time series plots provide the most important measure of model performance.

As with the stage and flow analysis, the scatter plots are produced by first running a cross-correlation between the observed data and model results to find the average phase lag over the entire record. The phase lag is removed from the computed record before creating the scatter plot and performing a linear regression analysis to find the best fit slope and offset. While there is a tidal signal in the EC time series records for most stations, the daily tidal variation is superimposed on the long term increasing trend as the Delta becomes more saline throughout summer and fall. Thus the phase lag estimate is not as meaningful as with the flow and stage plots. The statistics reported with the scatter plot include the following.

Mean Observed (EC)	Average value of observed EC from May 1 to September 30.
Mean Computed (EC)	Average value of computed EC from May 1 to September 30.

Lag (minutes)	Phase difference between observed and computed. A positive value indicates that the computed record lags behind the observed record.
Y = slope*X + offset (cfs)	Best linear fit where Y is computed and X is observed.
R2	Linear regression goodness of fit parameter.

Small location plots are also provided with each set of plots for convenient reference.

7.4 DETAILED COMMENTS

The model does an excellent job matching the transport of salt from the Martinez boundary through Suisun Bay to Antioch on the San Joaquin River. Both top and bottom EC is measured at Antioch (Figures 7-3 and 7-4). The tidally averaged model result is generally slightly higher than the top of the water column and lower than the bottom column. Given that the model uses a two-dimensional depth averaged approximation at that location, this is exactly the expected behavior. The general rise in observed EC over the calibration period as well as the spring-neap variation is well represented in both the dynamic and tidally averaged model result. The R2 value for this location is approximately 0.95, which is a very impressive fit for EC data.

Farther up the San Joaquin at Jersey Point (Figure 7-5) the model continues to do an excellent job matching both the dynamic and tidally averaged EC throughout the calibration period with an R2 value of 0.975.

On the Sacramento River at Rio Vista (Figure 7-6) the minimum daily EC throughout the year is strongly influenced by freshwater passing down from the north. As the year progresses and salt water moves farther into the Delta, flood tides bring increasing high EC peaks. The model matches the tidally averaged EC throughout the year very well. The dynamic variability is not as well represented as the previous two stations, although the range of minimum and maximum salinities for the computed and observed records is comparable.

Along the western edge of Franks Tract at the False River, Franks Tract West, Taylor Slough, and Sand Mound Slough stations (Figures 7-7 through 7-10) the model again closely matches the dry season rise and spring neap variations in tidally averaged EC. At False River the

daily EC variation is very well represented with a linear regression slope of 0.929 and an R2 of 0.979.

At Dutch Slough (Figure 7-11) the model under-predicts the rate of rise of EC such that by mid August the tidally averaged EC result is approximately 1,000 μmhos/cm while the observed EC is closer to 1,200 μmhos/cm. The spring neap variation is much less pronounced in the model result.

At San Andreas Landing on the San Joaquin (Figure 7-12) the minimum daily EC throughout the year is strongly influenced by freshwater from the Mokelumne River. As the year progresses and salt water moves farther up the San Joaquin, flood tides bring increasing high EC peaks. The model is showing the influence of the Mokelumne River at this station, but it is over-predicting the high salinity peaks in late summer by approximately 30% leading to an over estimation of tidally averaged EC by 15 to 20%. The model is moving a little too much salt up the San Joaquin, north of Franks Tract. This discrepancy would likely be improved if the net flows through Franks Tract were corrected as noted in the previous section on the flow calibration.

On the Mokelumne River near the San Joaquin (Figure 7-13) the observed data clearly shows that the typical EC value is established by fresh water moving downstream with high EC spikes occurring as the flood tide forces San Joaquin water back up the Mokelumne. As previously discussed, the model is not matching the peak flood flows in the Mokelumne, and so it follows that the model EC record does not show the same variability as the observed record. The tidal average EC, however, is well represented.

Comparison of computed and observed EC on the east side of Franks Tract (Figure 7-14) and subsequently at Holland Cut (USGS station shown in Figure 7-15 and permanent station shown in Figure 7-16) and Old River near Mandeville Island (Figure 7-17) indicated that the model does not move salt quickly enough through Franks Tract. During the first two weeks of July, the beginning of the period of rapidly rising EC, the tidally averaged model result tracks the observed data closely. However, as the summer progresses, the spring-neap variation in tidally averaged EC is much more pronounced in the observed record, and the overall rate of rise in

model EC is too slow. By mid August, the model EC is approximately 15% too low. This behavior is consistent with the assessment of net flows through Franks Tract.

The model is not providing a good representation of EC on Old River near the San Joaquin (Figure 7-18). Further calibration at this station will not be attempted until the net flows through Franks Tract are corrected.

There is an EC monitoring station at Old River near Bacon Island (Figure 7-19), however, the data from that station is highly suspect. The observed record has periods of very large and very small daily variation, which do not seem to be justified relative to other EC stations. Also, the typical salinity is to low relative to salinity observed at other stations on Old River. No attempt was made to calibrate the model for this station.

On Middle River at Victoria Island (Figure 7-20), the computed and observed records agree very well. The tidally averaged computed record is slightly higher (typically 25 to 50 μmhos/cm) than observed and matches the pattern of the observed record throughout the calibration period. There is slightly more daily variation in the observed record.

On the San Joaquin River near Stockton (Figure 7-21) EC is primarily a function of the San Joaquin River boundary condition at Vernalis. The computed and observed records match very well throughout the year.

The stations that are most important in evaluating the calibration are the SWP and CVP intake locations (Figures 7-22 and 7-23). The quality of water at these locations depends on mixture of water drawn from Old River near Franks Tract, Middle River, and the San Joaquin River through Old River at Head and Turner Cut. As shown, the model provides a good representation of EC in Middle River and the San Joaquin near Stockton, while the EC in Old River coming south from Franks Tract is approximately 15% low in the later part of the summer. At the CVP, which is more strongly dominated by Middle River and San Joaquin water, the model provides a very good representation of the tidally averaged EC throughout the summer. At the SWP, the influence of Old River is more important and the model underestimates the tidally averaged EC by 10 to 15%. At both stations the observed daily variability is much larger than predicted by the model. Currently the channels and junctions in the neighborhood of the

CVP and SWP intakes are represented as one-dimensional elements with cross-sections based on relatively old bathymetric data. Revising the geometry and moving to two-dimensional elements in this area may improve the representation of mixing and resolve more of the variability observed in EC.

ID Code	Name
RSAC101	Rio Vista
RSAC092	Emmaton
RSAN007	Antioch
RSAN018	Jersey Point
RSAN032	San Andreas Landing
RSAN058	SJR near Stockton
ROLD014	Old R. at Holland Cut
ROLD024	Old R. at Bacon Is.
RMID015	Middle R. at Bacon Is.
RMID023	Middle R. at Victoria Is.

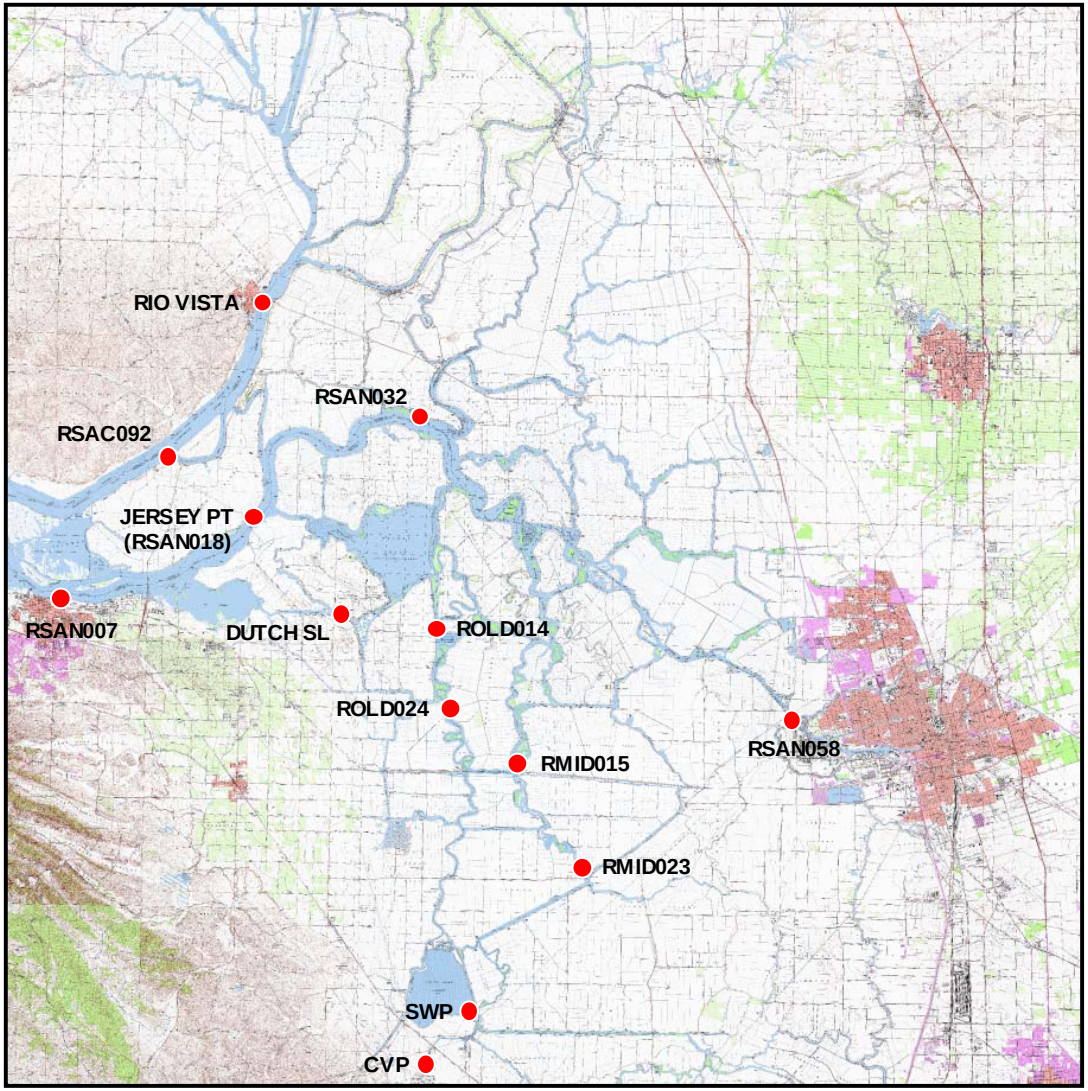

Figure 7-1 Delta EC monitoring stations.

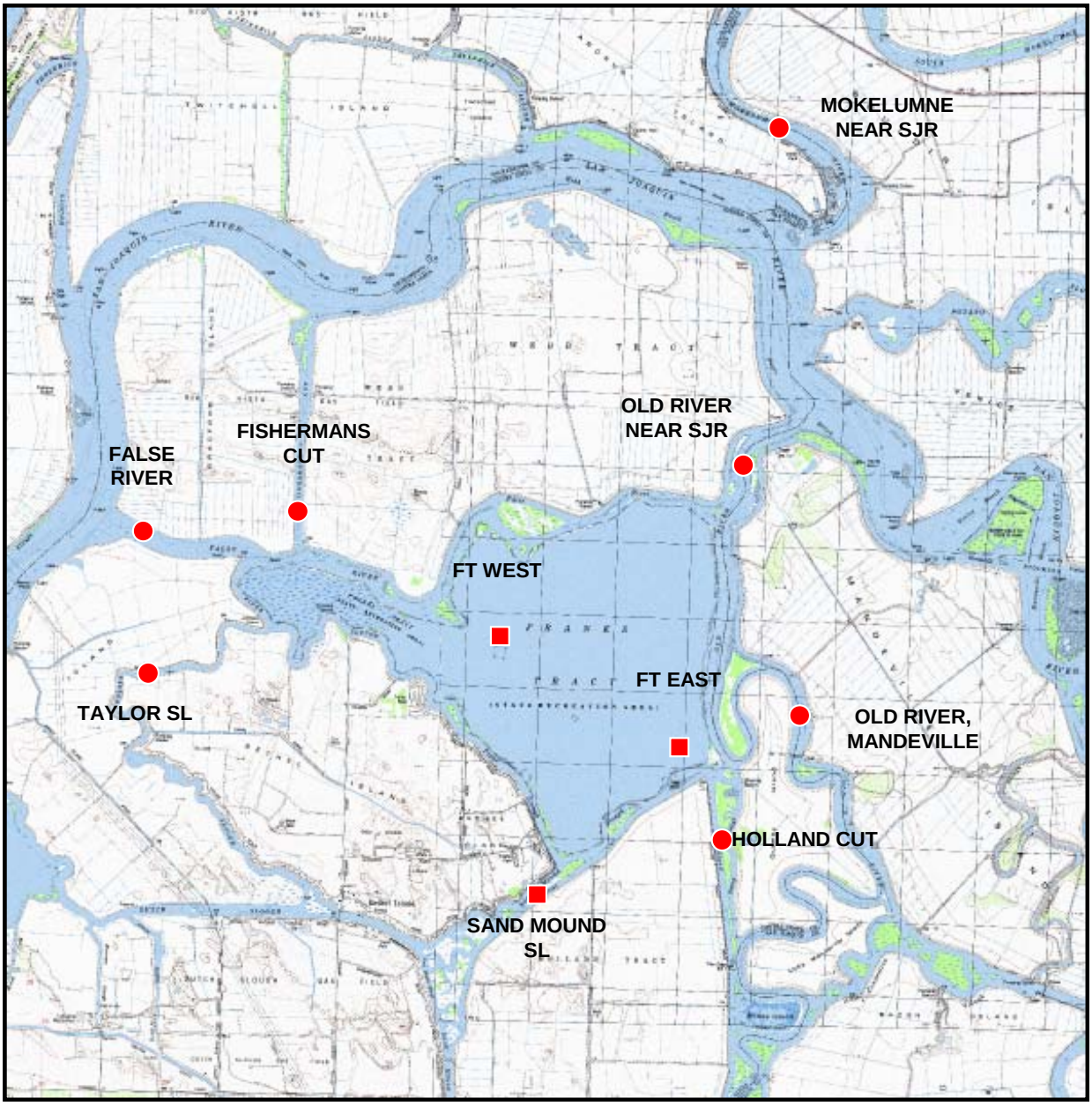

Figure 7-2 USGS monitoring locations.

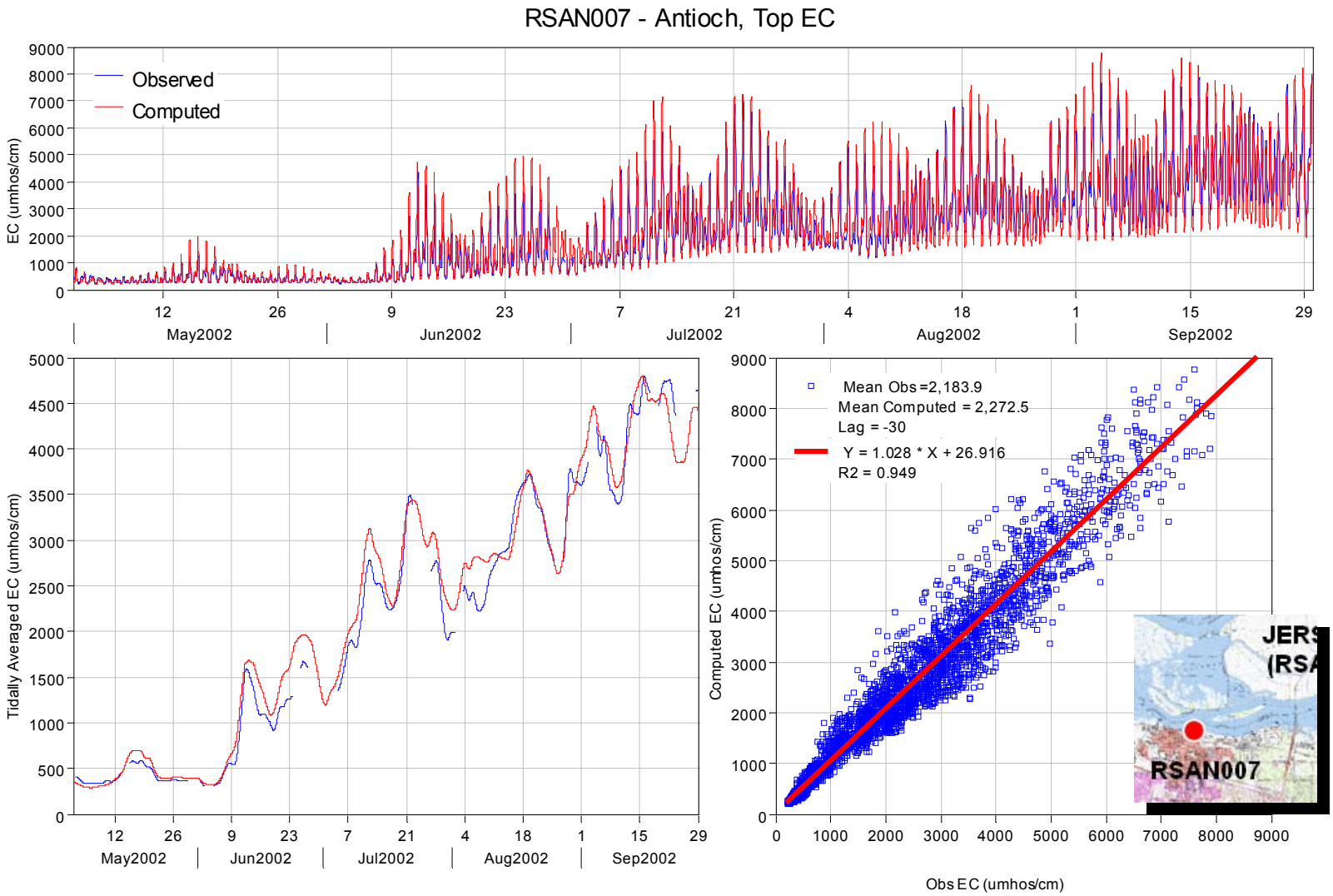

Figure 7-3 Computed EC with observed surface EC at RSAN007 - Antioch.

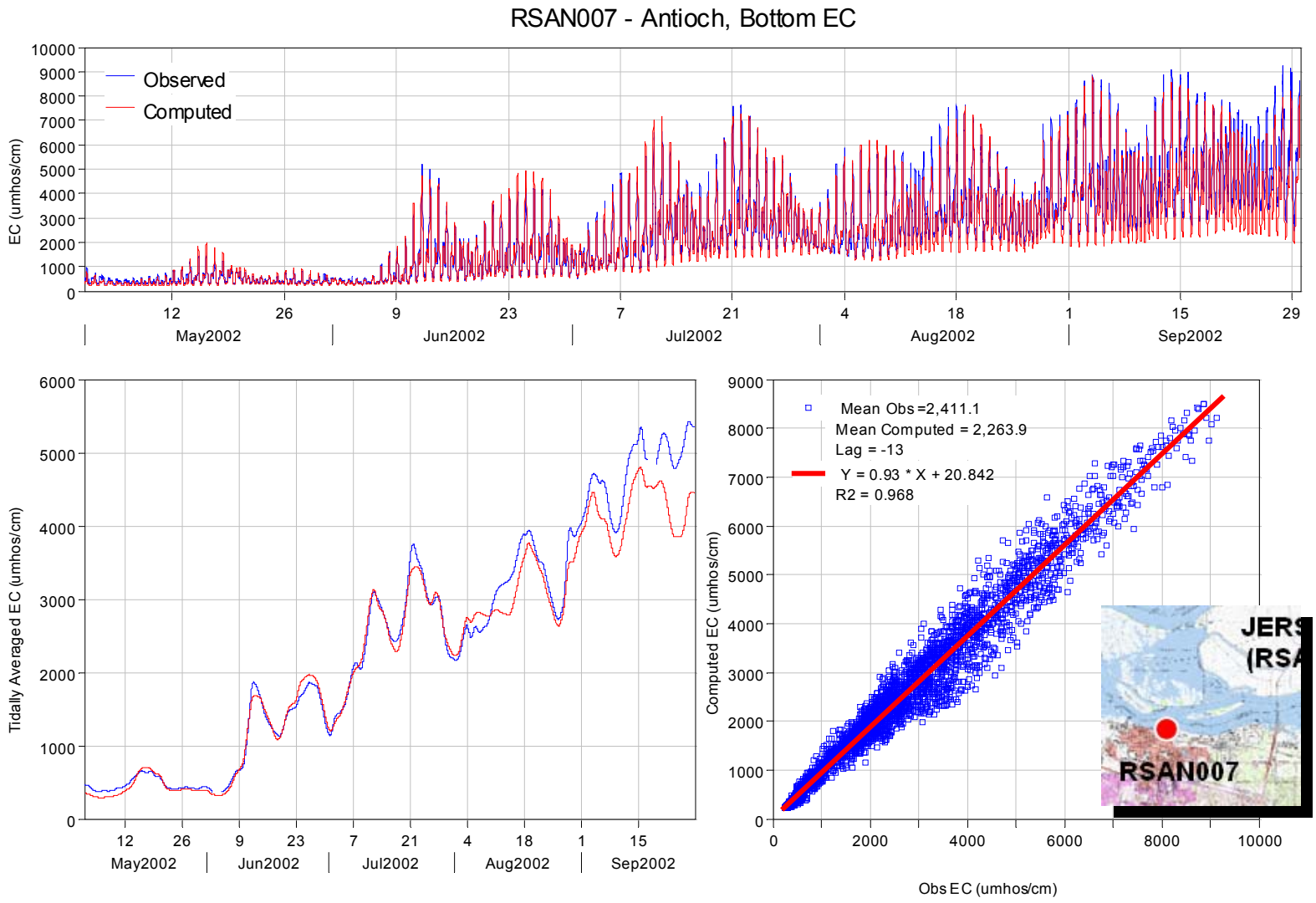

Figure 7-4 Computed EC with observed bottom EC at RSAN007 - Antioch.

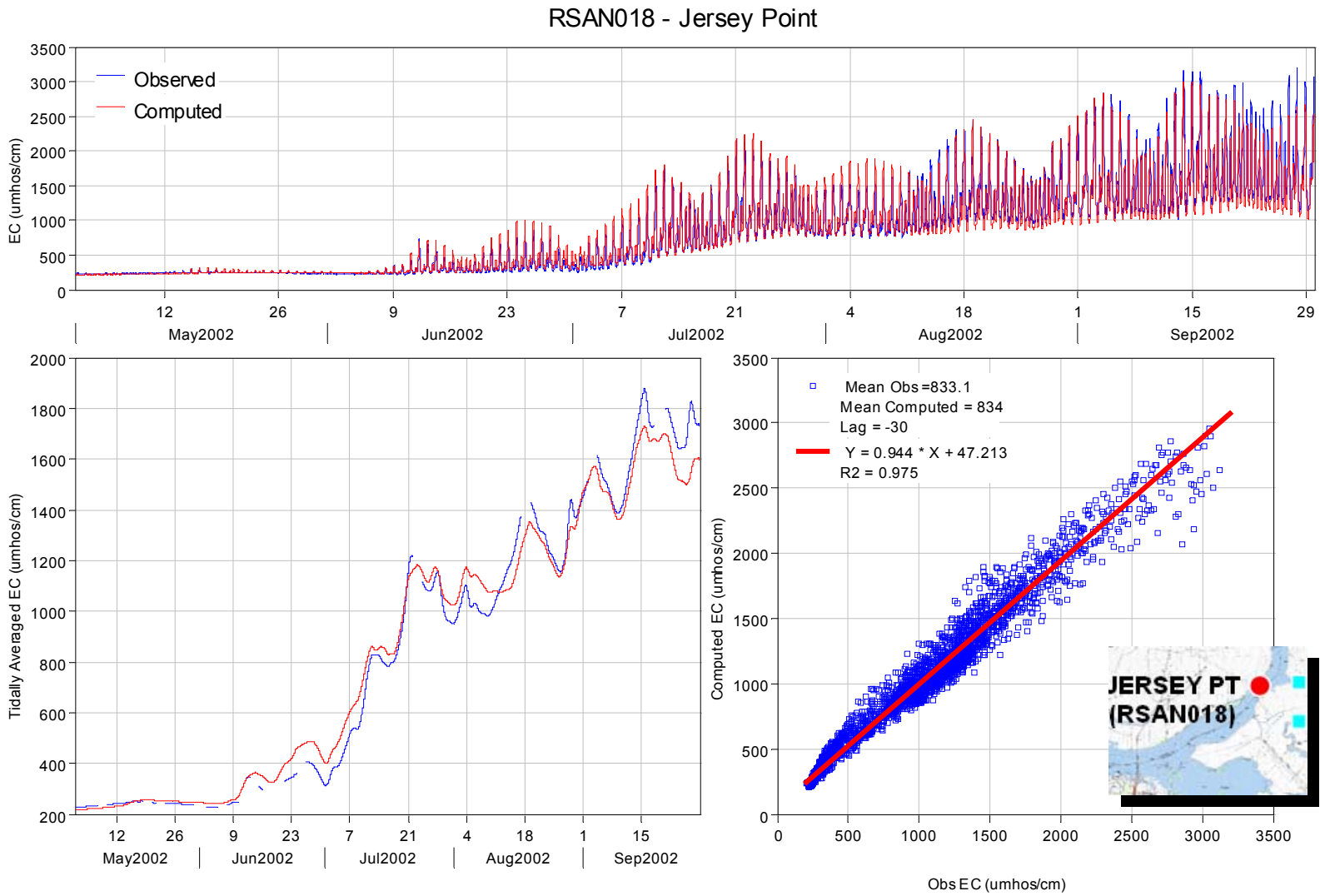

Figure 7-5 Computed and observed EC at RSAN018 - Jersey Point.

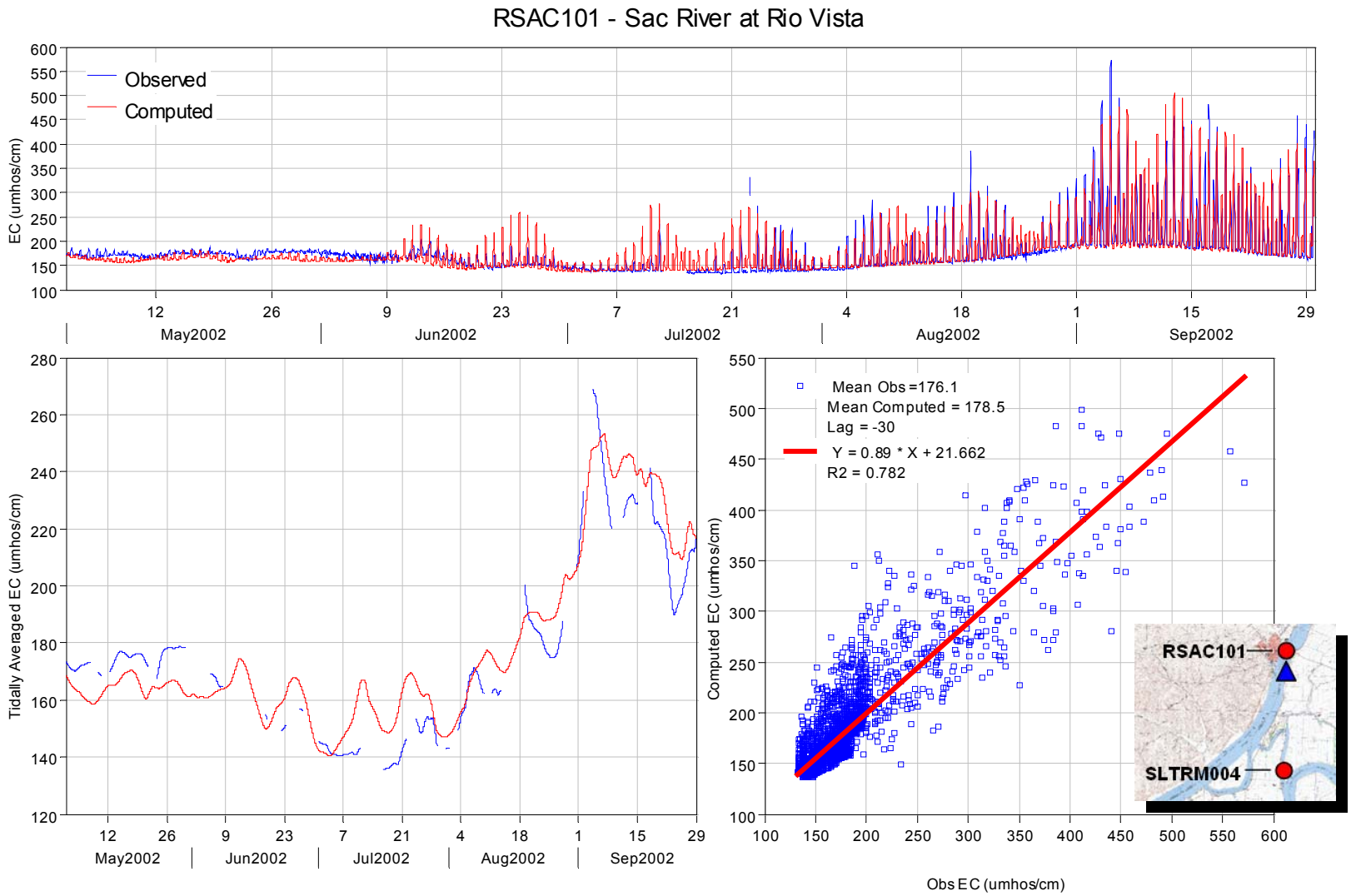

Figure 7-6 Computed and observed EC at Rio Vista - RSAC101.

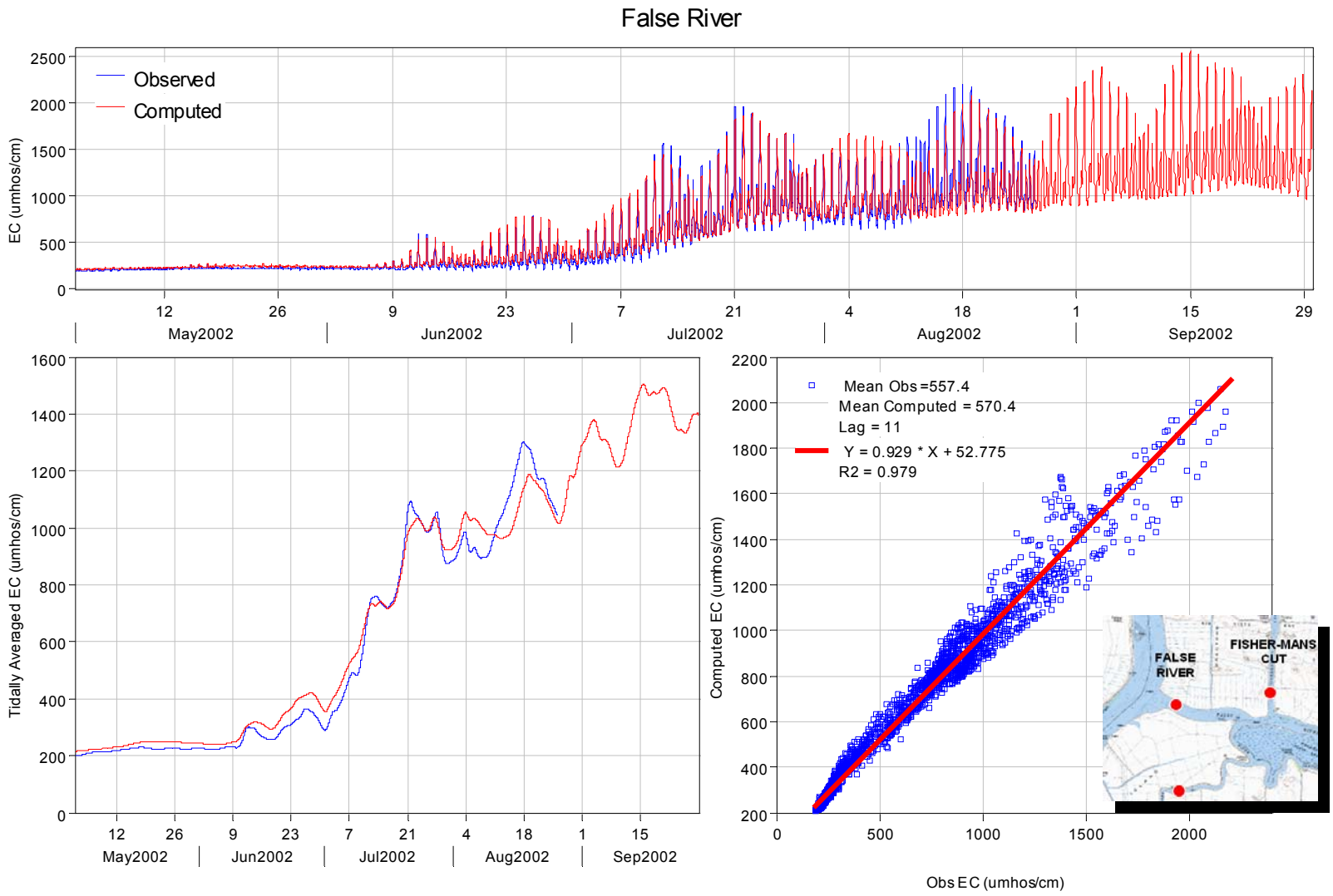

Figure 7-7 Computed and observed EC in False River.

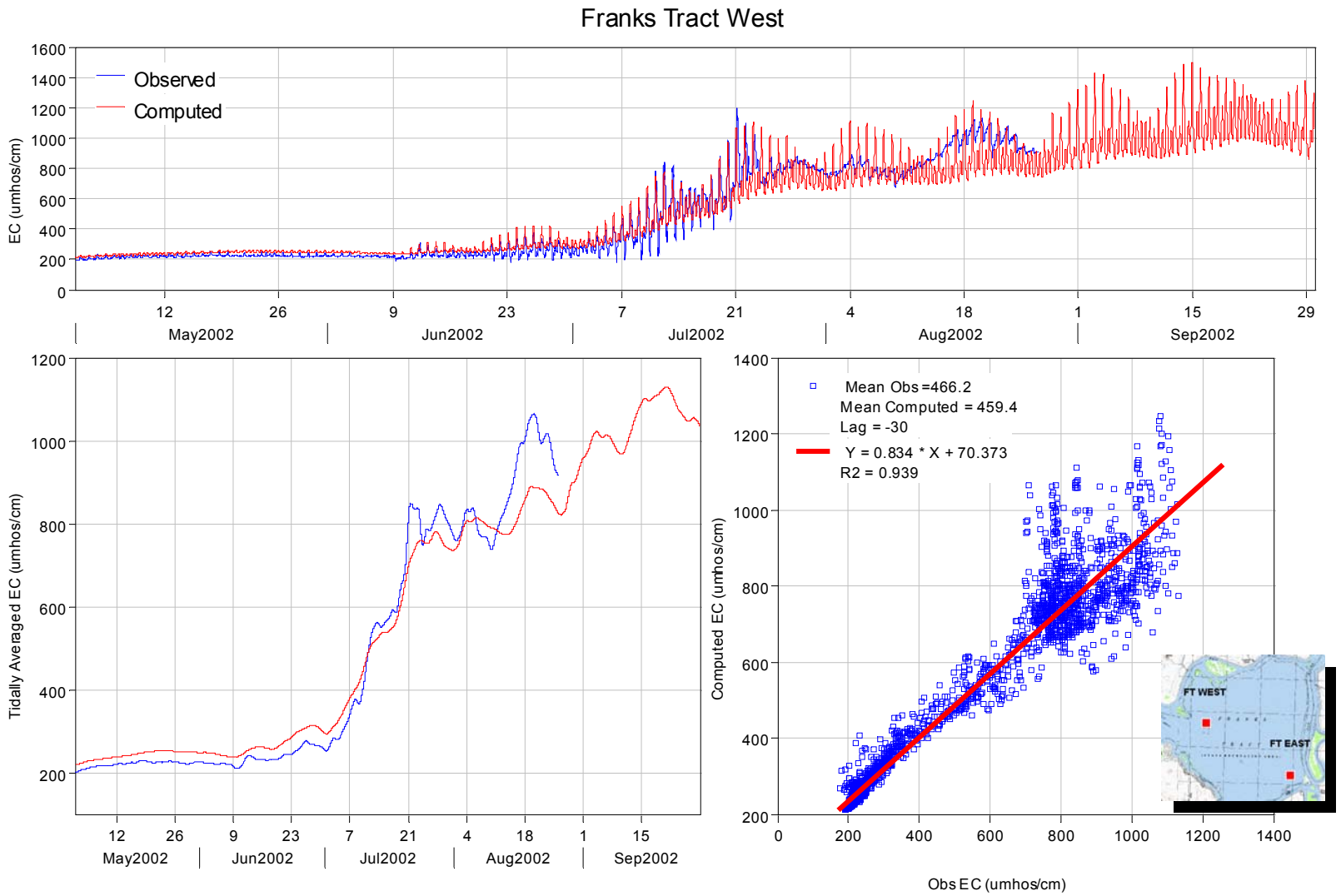

Figure 7-8 Computed and observed EC at Franks Tract West.

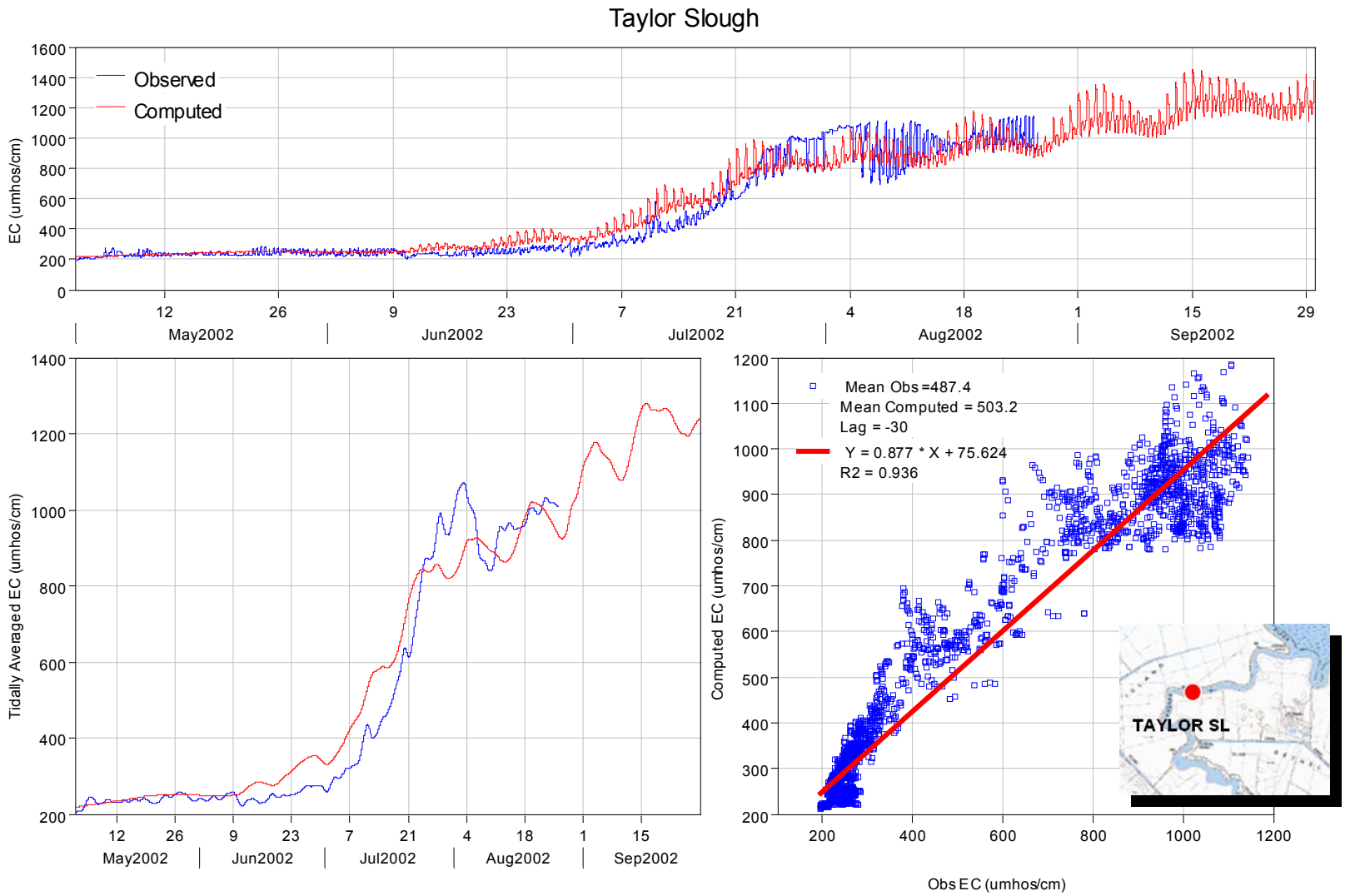

Figure 7-9 Computed and observed EC in Taylor Slough.

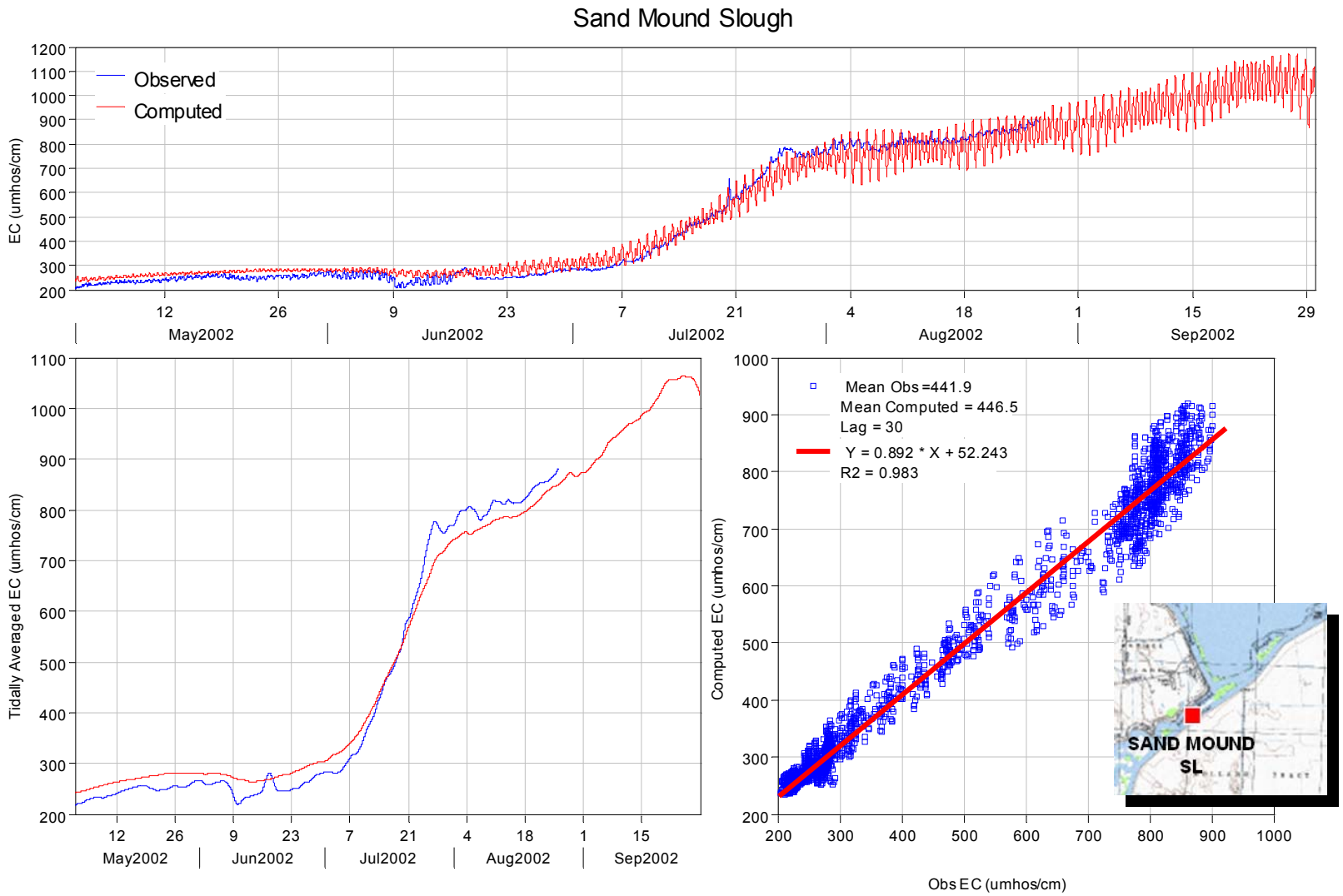

Figure 7-10 Computed and observed EC in Sand Mound Slough.

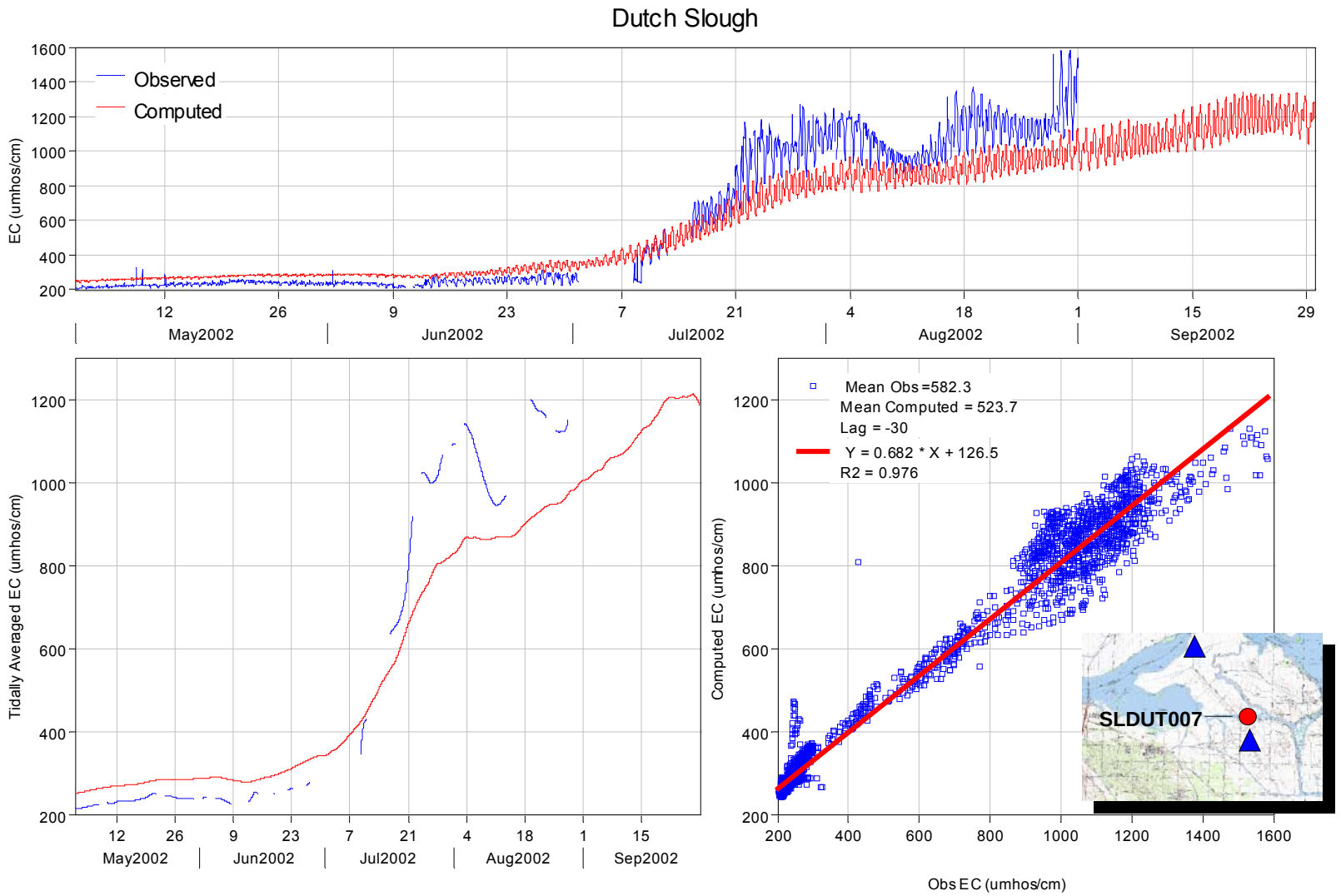

Figure 7-11 Computed and observed EC in Dutch Slough - SLDUT007.

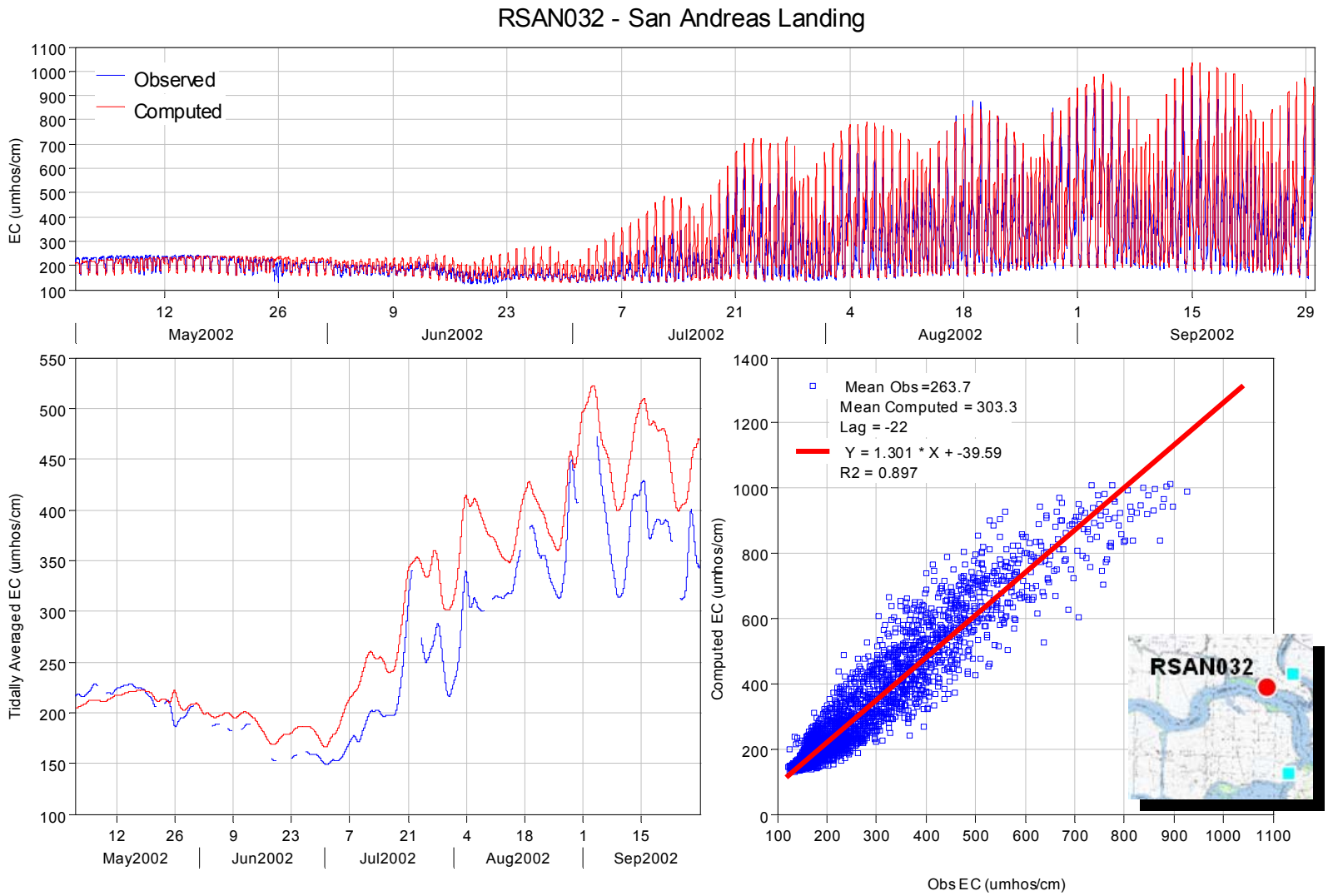

Figure 7-12 Computed and observed EC at RSAN032 - San Andreas Landing.

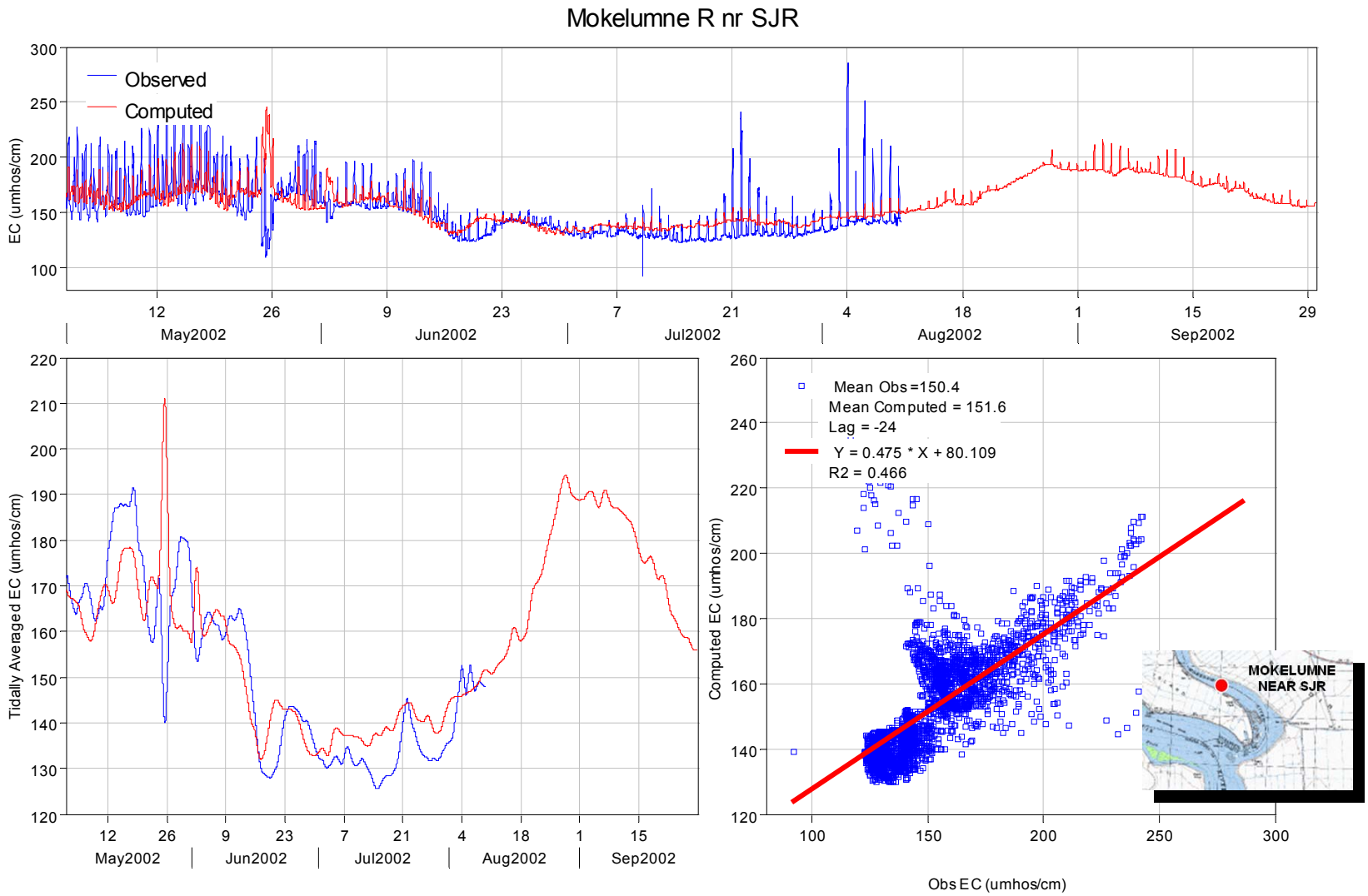

Figure 7-13 Computed and observed EC in Mokelumne River near San Joaquin River.

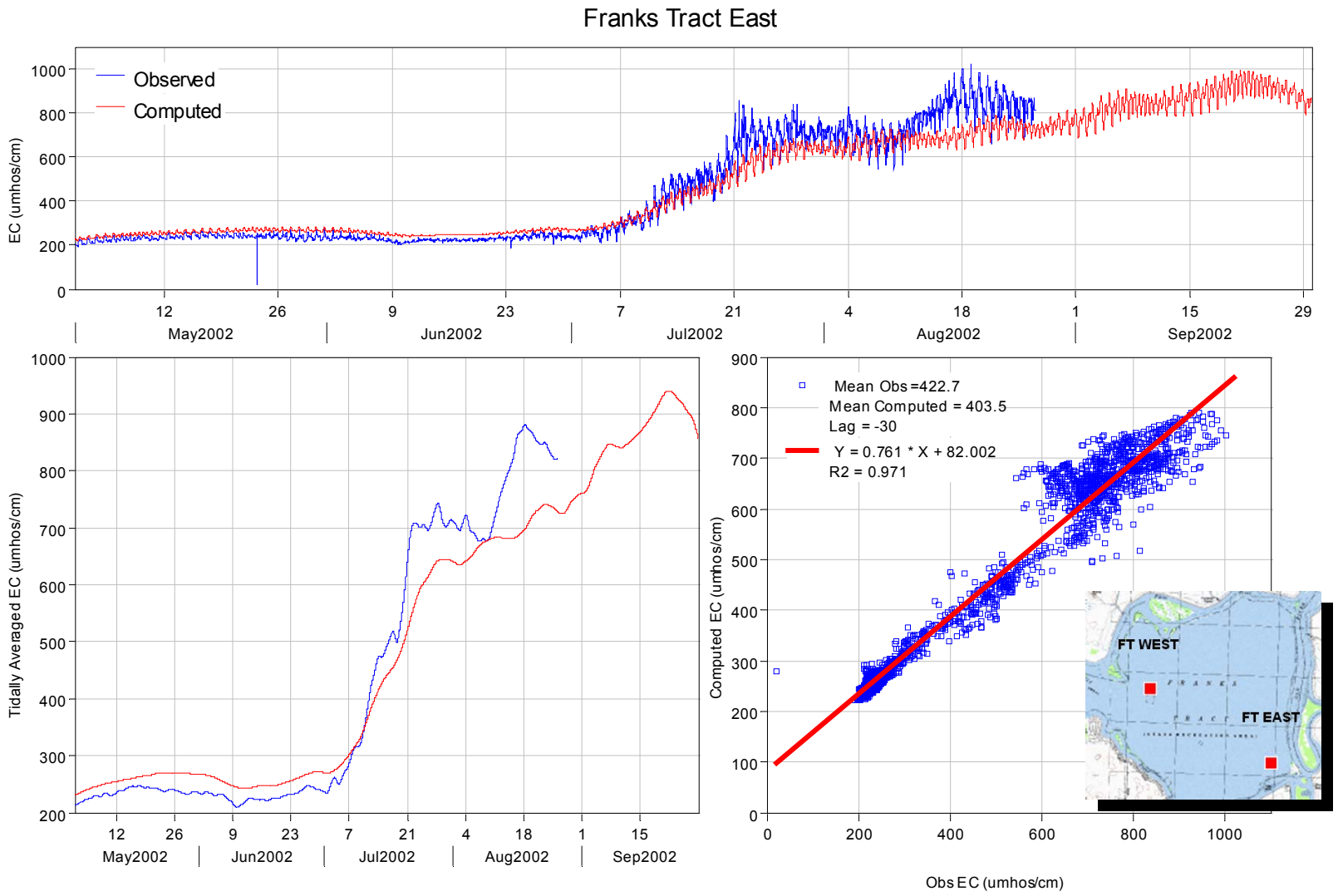

Figure 7-14 Computed and observed EC at Franks Tract East.

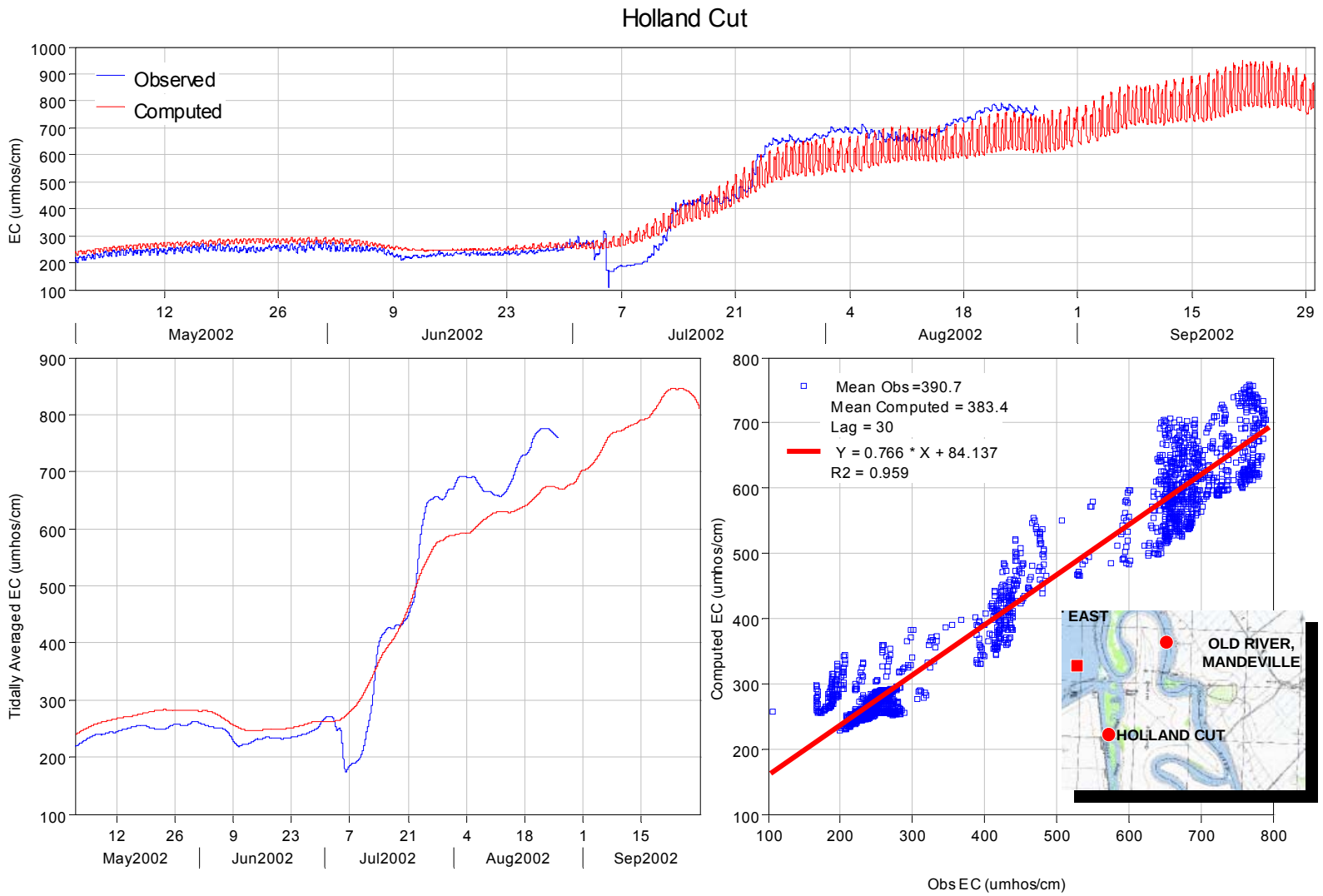

Figure 7-15 Computed and observed EC in Old River at Holland Cut (USGS station).

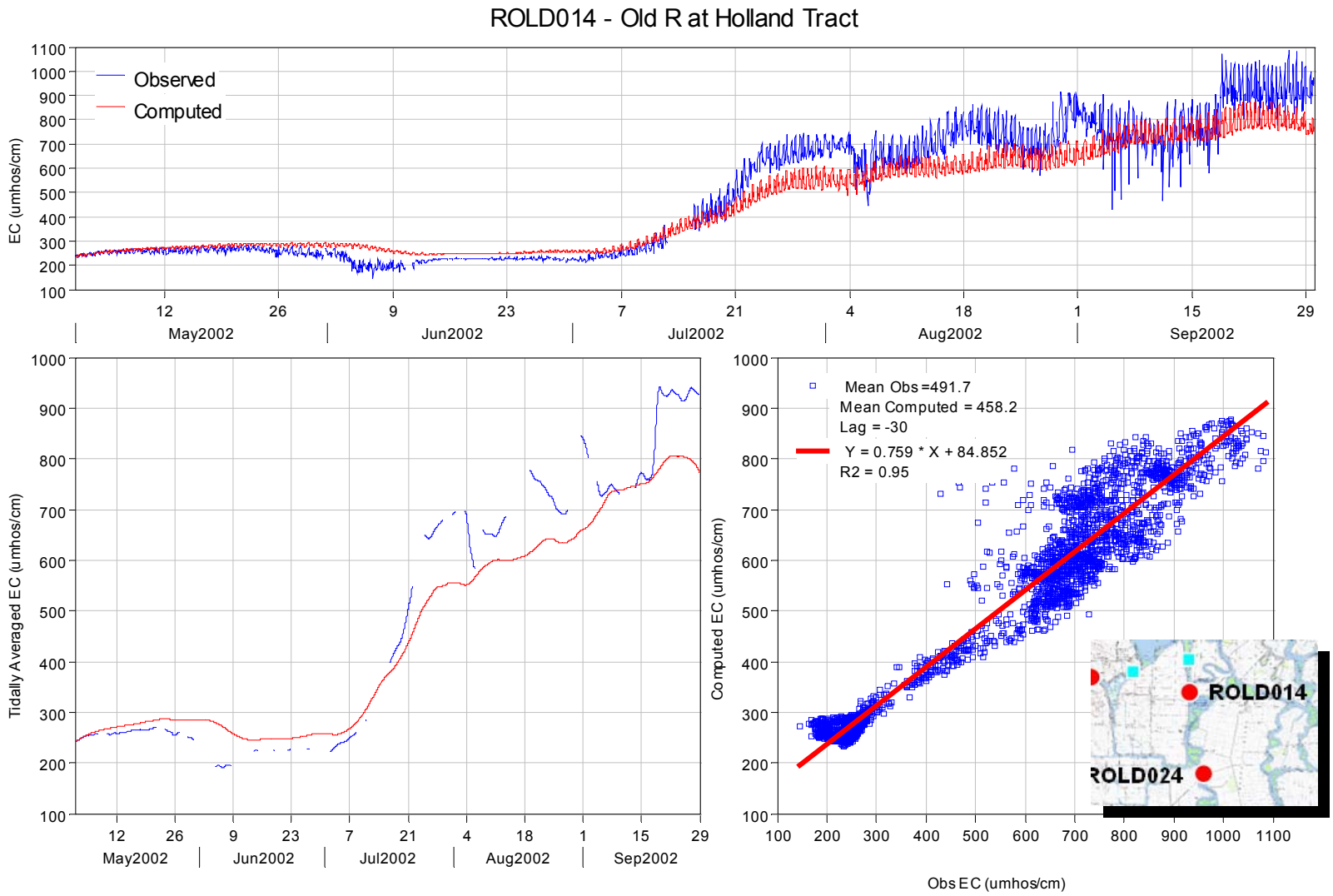

Figure 7-16 Computed and observed EC at ROLD014 - Old River at Holland Cut.

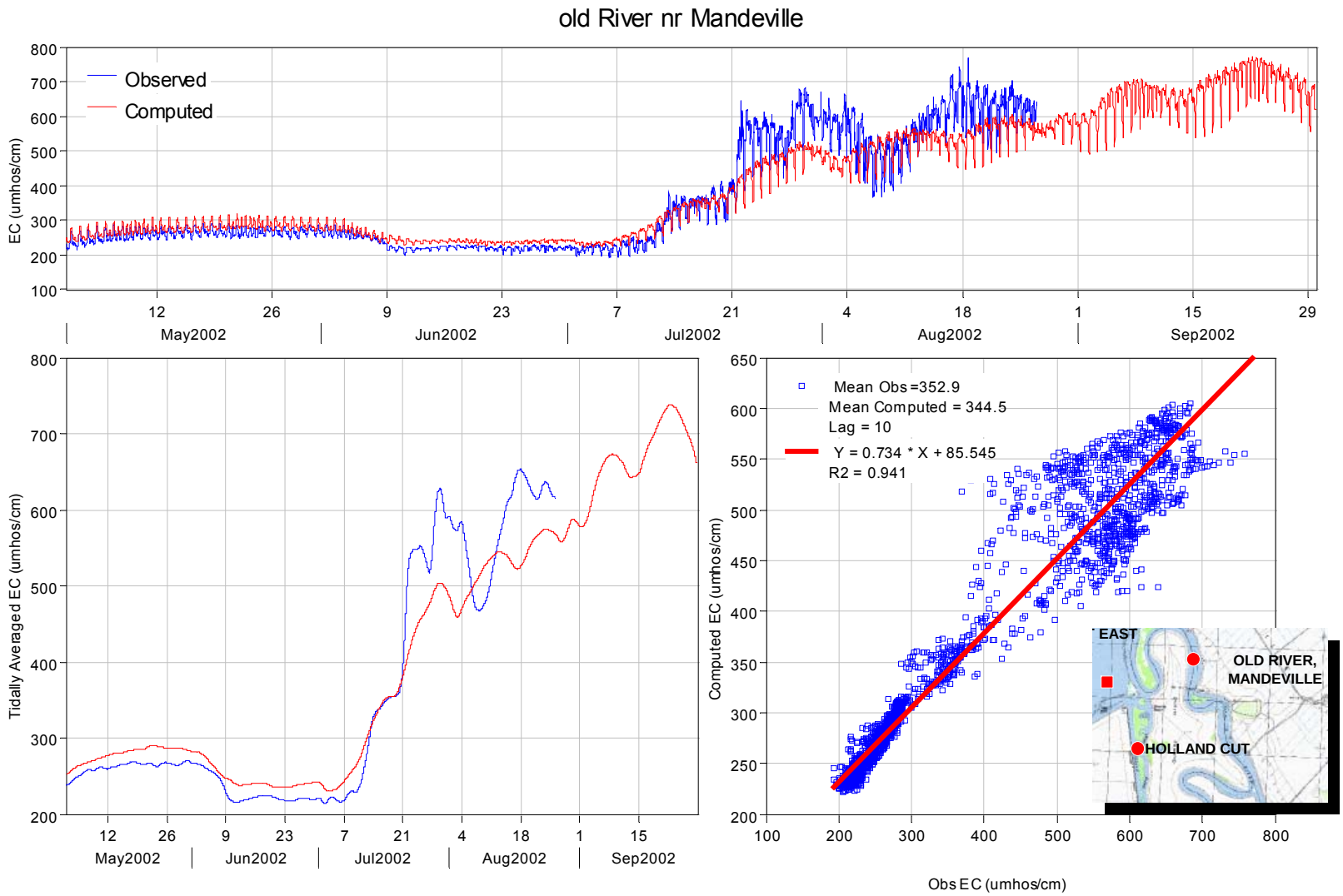

Figure 7-17 Computed and observed EC in Old River near Mandeville Island.

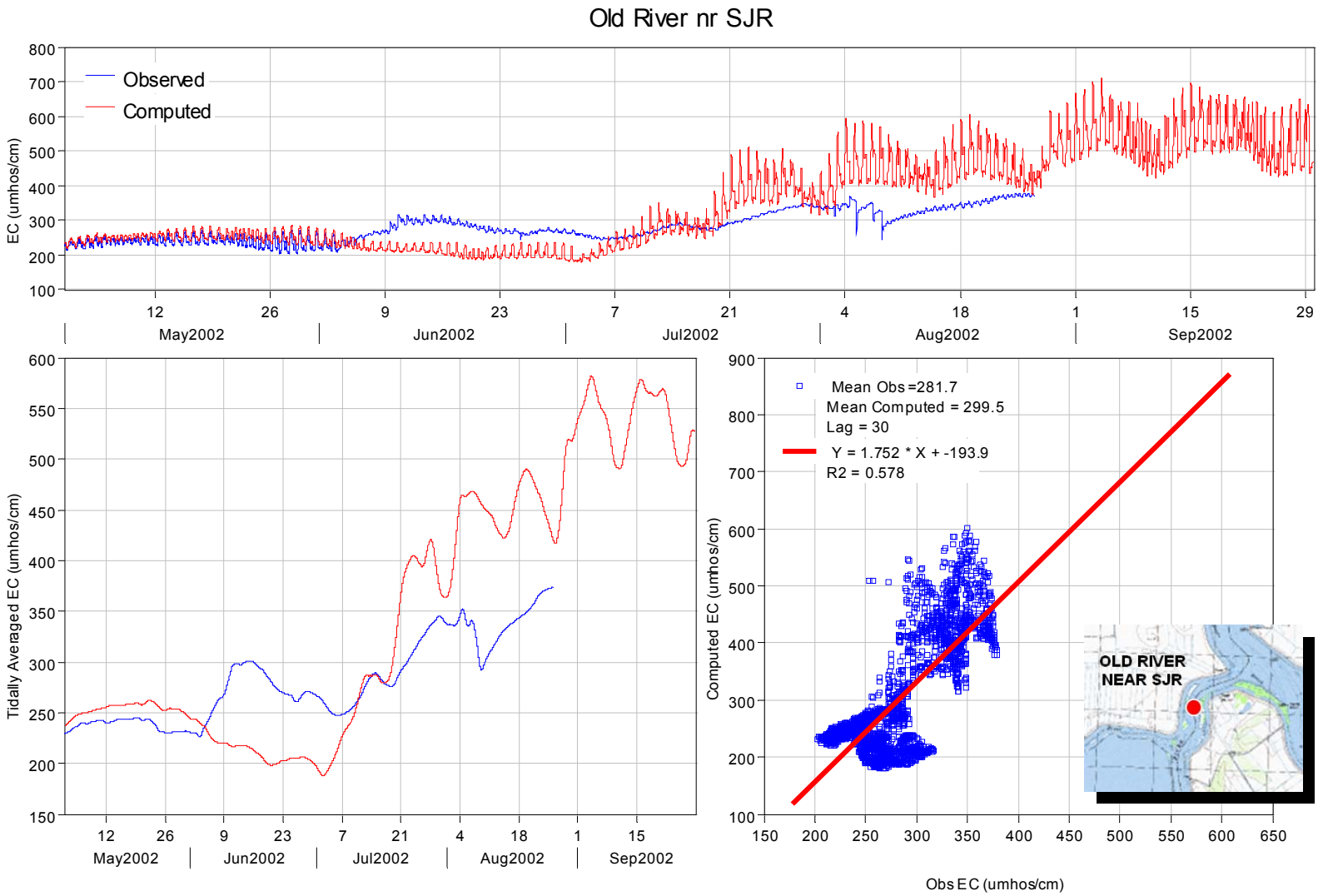

Figure 7-18 Computed and observed EC at Old River near San Joaquin River.

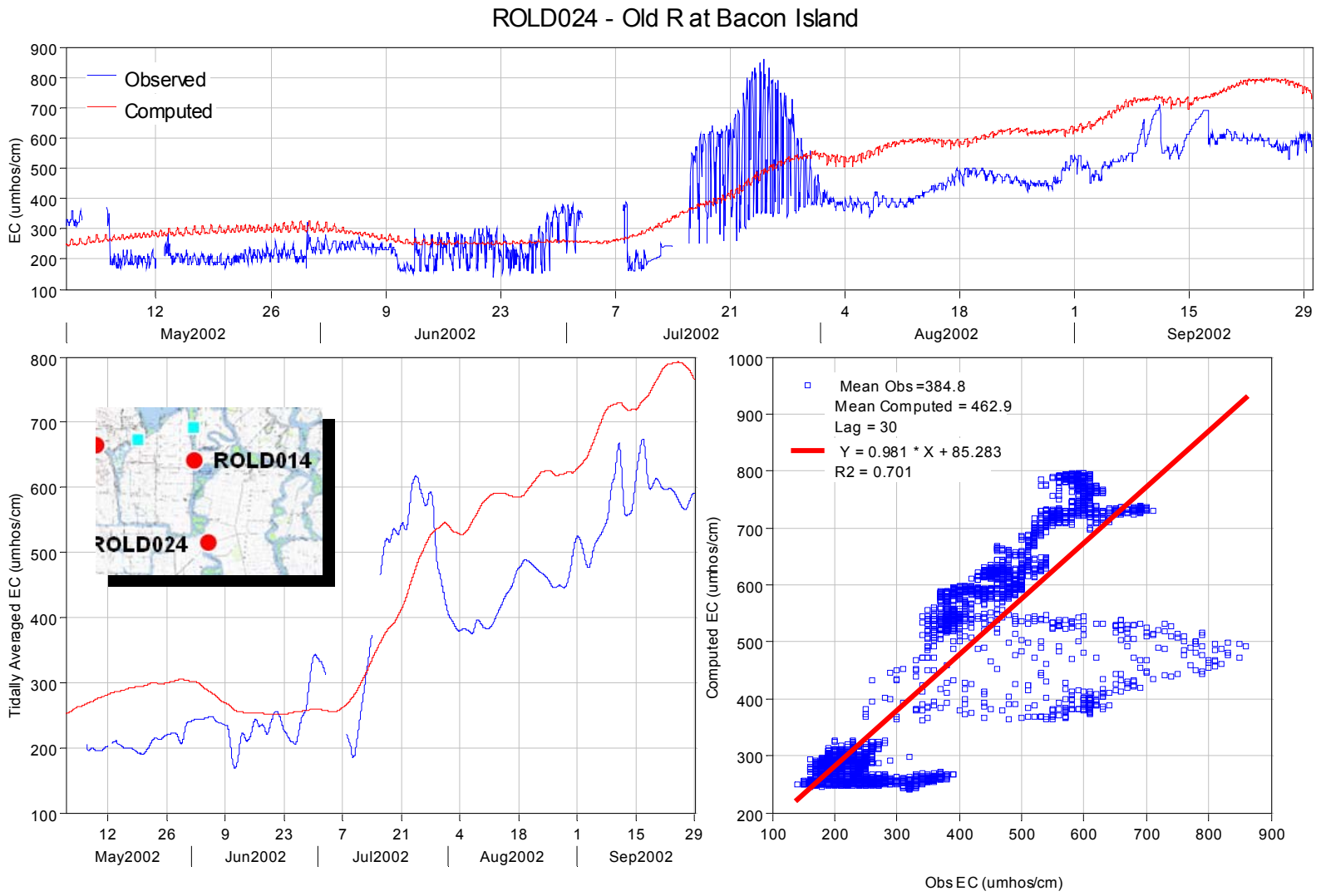

Figure 7-19 Computed and observed EC at ROLD024 - Old River at Bacon Island.

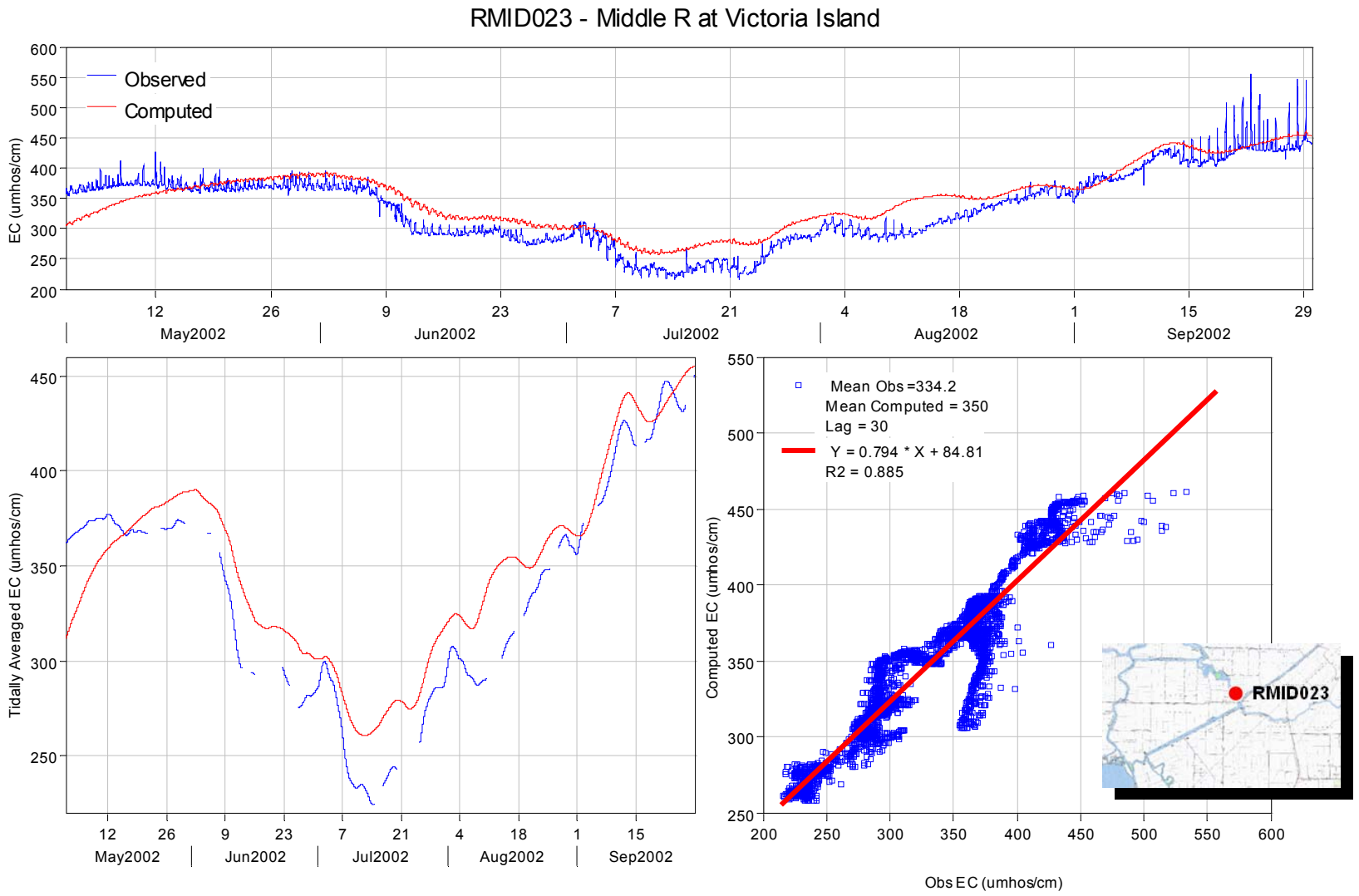

Figure 7-20 Computed and observed EC at RMID023 - Middle River at Victoria Island.

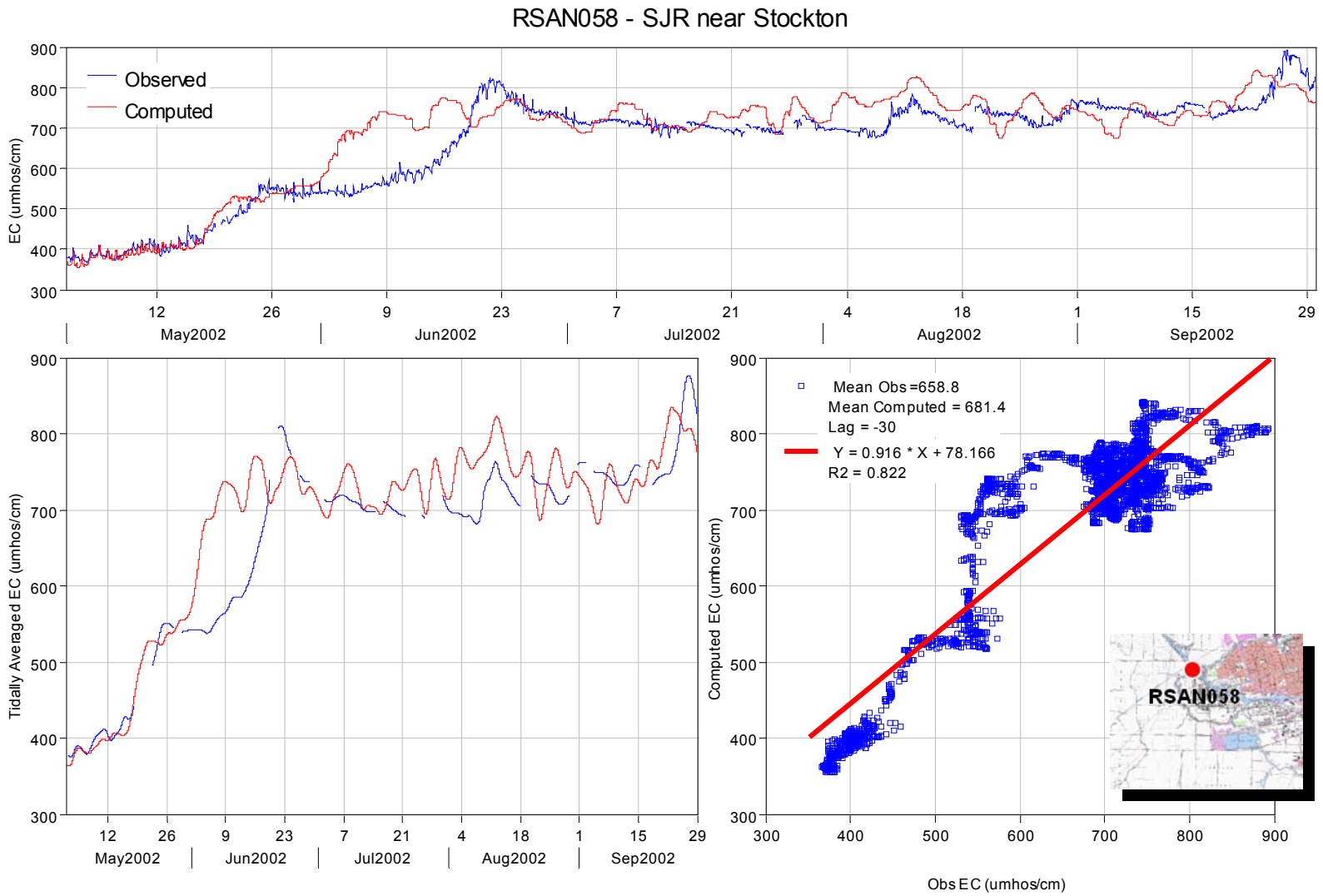

Figure 7-21 Computed and observed EC at RSAN058 - San Joaquin River near Stockton.

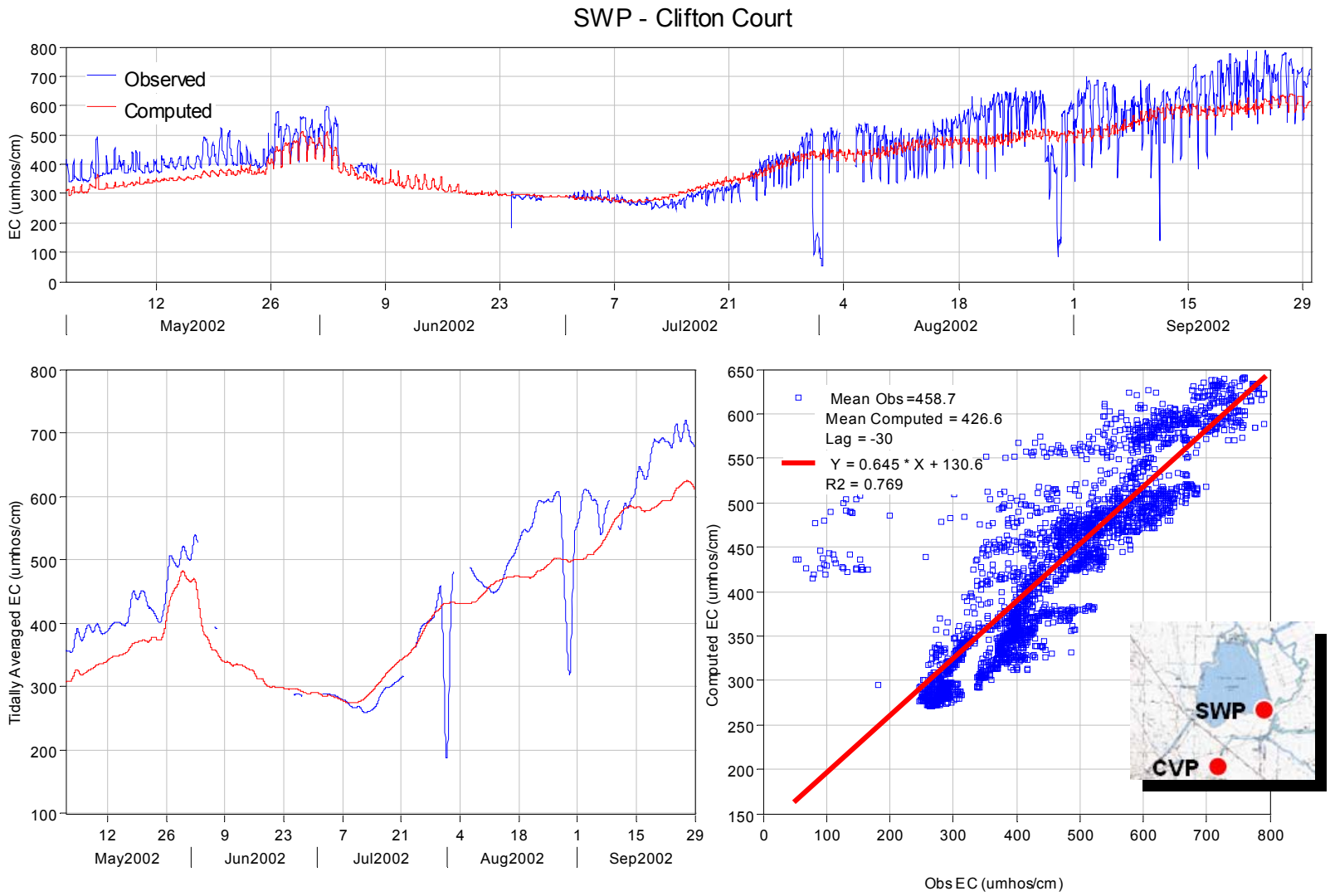

Figure 7-22 Computed and observed EC at the SWP - Clifton Court.

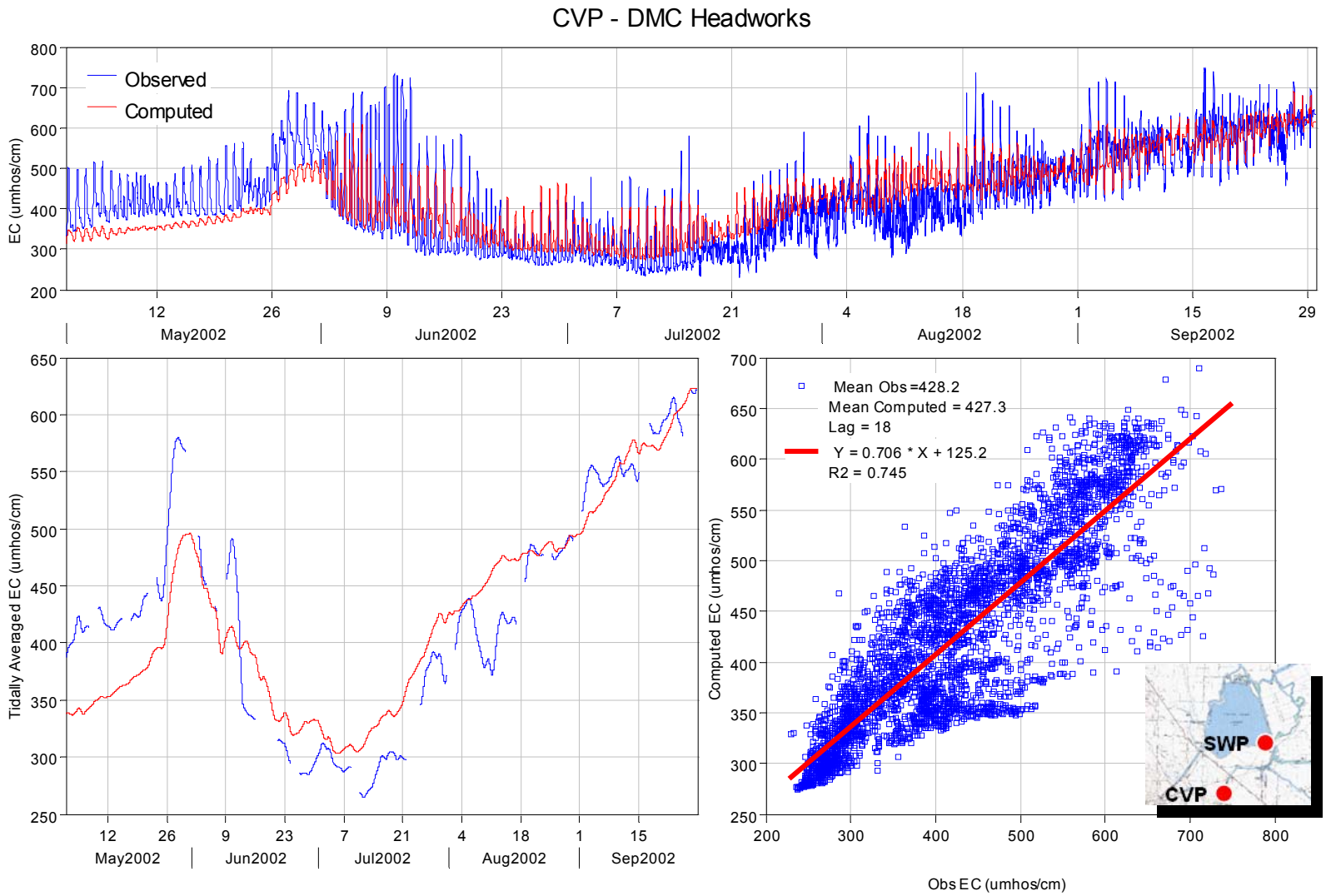

Figure 7-23 Computed and observed EC at the CVP – Delta-Mendota Canal Headworks.

8 CONCLUSIONS

8.1 SUMMARY OF STAGE CALIBRATION

The stage calibration for phase and amplitude is excellent overall. Tidal amplitude is typically within 5% of observed and phase errors are within 4 minutes. In general the model matches reported absolute stage within 0.05 to 0.25 feet, while at a few station the difference is as large as 0.5 to 0.7 ft. Performing coupled hydrodynamic and salinity simulation helped to improve the stage calibration overall in the Delta. Further effort calibrating for absolute stage is not warranted until uncertainties in the individual station datums have been resolved.

8.2 SUMMARY OF FLOW CALIBRATION

Flow calibration for the model is very good overall. Excellent results have been achieved in False River, San Joaquin River at Jersey Point and at the Old and Middle River UVM stations. Predicted tidal flow amplitude is typically within 5 to 10% of observed and linear regression R2 values are 0.97 and greater. Overall the model is doing a very good job simulating the tidal dynamics of a complex interconnected system. However, improvement is still needed to match net flows in Fisherman's Cut, Old River between Franks Tract and the San Joaquin, Mokelumne River near the San Joaquin, the Delta Cross Channel, and in Three Mile Slough.

Most significantly, the model over-predicts the net flow entering the northeast corner of Franks Tract from the San Joaquin River via Old River. This is mainly low salinity water which dilutes the higher salinity water coming from False River and the west side of Franks Tract. As a result, the model salinity on the east side of Franks Tract and ultimately Old River south of Franks Tract tends to be somewhat lower than observed. Similarly, the model under-predicts the net flow south on Fisherman's Cut, towards the west side of Franks Tract. These flows differences suggest a tidal asymmetry where flow enters the west side of Franks Tract on the flood tide with less resistance than the model is showing.

8.3 SUMMARY OF SALINITY CALIBRATION

The salinity calibration is very good in the western Delta. The net flow errors in the Franks Tract region slow the transport of salt through Franks Tract, leading to a 10 to 15% under estimation of tidally averaged EC late in the summer in Old River south of Franks Tract and subsequently at the SWP intake. Tidally averaged EC at the CVP intake matches observed data very closely.

8.4 DIRECTION FOR FUTURE WORK

Although the overall calibration of the model is excellent, there are still several areas where additional calibration effort is needed. Of primary concern are the net flows through Franks Tract. It appears that too much flow from False River is going through Fisherman's Cut to the San Joaquin River rather than going through Franks Tract and Old River to the San Joaquin River. There is a shift in Fisherman's Cut net flow of 900 cfs toward the San Joaquin, and a shift in net flow in Old River near the San Joaquin of 800 cfs toward Franks Tract. This results in slow movement of salinity through Franks Tract, dampened spring neap variation in salinity east of Franks Tract, slow rise of salinity levels through the summer east of Franks Tract and underestimation of salinity at the SWP export location. Conversely, too much salt moves up the San Joaquin River.

One possible cause of the net flow errors through Franks Tract is asymmetry in frictional resistance to flow in and out of Franks Tract near the major jet connection from Franks Tract to False River. Test simulations have shown that application of a directionally dependent manning's n in this area corrects the net flow error. If field data indicate that this approach is warranted, it will be incorporated into future calibration efforts.

In Three Mile Slough, a shift in model net flow of 1,100 cfs toward the San Joaquin River may also be due to asymmetry in frictional resistance. Large bed forms in this channel could explain the asymmetry. Test simulations have indicated that the directionally dependent manning's n application can correct net flow errors here as well. Again, if field investigations confirm the asymmetry, this method will be used in future calibration.

In Mokelumne River near the San Joaquin, there is a net flow shift of 1,100 cfs downstream. This results in variability in computed EC that is less than observed. The flow error could be related to conveyance capacity in Little Potato Slough and /or other channels west and north of the Mokelumne, perhaps as far up the system as Snodgrass Slough. This issue needs to be addressed in future calibration effort. Additional bathymetry and flow data are needed in order to proceed.

At the SWP and CVP exports, there is not enough variability in the EC. This could be the result of the use of 1-D channels in this area. Future efforts will involve extending 2-D elements into the south Delta in hopes of improving representation of mixing and resolving more of the variability seen in observed data.

Representation of south Delta Barriers will be investigated for potential improvement in stage results in Old River at Head and flow results in the San Joaquin River near Stockton.

9 REFERENCES

Department of Water Resources, "Methodology for Flow and Salinity Estimates in the Sacramento-San Joaquin Delta and Suisun Marsh, Twenty-second Annual Progress Report to the State Water Resources Control Board", August 2001.

Department of Water Resources, "Methodology for Flow and Salinity Estimates in the Sacramento-San Joaquin Delta and Suisun Marsh, Twenty-fifth Annual Progress Report to the State Water Resources Control Board", October 2004.

Foreman, M.G.G., "Manual for Tidal Heights Analysis and Prediction", Institute of Ocean Sciences, Patricia Bay, Sidney, B.C., 1977.

Hills, "New Flow Equations for Clifton Court Gates", Technical Memorandum. California Department of Water Resources, State Water Project Division of Operations and Maintenance, Sacramento California, 1988.

King, I. P., "Finite Element Model for Two-Dimensional Depth Averaged Flow, RMA2V, Version 3.3", Resource Management Associates, 1986.

King, I. P., "RMA11 – A Two-Dimensional Finite Element Quality Model", Resource Management Associates, 1995.

RMA, "Mathematical Modeling of Hydrodynamic and Water Quality Impacts of Suisun Marsh Levee Breaches", December 2000.

RMA, "Water Quality Impacts of Central Contra Costa Sanitary District Discharge on San Francisco Bay", August 2000.

RMA, "Impacts of the BADA Discharges on Copper Levels in the San Francisco Bay", March 1998.

RMA, "Dilution Analysis and Water Quality Impacts of the Palo Alto Regional Water Quality Control Plant on South San Francisco Bay", December 1997.

RMA, "Dilution Analysis and Water Quality Impacts of the Novato Sanitary District to San Pablo Bay", January 1997.

10 APPENDIX A: GOVERNING EQUATIONS

10.1 GOVERNING EQUATIONS FOR FLOW

The governing equations are presented for one and two-dimensional versions of the shallow water equations. This formulation assumes an incompressible flow that is vertically well mixed.

10.1.1 Two-dimensional Depth Averaged Flow

The notation used in this analysis is shown in Figure 10-1. It is worth noting that the principal variable for depth is (h) measured from the bottom elevation (a) and not the more conventional ξ measured from some nominal water surface. As will be seen later, this is because no linearizing approximations are made in the formulation.

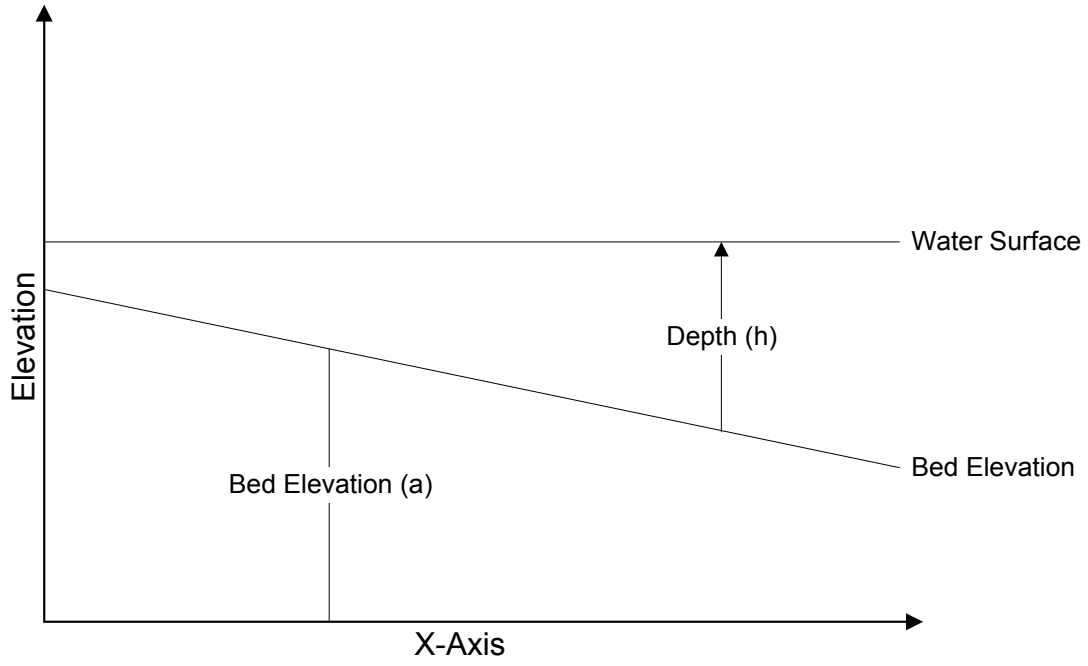

Figure 10-1 Notation definitions for depth averaged flow.

The governing equations consist of two conservation of momentum equations in the x and y direction and an equation of conservation of mass. The dependant variables are velocities (u) and (v) and depth (h).

Momentum Equation X-Direction

$$\rho\left(h\frac{\partial u}{\partial t} + hu\frac{\partial u}{\partial x} + hv\frac{\partial u}{\partial y} + gh\left(\frac{\partial a}{\partial x} + \frac{\partial h}{\partial x}\right) + \frac{g}{C^2}u|V|\right.$$

time transient | convective inertia | pressure gradient | bottom friction

$$\left. + uq_s - \Omega vh\right) + gh^2\frac{\partial \rho}{\partial x} - \frac{\partial}{\partial x}\left(\varepsilon_{xx}\, h\frac{\partial u}{\partial x}\right) - \frac{\partial}{\partial y}\left(\varepsilon_{xy}\, h\frac{\partial u}{\partial y}\right) - W_x = 0$$

tributary inflow | Coriolis | baroclinic | eddy viscosity | wind stress

Momentum Equation Y-Direction

$$\rho\left(h\frac{\partial v}{\partial t} + hu\frac{\partial v}{\partial x} + hv\frac{\partial v}{\partial y} + gh\left(\frac{\partial a}{\partial y} + \frac{\partial h}{\partial y}\right) + \frac{g}{C^2}v|V|\right.$$

time transient | convective inertia | pressure gradient | bottom friction

$$\left. + vq_s - \Omega uh\right) + gh^2\frac{\partial \rho}{\partial y} - \frac{\partial}{\partial x}\left(\varepsilon_{yx}\, h\frac{\partial v}{\partial x}\right) - \frac{\partial}{\partial y}\left(\varepsilon_{yy}\, h\frac{\partial v}{\partial y}\right) - W_y = 0$$

tributary inflow | Coriolis | baroclinic | eddy viscosity | wind stress

Continuity Equation

$$\left(h\frac{\partial u}{\partial x} + \frac{\partial v}{\partial y}\right) + u\frac{\partial h}{\partial x} + v\frac{\partial h}{\partial y} + \frac{\partial h}{\partial t} - q_s = 0$$

change of flow in x and y dir. | Change of water surface elev | specific inflow rate

where:

x, y = horizontal cartesian coordinates

t	=	time
u, v	=	the horizontal velocity components in the x and y directions respectively
h	=	depth
a	=	bottom elevation
ε_{xx}, ε_{xy}, ε_{yx} and ε_{yy}	=	the turbulent eddy coefficients.
C	=	Chezy bottom friction coefficient
V	=	Total water velocity
q_s	=	Tributary flow into the system
Ωvh and Ωuh	=	The coriolis forcing in the x and y directions respectively.
W_x and W_y	=	forces due to wind stresses in the x and y directions respectively.

10.1.2 Governing Equations for One-dimensional Flow

For this approximation, integration is applied in both the vertical and the horizontal direction normal to the desired flow direction. For consistency when integrating the conventional form of the equations is multiplied by the cross-sectional area. To introduce some generality when one-dimensional approximations are used the equations are constructed to permit trapezoidal cross-sections and off channel storage.

The final set of equations may be stated as:

Momentum Equation X-Direction

$$\rho \left[A\frac{\partial u}{\partial t} + Au\frac{\partial u}{\partial x}\right] - \frac{\partial}{\partial x}\left(\varepsilon_{xx}A\frac{\partial u}{\partial x}\right) + gA\left(\frac{\partial a}{\partial x} + \frac{\partial h}{\partial x}\right) + A\frac{g}{C^2}u|U|$$

time transient | convective inertia | eddy viscosity | pressure gradient | bottom friction

$$- \frac{gAh}{2}\frac{\partial \rho}{\partial x} - A\,\Gamma_x = 0$$

baroclinic | wind stress

Continuity Equation

$$A\frac{\partial u}{\partial x} + u\frac{\partial A}{\partial x} + \frac{\partial (A+As)}{\partial h}\frac{\partial h}{\partial t} - q_s = 0$$

change of flow in x dir. Change of water surface elev specific inflow rate

where:

A = the cross-sectional area

As = the non flowing cross-sectional area

Γ_x = wind stress forcing

Other terms have been previously defined.

The RMA2 program solves the governing equations for u,v and h by a finite element approach with Galerkin's criterion applied to the method of weighted residuals. For the two-dimensional approximations, the model employs 6-node triangular and 8-node quadrilateral elements (Figure 10-2). Three node line elements are used for approximating one-dimensional channel flow. Quadratic shape functions are used interpolate the velocity variables while linear shape functions are used for the depth, h. The quadratic functions allow for a curved element edge geometry. Because these equations can be highly non-linear, they are solved by a Newton-Raphson iterative technique. Time dependent solutions employ a Crank-Nicholson implicit finite difference scheme. Values of time integration constant, θ, can be varied by input. Typically a value of .526 is used for the RMA2 time dependent simulations.

Details of the model formulation in regards to horizontal turbulent transfer of momentum, wetting and drying scheme, wind formulas, bottom friction, boundary conditions, flow control structures (internal boundary conditions) are presented below

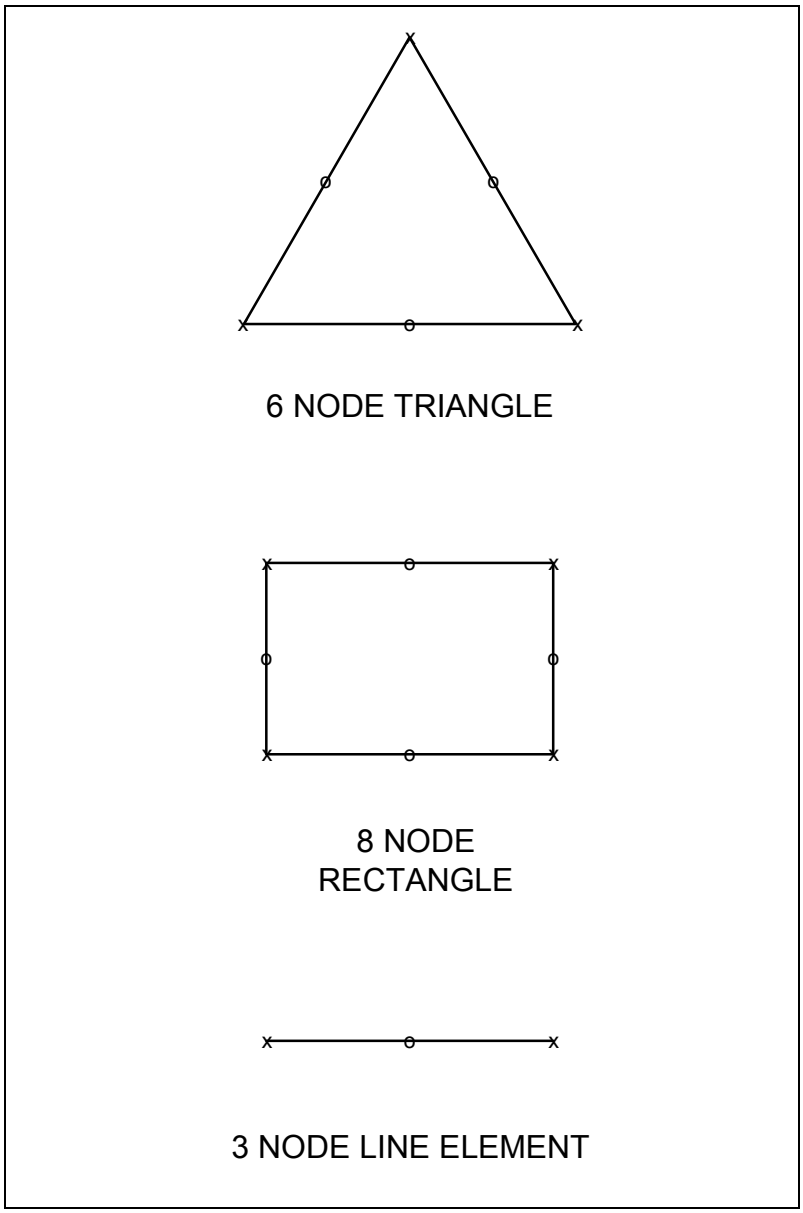

Figure 10-2 Basic element shapes.

10.1.3 Smagorinsky Method

Horizontal eddy viscosity in the momentum equations can be specified as constant values for ε_{xx}, ε_{xy}, ε_{yx} and ε_{yy} by element group type. Alternatively the Smagorinsky method for evaluating sub-grid scale momentum transport can be applied where eddy viscosities are approximated as the product of a scale factor that is dependent on the velocity gradients, and the element size.

As applied in RMA2 the turbulent eddy viscosity terms are given the following forms

For the x-momentum equation:

$$\frac{\partial}{\partial x}\left(2\, A_m\, h\, \frac{\partial u}{\partial x}\right) + \frac{\partial}{\partial y}\left(A_m\, h\, \left(\frac{\partial u}{\partial y} + \frac{\partial v}{\partial x}\right)\right)$$

For the y-momentum equation:

$$\frac{\partial}{\partial y}\left(2\, A_m\, h\, \frac{\partial v}{\partial y}\right) + \frac{\partial}{\partial x}\left(A_m\, h\, \left(\frac{\partial u}{\partial y} + \frac{\partial v}{\partial x}\right)\right)$$

where:

A_m = α (Area) $\left[\left(\frac{\partial u}{\partial x}\right)^2 + \left(\frac{\partial v}{\partial y}\right)^2 + 0.5\left(\frac{\partial u}{\partial y} + \frac{\partial v}{\partial x}\right)^2\right]^{0.5}$

α = a coefficient usually in the range 0.01 - 0.5.

Area = the area of the current element.

10.1.4 Bottom Friction

As implemented in RMA2, two friction loss formulations are permitted. The traditional forms for depth-averaged flow are given by:

(a) Manning's Equation $S_f = \frac{n^2 . u_m^2}{h^{1.33}}$ in metric units

(b) Chezy's Equation $S_f = \frac{u_m^2}{C^2 h}$

Where u_m is the mean velocity over the water depth

These formulations represent frictional shear applied as average forces over the entire depth. For the one-dimensional elements h is replaced by the hydraulic radius in the frictional loss equations.

For use as wall or boundary shears (two-dimensional elements), the factors must be multiplied by the wall depth (h). Thus:

(a) Manning's Equation $t_f = \frac{n^2.u_m^2}{h^{0.33}}$ in metric units

(b) Chezy's Equation $t_f = \frac{u_m^2}{C^2}$

10.2 OTHER FLOW MODELING CONSIDERATIONS

10.2.1 One-dimensional model geometry

Description of One-dimensional channel elements

The basic cross-sectional geometry of the RMA2 channel elements is shown in Figure 10-3.

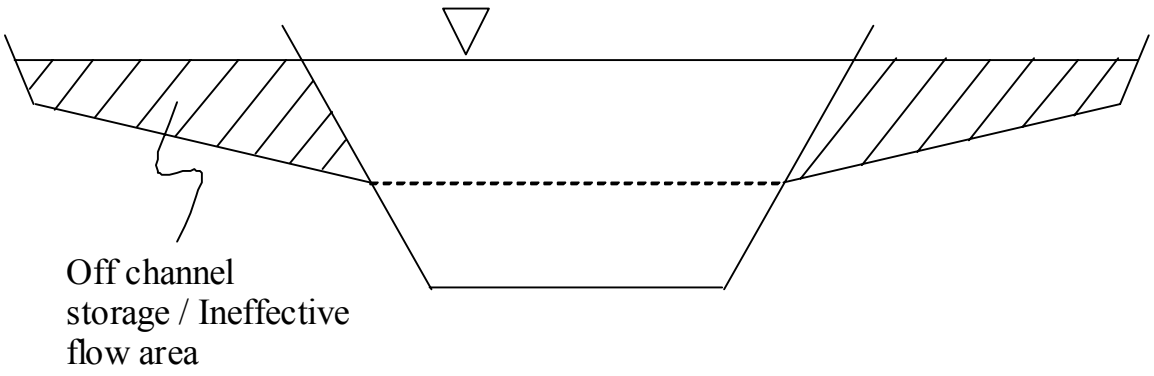

Figure 10-3 RMA2 1-D channel cross-section geometry.

The channel flow area is represented by a trapezoidal section defined by the bottom elevation, bottom width, and left and right channel side-slope. Optionally, the channel cross-section may be specified to also have an off-channel storage or ineffective flow area. The off-channel storage area is specified by beginning elevation, maximum width and side-slope. The off-channel storage contributes to the volume of water and tidal prism in the element, but does not convey flow.

Construction of One-dimensional Networks

One-dimensional systems are defined by interconnected line elements in an identical fashion to the two-dimensional layout. Nodes must however be given properties of bottom width, side-slopes and non-flowing storage width in addition to the coordinate location and bottom elevation. To ensure the correct length for a one-dimensional element the location of the mid-side may be adjusted until the correct length is achieved along the resulting curve. Because one-dimensional elements do not have fully two-dimensional sets of momentum equations, directional consistency is not required at a junction of two one-dimensional elements.

If it is desired to create junctions where more than two line elements join, special joint elements must be created. Thus, at junctions (three or more channels coming together), each node must be individually identified and the junction element defined by lists of each of the nodes at the intersection. Three types of one-dimensional junctions are defined:

1) Equal water surface elevation junctions.
2) Equal total head junctions.
3) Conservation of momentum junctions.

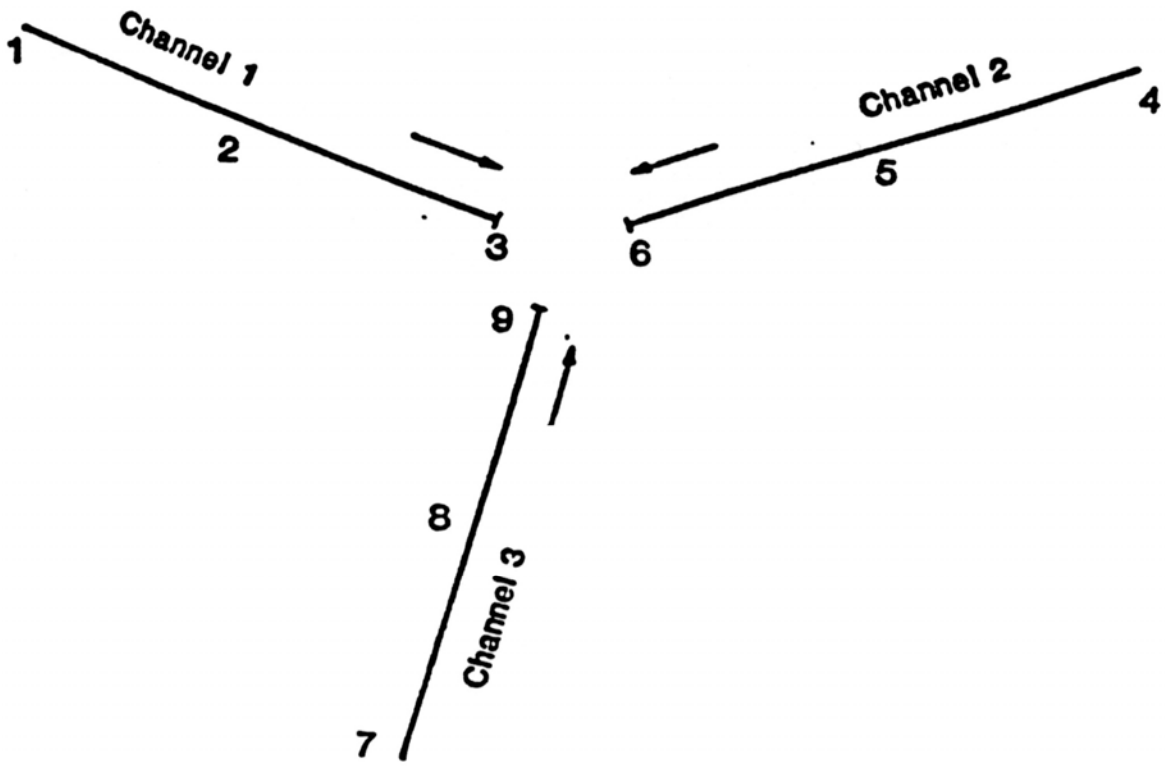

Figure 10-4 Junction element layout.

The conditions applied at intersections of three or more one-dimensional channels (Figure 10-4) are derived to ensure satisfaction of mass continuity (i.e., flow in equals flow out) and in some sense, elevation consistency. Preservation of flow continuity is a straightforward application of a continuity condition. For the case of the figure the following equation results:

$$A_3.V_3 + A_6.V_6 + A_9.V_9 = 0$$

In this case V_n represents the velocity along the channel at node n into the junction and A_n, the cross-sectional area at this point.

The condition of elevation consistency is more difficult to resolve. The use of a one-dimensional element at junctions introduces significant approximations and if this is a real concern it is always possible to construct an intersection from two-dimensional elements and model the system more precisely.

Three possible alternatives for treatment of elevation consistency at junctions have been programmed. They allow the user to choose one of the following methods for each junction in the system:

1) Force equal water surface elevation for all nodes entering a junction., i.e.,

$H_3 = H_6 = H_9$

where H_n = the water surface elevation at node n

2) Force equal velocity head for all nodes entering a junction,

$H_3 + V_3^2/2g = H_6 + V_6^2/2g = H_9 + V_9^2/2g$

3) Preserve momentum at intersections

A set of equations for intersections where relatively small tributaries flow into a main stream may be constructed so that momentum is conserved in the main stream. Two conditions are required.

(a) There must be conservation of momentum or force equilibrium along the stream.
(b) There must be some specification of water surface elevation for the tributary.

If channels 1 and 2 in figure form the main river, the latter condition can be satisfied when:

$H_9 = (H_3 + H_6)/2$

That is the tributary is set to the mean water surface elevation of the main river nodes at the junction. Note that conservation of momentum eliminates the condition that $H_3 = H_6$. A momentum continuity condition may be derived by conceptually balancing the forces that act only on the two main channels entering the junction. The tributary channel is assumed to be small and at an unknown direction and its force contribution is therefore neglected.

Then:

$F_{m3} + F_{p3} = F_{m6} + F_{p6}$

Where:

F_m = The momentum force at node n

F_p = The hydrostatic pressure force at node n

For the constant width case would reduce to,

$Au_3^2 + w_3gh_3^2/2 = au_6^2 + w_6gh_6^2/2$

10.2.2 Marsh Elements / Flooding And Drying

The marsh element or equivalent porosity formulation has been added to RMA2 to improve performance when simulating areas the flood and dry during the tidal cycle or flood event.

Historically the first approach used for simulation of these types of system was to automatically drop from the system any element where any **one** corner water depth dropped below a nominal minimum value (an input parameter). This technically works. The problems found were:

- Inconsistent performance when irregular boundaries resulted.
- Elements dropped out too soon, because one corner showed negative depth and was considered dry.
- Poor convergence at some times when elements cycled in and out the system.
- When an element was dropped or added the total water stored in this element was removed or added and there was a loss of mass consistency.

For these reasons an improved method was sought. Preferable a method where elements dropped out steadily (in a sense faded away) and would only be removed when **all** nodes were below the minimum.

The equivalent porosity/marsh method is the result. Conceptually, the system was considered as an integration of both surface waters and subsurface groundwater. When the water surface elevation is below the ground surface, flow is presumed to occur in the low-porosity groundwater zone. However the governing equations are still the shallow water equations. Figure 10-5 below illustrates this concept. As a practical consideration the transition in porosity at the ground surface cannot occur with the infinite gradient shown. Instead an approximate system was conceptualized where porosity changed over a finite range, as shown. This range has some physical basis. For example in sandy beach areas and overbank flood plains there are

frequently uneven sections, in marshes there are small channels that are below the level of discretization and drying is in fact a transition over a water surface range.

In order to assure mathematical consistency and not create water at any time the actual level of the transition must be slightly adjusted and the bottom elevation of the groundwater section had to be kept finite. The elevation of the groundwater section is thus best set to be just above the anticipated lowest water level.

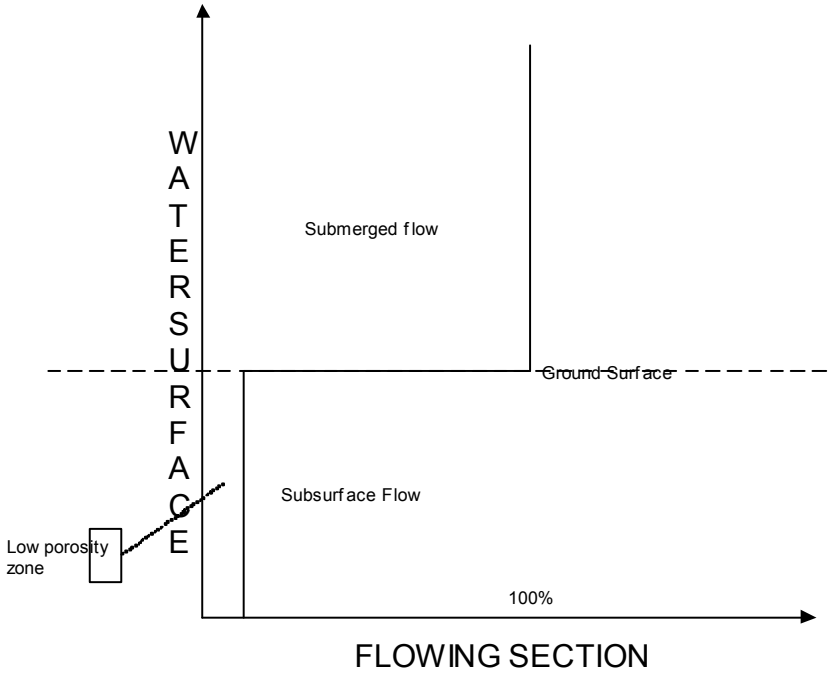

Idealized Representation

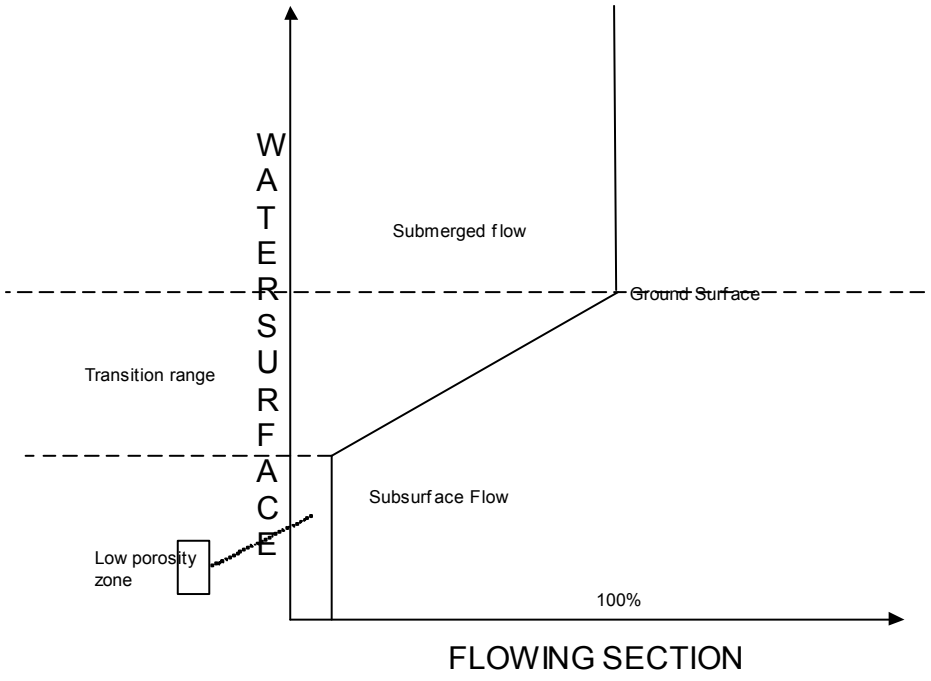

Approximate Representation

Figure 10-5 Idealized and approximate marsh/porosity method representation.

Modeling Consequences of Marsh Elements

The model incorporates this process by formal integration into the differential equations. Without going into full details, the result is that the model operates with a transformed equivalent depth. When the water surface is above the transition level, this equivalent depth is identical to the conventional depth and the water surface elevation is equal to the bottom elevation plus the depth. Below the start of the transition this relationship no longer holds. The depth decreases at a smaller rate than the water surface, or in other words the effective bottom moves down as the depths falls. The figure below illustrates this concept. Note that the curve below is a mathematical result and there are no consequences from the perspective of overall flow conservation.

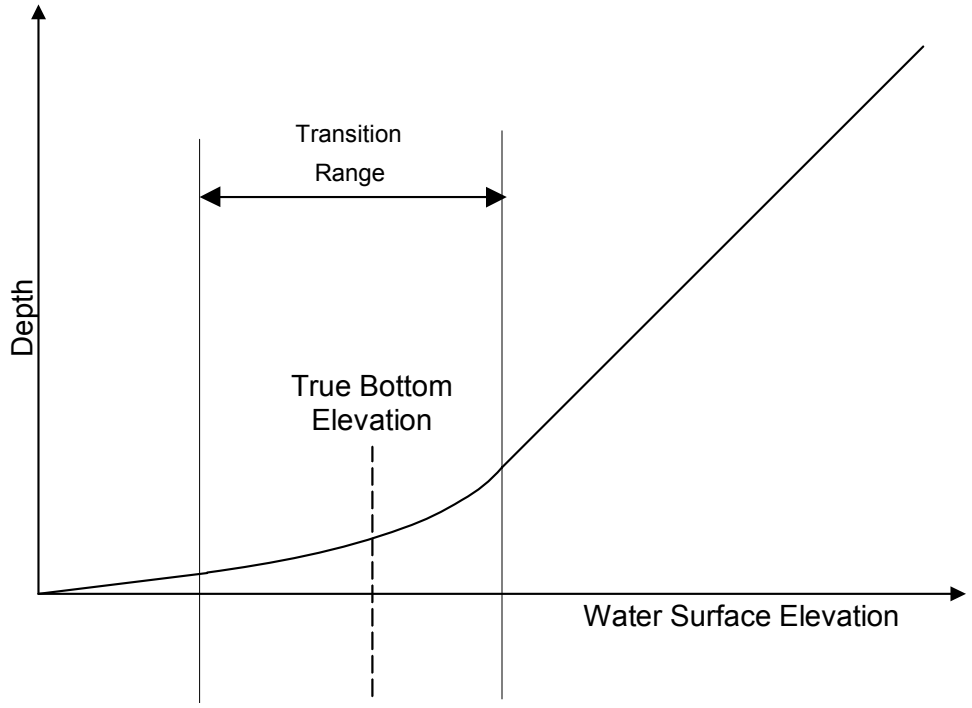

Figure 10-6 Water surface vs. depth for the marsh approximation.

From a numerical perspective the greatest difficulty and cause of instability for this method is the sharp break in gradient as the depth decreases through the transition. This may be demonstrated by observing that the Newton Raphson correction to depth when a point in the system is fully submerged or low in the porous zone will not mathematically expect the

transition and over-correction can result. The model has been modified to automatically switch to under-relaxation for these cases. Model convergence can be significantly slowed by these conditions.

10.2.3 Boundary Conditions

The default boundary condition along the finite element network boundary is the no flow condition. Typically flow or elevation is specified for a single node or line of nodes at the ends of the finite element network to simulate river inflows and to force tidal conditions. Some boundary conditions, such as water surface elevation or velocity, may be specified at interior node locations. Boundary conditions may be constant or entered as time series data. The common type of boundary conditions available in RMA2 are: specified elevation (e.g. tidal boundary), specified flow (e.g. river inflows), and stage/flow.

In addition to boundary conditions applied at one or more nodes along the network boundaries, inflows and withdrawals may be applied to individual or groups of elements. This method is commonly used to simulate inflows or diversions from the interior locations of the finite element network, such as those from the Delta Island Consumptive Use (DICU). The element inflow/withdrawal method may also be used apply evaporation/precipitation over a group of elements or the entire network.

Boundary conditions for the water quality module must be closely coordinated with the flow boundary conditions. The water quality constituent concentration needs to be specified for any location along the boundary in which inflow occurs. When the element inflow option is used, the inflow rate as well as the constituent concentration is required to correctly compute the mass loading in the water quality model.

10.2.4 Control Structures

The RMA2 model supports control structures for the one and two-dimensional elements. For the one-dimensional elements, the equations are for total flow. In the case of the two-

dimensional elements, the equations are developed for lineal flow. In the most general form, flow across the control structure is expressed by the equations:

Flow as a function of head loss,

$Q = A_{J1} + B_{J1}*(H_{N1}-H_{N2}-C_{J1})**GAM1$

where H_{N1} and H_{N2} are water surface elevations at the nodes of the control structure element and $A_{J1,}$ $B_{J1,}$ C_{J1} and GAM1 are coefficients. Q is total for one-dimensional control structures and lineal flow for two-dimensional flow control elements.

Flow as a function of water surface elevation,

$Q = A_{J1} + B_{J1}*(H_{N1}-C_{J1})**GAM1$

where H_{N1} is the water surface elevation at the first node of control structure element.

The basic one and two-dimensional flow control structures behave as "tide gates" allowing only unidirectional flow

Flow in one-dimensional control structures is more typically specified by defining the physical parameters of the available flow control components. These components include weirs, culverts and gates. The properties for defining weir flow include crest elevation, length of the weir, and the weir coefficient.

$Q = 0.$ when $WS_{up} < WeirElev$

$Q = C*L * (WS_{up} - WeirElev)^{3/2}$ for free flow over the weir

$Q = 2.6*C*L * (WS_{dn} - WeirElev) * (WS_{up} - WS_{dn})^{1/2}$
for submerged flow over the weir.

where,

WS_{up} = water surface elevation at the upstream node
WS_{dn} = water surface elevation at the downstream node
WeirElev = crest elevation of the weir
C = weir coefficient
L = weir length

Submerged flow is estimated to occur when,

$(WS_{dn} - WeirElev) / (WS_{up} - WeirElev) > 2/3$

The equation and threshold used for submerged weir flow was based upon the submerged weir flow formulas documented in the UNET Manual.

The one-dimensional control structures are capable of modeling the complex flow in culverts. The computation of culvert flow is similar to that of the steady flow module of the HEC-RAS program. Culverts in the RMA2 program are currently limited to circular or box shape. Test cases have shown for these culvert types, the RMA2 program produces flow and head loss similar to the HEC-RAS steady flow program.

The flow analysis in culverts includes entrance losses, friction losses for flow within the culvert and exit losses. The computation of the culvert flow follows an iterative procedure, in which a backwater computation for a trial flow proceeds upstream from the downstream flow control node. The iterations continue until the flow required to match the water surface at the upstream node is determined. The backwater calculation begins by determining the downstream controlling water surface elevation. When the upstream and downstream ends of the culvert are fully submerged the entrance, exit and frictional losses are fairly simple to compute. Flow in the non-submerged case begins by determining the downstream controlling water surface elevation, either the water surface at the downstream node or the critical depth at the culvert exit. Frictional losses in a partially full culvert require the water surface profile. This is computed using the direct step method (HEC-RAS Hydraulic Reference Manual, 2002).

Gates are the third available component for a one-dimensional flow control structure. Gate flow is computed by:

$$Q = C * A * (2 * g * dh)^{1/2}$$

g = gravitational acceleration

$dh = WS_{up} - WS_{dn}$

A = Gate Width * [min(WS_{up}, Gate Opening Height) – Gate Bottom]

C = Gate flow coefficient

Currently the gate flow equation does not account for the approach velocity. If the gate area approximates the channel cross-section, “C” is set sufficiently high to reduce unintended head loss across the gate structure.

A one-dimensional control structure may include any number weirs, culverts and gates in parallel. A "Gate Operations" file can be used to schedule the opening, closing and removal of the flow control structure and any individual or group of components. The components may be specified to behave as "tide gates" in order to permit flow in only one direction. Structures such as the South Delta temporary barriers are typically represented using a one-dimensional control structure composed as combination of one or more culvert sets and weirs.

The two-dimensional flow control elements do not currently support the complex structures available for the one-dimensional control elements. However, special two-dimensional "weir" elements are available. These elements model free flow over a weir, submerged weir flow, and the no flow condition when the upstream water surface is below the weir crest. For fully submerged flow, the weir element may be switched to behave as a regular two-dimensional element with flow rate set using the shallow water equations. The weir crest elevation may be independently set for each upstream corner node. The weir crest elevation may be changed over time. The two-dimensional weir elements have been used extensively to simulate levee failure along Delta Islands. As an example, the weir elements were used to simulate the Jones Tract levee failure in June, 2004. Weir elevation was lowered from +2.0 m to -9.0 m over a three hour period. The weir elevations were then slowly raised back up to +2.0 m to simulate the repair period.

Figure 10-7 One-dimensional flow control structure representation (shown for the Suisun Marsh Salinity Control Gate).

10.3 GOVERNING EQUATIONS FOR TRANSPORT

10.3.1 Two-dimensional Depth Averaged Transport

The results of the RMA2 flow simulation (x and y velocity components, and depth of water) are saved every time step for all nodal locations to a binary file. The flow result file then may be used by the finite element water quality model, RMA11, to compute salinity transport or the transport of other water quality constituents with more complex interactions. The RMA11 water quality model is capable of simulating water temperature, DO/BOD, algae growth and decay including interaction with the nitrogen and phosphorous cycles, cohesive and non-cohesive sediment transport, coliform with associated decays, and arbitrary conservative and non-conservative constituents with user defined interactions.

EC or salinity transport may also be computed during the flow simulation using the "salinity-coupled" version of the RMA2 model. The governing equations for water quality transport are presented here only for the case of modeling EC. The equations apply both to conservative transport in the RMA11 water quality model and to EC/salinity transport in the "salinity-coupled" version of the RMA2 flow model.

The governing transport equations may be integrated over the vertical dimension with the assumption that C is independent of elevation (z). Under these conditions all derivatives with respect to z are eliminated.

Continuity

$$(h\frac{\partial u}{\partial x} + \frac{\partial v}{\partial y}) + u\frac{\partial h}{\partial x} + v\frac{\partial h}{\partial y} + \frac{\partial h}{\partial t} - q_1 = 0$$

Constituent transport

$$\frac{\partial(hC)}{\partial t} + u\frac{\partial(hC)}{\partial x} + v\frac{\partial(hC)}{\partial y} - \frac{\partial}{\partial x}\left(D_x\, h\, \frac{\partial C}{\partial x} + D_{xy}\, h\, \frac{\partial C}{\partial y}\right) - \frac{\partial}{\partial y}\left(D_{xy}\, h\, \frac{\partial C}{\partial x} + D_y\, h\, \frac{\partial C}{\partial y}\right)$$

$$- KhC - h\theta_s = 0$$

where

x, y	=	horizontal coordinates
t	=	time
u, v	=	velocity components
h	=	water depth
q_1	=	inflow per unit area.
C	=	constituent concentration
Dx, Dxy, Dy	=	diffusion tensor coefficients
R_k	=	a concentration dependent growth rate. Note that in this formulation settling is incorporated into this 1st order rate coefficient
θ_s	=	source rate

After substitution of the continuity equation the transport equation may be written as

$$h\left(\frac{\partial C}{\partial t} + u\frac{\partial C}{\partial x} + v\frac{\partial C}{\partial y}\right) - \frac{\partial}{\partial x}\left(D_x\, h\, \frac{\partial C}{\partial x} + D_{xy}\, h\, \frac{\partial C}{\partial y}\right) - \frac{\partial}{\partial y}\left(D_{xy}\, h\, \frac{\partial C}{\partial x} + D_y\, h\, \frac{\partial C}{\partial y}\right)$$

$$+ (q_1 - R_k\, h)C - h\theta_s = 0$$

For the finite element formulation partial integration is applied to the diffusive terms. The element residual contribution may then be written:

$$\mathbf{f_c} = \int_{A_h} \mathbf{N}^T \left[h\left(\frac{\partial C}{\partial t} + u\frac{\partial C}{\partial x} + v\frac{\partial C}{\partial y}\right) + (q_1 - R_k\, h)\, C - h\theta_s\right] + \mathbf{N_x}^T\left[h\left(D_x \frac{\partial C}{\partial x} + D_{xy}\frac{\partial C}{\partial y}\right)\right]$$

$$+ \mathbf{N_y}^T\left[h\left(D_{xy}\frac{\partial C}{\partial x} + D_y\frac{\partial C}{\partial y}\right)\right] dA$$

For salinity transport, R_k and θ_s are zero.

10.3.2 One-dimensional Transport

For this approximation, integration is applied in both the vertical and the horizontal direction normal to the desired flow direction. The basic equations for this approximation are once again independent of depth, however to introduce some generality when one-dimensional approximations are used the equations are constructed to permit trapezoidal cross-sections and off channel storage.

Once again two alternative formulations have been created. The basic form is suitable for applications that consist only of one-dimensional and depth-averaged two-dimensional elements. The transformed form is suitable for combinations of all element types. The basic equations may be stated as follows:

Continuity

$$\frac{\partial A_S}{\partial t} + A\frac{\partial u}{\partial x} + u\frac{\partial A}{\partial x} - q_3 = 0$$

Constituent transport

$$\frac{\partial (A_S C)}{\partial t} + \frac{\partial (AuC)}{\partial x} - \frac{\partial}{\partial x}\left(D_x A \frac{\partial C}{\partial x}\right) - R_k A_S C - A_S \theta_S = 0$$

where:

A	=	flowing cross-sectional area of the one-dimensional element
A_S	=	storage cross-sectional area of the one-dimensional element
q_3	=	inflow per unit length

After substitution of the continuity equation, the transport equation may be written as

$$A_S\frac{\partial C}{\partial t} + Au\frac{\partial C}{\partial x} - \frac{\partial}{\partial x}\left(D_x A \frac{\partial C}{\partial x}\right) + (q_3 - R_k A_S) C - A_S \theta_S = 0$$

For the finite element formulation partial integration is applied to the diffusive term. The element residual contribution may then be written:

$$\mathbf{f_C} = \int_L \mathbf{N^T}\left[A\frac{\partial C}{\partial t} + Au\frac{\partial C}{\partial x} + (C\,(q_3 - R_k\,A_S) - A_S\theta_{S\text{-}})\right] + \mathbf{N_X^T} D_X\,A\,\frac{\partial C}{\partial x}\,dL$$

The RMA11 finite element water quality model supports the same elements types as the RMA2 flow model. Quadratic shape functions are used interpolate the constituent concentrations as well as velocity variables while linear shape functions are used for the depth, h. The quadratic functions allow for a curved element edge geometry.

Diffusion Tensor

In setting the diffusion or mixing coefficients, the user enters factors in the water quality input file which control the computation of the longitudinal diffusion coefficient, D_ℓ, and the transverse diffusion coefficient, D_t. D_ℓ represents the diffusion or mixing coefficient aligned with the direction of flow. D_t represents the diffusion or mixing coefficient transverse to the direction of flow. The diffusion coefficients are a tensor quantity and must be properly treated when transforming to the x-y model coordinate system. The equations for the diffusion coefficients in the x-y coordinate system become:

$$D_x = D_\ell \cos^2\theta + D_t \sin^2\theta$$
$$D_{xy} = \tfrac{1}{2} \cdot \sin 2\theta \cdot (D_\ell - D_t)$$
$$D_y = D_t \cos^2\theta + D_\ell \sin^2\theta$$

where,

θ = flow direction relative to the x-axis.

The longitudinal and transverse diffusion coefficients are computed from user entered scale factors:

$$D_\ell = d_\ell \cdot (u^2 + v^2)^{1/2}$$
$$D_t = d_t \cdot D_\ell$$

where,

u, v	=	x,y velocity components
d_ℓ	=	user scale factor for the longitudinal diffusion
d_t	=	user scale factor for the transverse diffusion

The first factor scales the longitudinal diffusion according to the velocity magnitude. The second factor sets the transverse diffusion as a fractional value of the longitudinal diffusion.

11 APPENDIX B: OBSERVED VS. MODEL PERFORMANCE EVALUATION

For the most part, Delta flow and stage time series exhibit a strong tidal signal as well as a net flow or average stage component. Several data analysis methods were applied to evaluate the performance of the model in reproducing the tidal components as well as the tidally averaged components.

A simple performance measure for evaluating computed and observed time series data is to perform a linear regression analysis of the two data sets. However, a direct application of the regression analysis may not be the most useful method for evaluating the performance of the model. For a parameter such as tidal flow, even a minor phase difference between computed and observed records will skew the regression results if the phase difference is not removed. In addition, the phase difference of the model vs. observed data is itself a measure of model performance.

The phase difference between the model and measured time series was determined using a cross-correlation procedure. Figure 11-1 illustrates the cross-correlation procedure for determining the phase difference of the model time series record relative the observed data record. The process entails repeatedly time shifting the model record relative to the observed time series while computing the correlation coefficient between the model and observed data set at each time shift. The correlation has a maximum value when the shifted model time series best aligns with the observed data time series. The time shift at this point represents the phase difference (expressed in minutes) between the two data sets. The model data were shifted at one-minute increments in cross-correlation computations. Typically the model and observed data points are at a 15-minute interval. The model values were interpolated to the shifted time points using a cubic-spline interpolation.

The shifted time series which results in the peak correlation value was saved for further processing. A linear regression analysis was then performed between the time shifted model result and the observed data record. The results of the linear regression analysis are presented as a scatter plot of observed vs. the time shifted model data, along with the least-squares line and regression statistics.

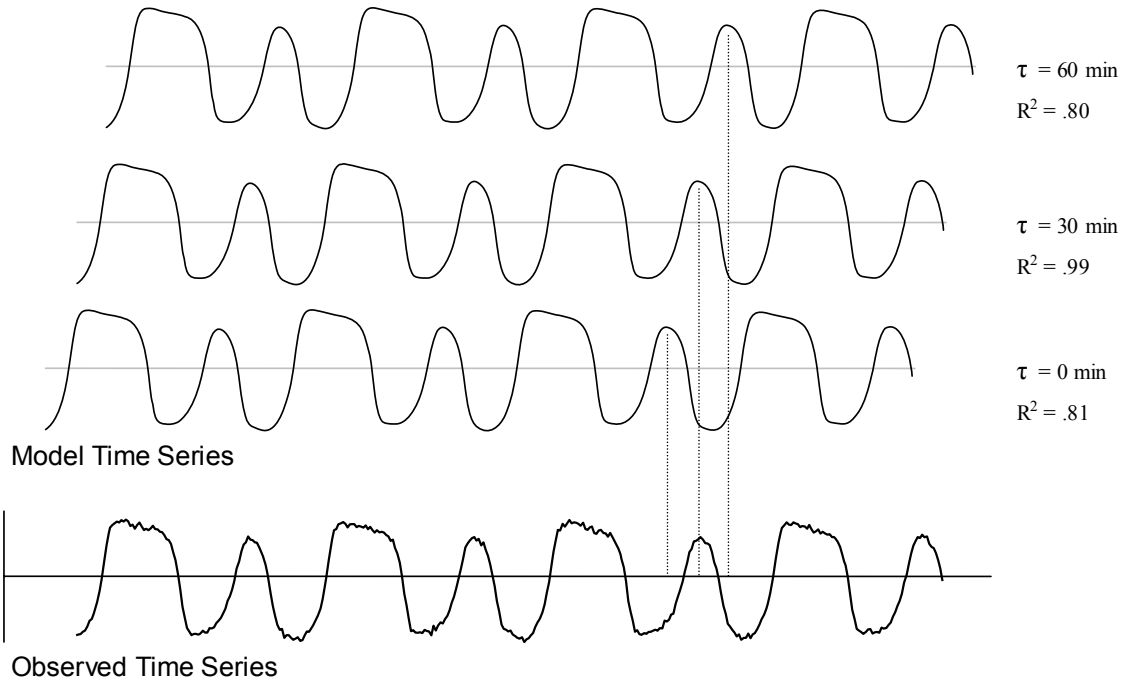

Figure 11-1 Illustration of the cross-correlation technique for determining phase difference between observed and model time series. The model time series is repeatedly shifted in time and the correlation coefficient is computed for the shifted time series and the observed time series.

Figure 11-2 shows the scatter plot and the results of the regression analysis for computed and observed flow at the False River station. The slope of the line approximates the amplitude ratio for model vs. observed tidal flow. The mean values indicate for the analysis period, the computed flow, on average, was 476 cfs higher in the flood direction relative to the observed flow.

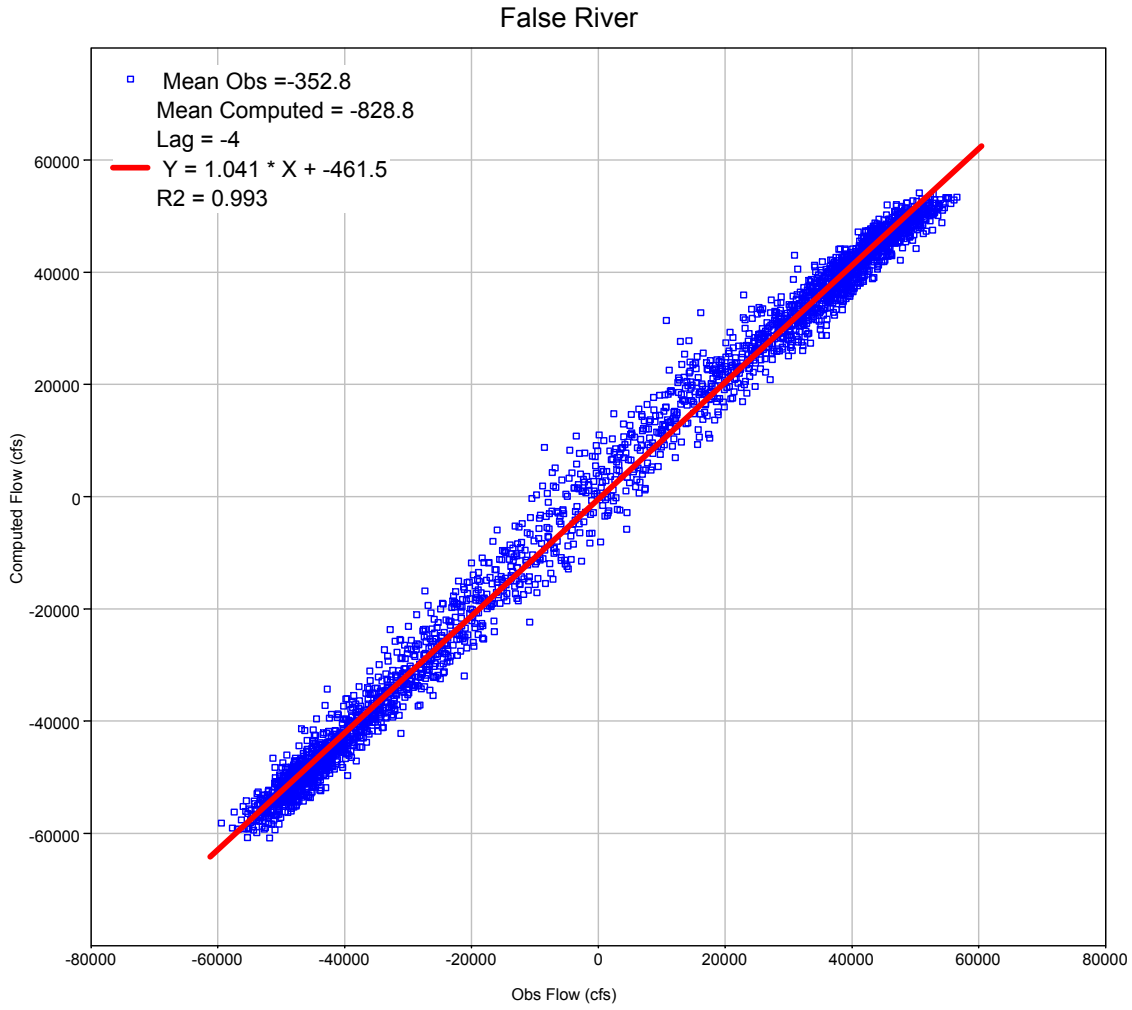

Figure 11-2 Scatter plot of observed vs. time shifted computed data, showing best fit line and linear regression coefficients. The value for the phase lag, in minutes, is determined from the cross-correlation analysis is also shown.

A harmonic analysis of tidal stage and flow was also performed. The tidal constituents for observed and model stage were analyzed using the "Tidal Heights Analysis Computer Program" developed by Foreman (1977). The program uses a least-squares method of analysis to evaluate the amplitude and phase of the standard set of tidal constituents. The input format of the Foreman program did not readily accommodate values for flow. In this case, M2 and K1

tidal phase and amplitude were determined using Fourier analysis. Tests with stage time series showed the Fourier analysis method reproduced the least squares analysis M2 amplitude and phase, but was 5% higher in the estimate of K1 amplitude. Computation of the K1 phase lag was off +1 minute using the Fourier analysis method vs. the least-squares analysis.